

**CRC Report No. AVFL-13b**

**ETHANOL EFFECTS ON GASOLINE-  
LIKE HCCI COMBUSTION**

**August 2009**



**COORDINATING RESEARCH COUNCIL, INC.**  
3650 MANSELL ROAD·SUITE 140·ALPHARETTA, GA 30022

**The Coordinating Research Council, Inc. (CRC) is a non-profit corporation supported by the petroleum and automotive equipment industries. CRC operates through the committees made up of technical experts from industry and government who voluntarily participate. The four main areas of research within CRC are : air pollution (atmospheric and engineering studies); aviation fuels, lubricants, and equipment performance, heavy-duty vehicle fuels, lubricants, and equipment performance (e.g., diesel trucks); and light-duty vehicle fuels, lubricants, and equipment performance (e.g., passenger cars). CRC's function is to provide the mechanism for joint research conducted by the two industries that will help in determining the optimum combination of petroleum products and automotive equipment. CRC's work is limited to research that is mutually beneficial to the two industries involved, and all information is available to the public.**

**CRC makes no warranty expressed or implied on the application of information contained in this report. In formulating and approving reports, the appropriate committee of the Coordinating Research Council, Inc. has not investigated or considered patents which may apply to the subject matter. Prospective users of the report are responsible for protecting themselves against liability for infringement of patents.**



47519 HALYARD DRIVE  
PLYMOUTH, MI 48170-2438  
PHONE: (734) 414 9618  
FAX: (734) 414 9690

## **REPORT PEI-0341 Revision 3 September 2009**

### **Ethanol Effects on Gasoline-like HCCI Combustion (CRC Project #AVFL-13B)**

**Written by**

A handwritten signature in black ink, appearing to read "Jennifer Wheeler".

Jennifer Wheeler  
Project Engineer  
Engine Development

**Reviewed by**

A handwritten signature in black ink, appearing to read "Daniel Schwarz".

Daniel Schwarz  
Skill Team Leader  
Engine Development

**Approved by**

A handwritten signature in black ink, appearing to read "Gary Hunter".

Gary Hunter  
Chief Technologist  
CI Engine Development

**Distributed to**

Coordinating Research Council

AVL PEI

AVL Graz Abteilung DEC, DGD





## Executive Summary

Homogeneous charge compression ignition (HCCI) combustion offers the potential of producing diesel-like fuel economy combined with ultra-low Oxides of Nitrogen ( $\text{NO}_x$ ) emissions in gasoline-fueled spark-ignition engines. Since HCCI combustion occurs by auto-ignition of the fuel/air mixture, fuel parameters such as octane rating, composition, and distillation are likely to play a role in HCCI engine operation and performance. However, the precise impacts of these parameters are not presently known. Also unknown is what HCCI operating mode will dominate future HCCI engines. Therefore, it is the goal of this Coordinating Research Council (CRC) Advanced Vehicles, Fuels and Lubricants (AVFL) Committee funded project to quantify fuel effects for various conditions and modes of HCCI engine operation. This project is the second of two phases of testing and includes the effect of ethanol in addition to the fuel component effects studied in the first phase [1].

In the first study, ten gasoline-like test fuels of varying octane quality, composition, and distillation were tested by AVL of Plymouth, MI on a single cylinder research engine equipped with a hydraulic variable valve train (VVT) and a gasoline direct injection (GDI) system. The second study looks at five repeat fuel blends from the first study, one additional fuel blend, and ten fuel blends with varying levels of ethanol based on the five repeat test fuels. There were 26 fuels in total. These fuels were tested using two different HCCI operating modes: Re-compression early injection (RCEI) and re-breathing early injection (RBEI). For each mode, three engine operating conditions were investigated: a near-idle condition, a mid-load HCCI condition, and a high-speed HCCI condition. At higher engine loads and speeds, it is anticipated that an HCCI engine will switch to normal closed-loop spark-ignition operation.

The most prevalent refinery streams used for gasoline blending are reformat (about 50% aromatic), alkylate (about 100% iso-paraffin), cat cracker gasoline (about 25% olefin), and straight run gasoline (about 100% normal paraffin). Therefore, these four streams were used to blend the eleven base test fuels and are represented in this study by the letter designations A, B, C and D, respectively. The ethanol content of each fuel is represented by the letter designation E.

The first step in the engine testing was to determine the baseline engine operating conditions (valve timings, fuel-rail pressure, single injection timing, split injection timings and quantities, and overall fueling quantities). This determination was completed at the beginning of the first study [1]. These baseline tests were conducted for each HCCI mode and for each of the three operating conditions for each mode. Indolene was used as the fuel for these baseline tests. These baseline engine-operating conditions were used as the starting conditions for testing each of the test fuels and then only the valve timings were changed to achieve the required combustion phasing and engine load. Repeatability tests with indolene were interspersed in the test fuel matrix to assure the engine operation remained consistent throughout testing. The engine parameters of

---

### CUSTOMER CONFIDENTIAL



interest in both the baseline testing and test fuel testing were: indicated specific fuel consumption (ISFC), indicated thermal efficiency (ITE), indicated specific  $\text{NO}_x$  emissions (IS $\text{NO}_x$ ), indicated specific hydrocarbon emission (ISHC), indicated specific carbon monoxide emission (ISCO), filter smoke number (FSN), combustion duration, combustion noise, coefficient of variance (COV) of indicated mean effective pressure (IMEP), and peak cylinder pressure (PP).

The repeatability tests with indolene showed test-to-test variability correlated with engine operating parameters which were measured but could not be precisely controlled. To account for variations in operating conditions, normalization models were developed using the indolene data and data from the five repeated test fuels to adjust each relevant engine parameter for every test fuel prior to further data analysis.

After the data was normalized, the effect of ethanol was examined for each of the ten engine performance parameters. Only the ethanol blends and their respective base fuels were used for this analysis. Then regression models for each engine performance parameter were fit to all possible combinations of two fuel properties and their interaction using data from testing of the eleven base fuels. The best “2-factor” model was then chosen for each of the ten performance parameters.

For all ten engine parameters there was no universally “best” model in which all individual speed/mode regressions were highly statistically significant. However, there were several cases where subgroups of speed/mode conditions did exhibit statistically significant results. These were further evaluated to determine if they showed consistency in level of significance and form of relationship (i.e. increase in fuel property produces same response in different modes).

Ethanol has a smaller lower heating value (LHV) than gasoline and thus contains less energy on a mass and volumetric basis. Therefore, fuel consumption is expected to increase as the volumetric ethanol content is increased. This trend was observed as statistically significant for all six speed/mode combinations. The fuel consumption was also found to be related to butane content and T10 at 2000 rpm and 3000 rpm. However, at 1000 rpm, where combustion stability is poor, the ISFC is highly dependent on COV of IMEP.

The indicated thermal efficiency increased significantly as the volumetric ethanol content of the fuel was increased. Ethanol had a cooling effect on the combustion temperatures, indicated by decreasing  $\text{NO}_x$  emissions. Heat transfer losses were reduced resulting in the observed increased efficiency. Thermal efficiency was also affected by n-paraffin content without butane and T10 at 2000 rpm and 3000 rpm. Because ITE is a function of ISFC, both these parameters are likely to be dependent on total normal paraffin content, although this parameter was not part of the statistical analysis.

---

**CUSTOMER CONFIDENTIAL**



As previously mentioned, the ISNO<sub>x</sub> emissions decreased as the ethanol content of the fuel increased due to the cooling effects of ethanol. The ISNO<sub>x</sub> was also statistically related to olefin content and butane content.

The ISHC emissions were not statistically related to ethanol. In addition no 2-factor model could be used to successfully predict the hydrocarbon emissions. In this study, the hydrocarbon emissions were highly dependent on the engine operating conditions and had little relationship to fuel composition.

As ethanol was increased, the ISCO emissions at 1000 rpm illustrated an increasing trend due to a decrease in combustion stability indicated by a higher COV of IMEP. Also at 1000 rpm, the ISCO emissions showed a strong relationship to aromatics and iso-paraffin content. At higher engine speeds, the ISCO emissions did not show any consistent relationships to fuel composition. The ISCO emissions are very low at 2000 rpm across the entire range of fuels tested. At 3000 rpm, the ISCO emissions are strongly dependent on air-fuel ratio since the engine runs closer to stoichiometry at this engine speed.

In general, this study shows that blending ethanol with gasoline in moderate amounts is beneficial to thermal efficiency and reduced NO<sub>x</sub> emissions for part-load lean HCCI operation with little to no effect on hydrocarbon emissions. However, this benefit must be balanced with a loss in combustion stability at idle conditions and an associated increase in ISCO emissions. However, this effect could be mitigated by using stoichiometric spark-ignited operation when necessary. Increasing the ethanol content of the fuel is also beneficial for full load spark-ignited operation where the anti-knock properties of ethanol can be used to enable more advanced spark timings and increased engine performance. Therefore, a combined HCCI and spark-ignited strategy would appear to benefit from the use of ethanol-blended fuels.

Although the models for ethanol content are separate from those for the other fuel components, these models can still be used together to estimate fuel effects on HCCI combustion. In addition, these models could be combined if more testing is performed with ethanol blends of the other 6 base fuels. An investigation of fuels with higher percentages of ethanol content is also recommended to determine if the cooling effects of ethanol ultimately hinder HCCI operation.



## Contents

<b>Revision History</b> .....	<b>i</b>
<b>Executive Summary</b> .....	<b>ii</b>
<b>Contents</b> .....	<b>v</b>
<b>List of Tables</b> .....	<b>vi</b>
<b>List of Figures</b> .....	<b>viii</b>
<b>1. Introduction</b> .....	<b>1</b>
1.1. Background .....	1
1.2. Project Objectives .....	2
<b>2. Technical Methodology</b> .....	<b>3</b>
2.1. Description of Test Plan .....	3
2.2. Fuel Parameter Matrix .....	6
2.3. Analysis Techniques .....	9
<b>3. Experimental Set-up</b> .....	<b>11</b>
3.1. Test Engine Specifications .....	11
3.2. Test Cell Configuration .....	12
3.3. Test Procedures .....	14
3.4. Fuel Specification .....	16
3.5. Data Quality .....	17
<b>4. Test Results</b> .....	<b>24</b>
4.1. Test Results from Phase II-a .....	24
4.2. Test Results from Phase II-b .....	38
<b>5. Statistical Data Analysis</b> .....	<b>51</b>
5.1. Data Handling .....	51
5.2. Data Analysis Methods .....	53
5.3. Fuel Selection Analysis Results .....	58
5.4. Indolene and Repeat Fuel Test Adjustments .....	66
5.5. Analysis of Engine Performance versus Fuel Composition and Properties .....	69
<b>6. Conclusions</b> .....	<b>100</b>
6.1. Volumetric Ethanol Content .....	100
6.2. Base Fuel Composition .....	100
<b>7. Recommendations</b> .....	<b>102</b>
<b>8. References</b> .....	<b>103</b>
<b>Appendix A – Definition of Acronyms</b> .....	<b>105</b>
<b>Appendix B – Measured and Calculated Parameters</b> .....	<b>106</b>
<b>Appendix C – Fuel Analysis</b> .....	<b>107</b>
<b>Appendix D – Motored Engine Pressure Data</b> .....	<b>111</b>
<b>Appendix E – Numerical Results</b> .....	<b>112</b>
<b>Appendix F – Regression Models</b> .....	<b>113</b>



## List of Tables

Table 2.1 – Engine Operating Points .....	5
Table 2.2 – Fuel Properties used for Analysis.....	7
Table 2.3 – Fuel Test Matrix.....	8
Table 3.1 – Engine Specifications .....	11
Table 3.2 – Fuel Test Order for Phase II-a.....	15
Table 3.3 – Fuel Test Order for Phase II-b.....	15
Table 3.4 – Operating Point Test Order for Each Fuel .....	15
Table 3.5 – Indolene Baseline Valve and Injection Timings .....	16
Table 5.1 - Unusual Data Record Values.....	52
Table 5.2 - Normalization of Measured Response Variables .....	68
Table 5.3 - Best Ethanol Content Statistical Model for ISFC.....	71
Table 5.4 - Best Ranked R-Square Model for ISFC .....	71
Table 5.5 - Best Ethanol Content Model for ITE.....	74
Table 5.6 - Best Ranked R-Square Model for ITE.....	74
Table 5.7 - Best Ethanol Content Model for ISNO <sub>x</sub> .....	77
Table 5.8 - Best Ranked R-Square Model for ISNO <sub>x</sub> .....	77
Table 5.9 - Best Ethanol Content Model for ISHC.....	80
Table 5.10 - Best Ranked R-Square Model for ISHC.....	80
Table 5.11 - Best Ethanol Content Model for ISCO.....	82
Table 5.12 - Best Ranked R-Square Model for ISCO.....	82
Table 5.13 - Best Ranked R-Square Model for IS_SMK .....	85
Table 5.14 - Best Ethanol Content Model for Combustion Duration.....	87
Table 5.15 - Best Ranked R-Square Model for Combustion Duration.....	87
Table 5.16 - Best Ethanol Content Model for COV of IMEP .....	89
Table 5.17 - Best Ranked R-Square Model for COV of IMEP .....	89
Table 5.18 - Best Ethanol Content Model for Noise .....	91
Table 5.19 - Best Ranked R-Square Model for Noise .....	93
Table 5.20 - Best Ethanol Content Model for Peak Cylinder Pressure.....	93
Table 5.21 - Best Ranked R-Square Model for Peak Cylinder Pressure.....	93
Table 5.22 - Best Ethanol Content Model for EVC .....	95
Table 5.23 - Best Ranked R-Square Model for EVC .....	95
Table 5.24 - Best Ethanol Content Model for IMEP @ 3000 rpm.....	97
Table 5.25 - Best Ranked R-Square Model for IMEP @ 3000 rpm.....	97
Table 5.26 - Best Ethanol Content Model for MRPR.....	98
Table 5.27 - Best Ranked R-Square Model for MRPR.....	99

---

### CUSTOMER CONFIDENTIAL



Table B.1 – Measured & Calculated Parameters .....	106
Table C.1 – Phase I (AVFL-13) Fuel Analysis.....	107
Table C.2 – Phase II-a (AVFL-13b) Fuel Analysis.....	108
Table C.3 – Phase II-b (AVFL-13b) Fuel Analysis.....	109
Table C.4 – Indolene Fuel Analysis.....	110
Table D.1 – Motored Pressure Data 5/25/07 .....	111
Table D.2 – Motored Pressure Data 11/23/08.....	111



## List of Figures

Figure 2.1 – Injection, Valve & Cylinder Pressure Traces @ 2000 rpm, RCEI .....	4
Figure 2.2 – Injection, Valve & Cylinder Pressure Traces @ 2000 rpm, RBEI .....	5
Figure 3.1 – Engine Set-up .....	12
Figure 3.2 – Test Cell Set–up & Measurement Locations .....	13
Figure 3.3 – Test Cell GDI System Measurement Locations.....	14
Figure 3.4 – Indolene Baseline Data @ 2000 rpm .....	18
Figure 3.5 - Indolene Baseline Data @ 2000 rpm (2).....	19
Figure 3.6 – Indolene Baseline Data @ 3000 rpm .....	20
Figure 3.7 - Indolene Baseline Data @ 3000 rpm (2).....	21
Figure 3.8 – Indolene Baseline Data @ 1000 rpm .....	22
Figure 3.9 - Indolene Baseline Data @ 1000 rpm (2).....	23
Figure 4.1 - Phase II-a Results for 2000 rpm, RCEI.....	25
Figure 4.2 - Phase II-a Results for 2000 rpm, RCEI (2).....	26
Figure 4.3 - Phase II-a Results for 2000 rpm, RBEI .....	27
Figure 4.4 - Phase II-a Results for 2000 rpm, RBEI (2).....	28
Figure 4.5 - Phase II-a Results for 3000 rpm, RCEI.....	30
Figure 4.6 - Phase II-a Results for 3000 rpm, RCEI (2).....	31
Figure 4.7 - Phase II-a Results for 3000 rpm, RBEI .....	32
Figure 4.8 - Phase II-a Results for 3000 rpm, RBEI (2).....	33
Figure 4.9 - Phase II-a Results for 1000 rpm, RCEI.....	34
Figure 4.10 - Phase II-a Results for 1000 rpm, RCEI (2).....	35
Figure 4.11 - Phase II-a Results for 1000 rpm, RBEI .....	36
Figure 4.12 - Phase II-a Results for 1000 rpm, RBEI (2).....	37
Figure 4.13 - Phase II-b Results for 2000 rpm, RCEI .....	39
Figure 4.14 - Phase II-b Results for 2000 rpm, RCEI (2).....	40
Figure 4.15 - Phase II-b Results for 2000 rpm, RBEI .....	41
Figure 4.16 - Phase II-b Results for 2000 rpm, RBEI (2).....	42
Figure 4.17 - Phase II-b Results for 3000 rpm, RCEI .....	43
Figure 4.18 - Phase II-b Results for 3000 rpm, RCEI (2).....	44
Figure 4.19 - Phase II-b Results for 3000 rpm, RBEI .....	45
Figure 4.20 - Phase II-b Results for 3000 rpm, RBEI (2).....	46
Figure 4.21 - Phase II-b Results for 1000 rpm, RCEI .....	47
Figure 4.22 - Phase II-b Results for 1000 rpm, RCEI (2).....	48
Figure 4.23 - Phase II-b Results for 1000 rpm, RBEI .....	49
Figure 4.24 - Phase II-b Results for 1000 rpm, RBEI (2).....	50

---

### CUSTOMER CONFIDENTIAL



Figure 5.1 - Pairwise Fuel Properties for Phase I and Phase II.....	61
Figure 5.2 - Pairwise Fuel Properties for Phase I and Phase II (2) .....	62
Figure 5.3 - Pairwise Fuel Properties for Phase I and Phase II (3) .....	63
Figure 5.4 - Pairwise Fuel Properties for Phase I and Phase II (4) .....	64
Figure 5.5 - Pairwise Fuel Properties for Phase I and Phase II (5) .....	65
Figure 5.6 - Pairwise Fuel Properties for Phase I and Phase II (6) .....	66
Figure 5.7 - Relationship between Ethanol Content and ISFC.....	72
Figure 5.8 - Contour Plots of Modeled ISFC .....	73
Figure 5.9 - Relationship between Ethanol Content and ITE.....	75
Figure 5.10 - Contour Plots of Modeled ITE .....	76
Figure 5.11 - Relationship between Ethanol Content and ISNO <sub>x</sub> .....	78
Figure 5.12 - Contour Plots of Modeled ISNO <sub>x</sub> .....	79
Figure 5.13 - Relationship between Ethanol Content and ISHC.....	81
Figure 5.14 - Relationship between Ethanol Content and ISCO .....	83
Figure 5.15 - Contour Plots of Modeled ISCO.....	84
Figure 5.16 - Contour Plots of Modeled IS_SMK .....	86
Figure 5.17 - Relationship between Ethanol Content and Combustion Duration.....	88
Figure 5.18 - Relationship between Ethanol Content and COV of IMEP .....	90
Figure 5.19 - Contour Plots of Modeled COV of IMEP .....	91
Figure 5.20 - Relationship between Ethanol Content and Noise .....	92
Figure 5.21 - Relationship between Ethanol Content and Peak Cylinder Pressure.....	94
Figure 5.22 - Relationship between Ethanol Content and EVC.....	96
Figure 5.23 - Relationship between Ethanol Content and IMEP .....	97
Figure 5.24 - Relationship between Ethanol Content and MRPR.....	98



# 1. Introduction

## 1.1. Background

The use of homogeneous charge compression ignition (HCCI) combustion in internal combustion engines is of interest because it has the potential to produce low  $\text{NO}_x$  and low particulate matter emissions while providing diesel-like efficiency. In HCCI combustion, a premixed charge of fuel and air auto-ignites at multiple points in the cylinder near top dead center, resulting in rapid combustion with very little flame propagation. Since ignition occurs in an HCCI engine by auto-ignition of the fuel/air mixture, the choice of fuel will have a significant impact on both engine design and control strategies. The start of ignition depends on the temperature, pressure, and concentration history during the compression stroke, and the unique reaction kinetics of the fuel/air mixture. To control the temperature, pressure, and concentration of fuel/air mixture, different dilution strategies, valve timings, and injection schemes are proposed for HCCI engines.

AVL conducted HCCI single cylinder testing for CRC in which 10 fuels with various fuel properties were studied. Although this study, referred to as AVFL-13, provided no definitive associations between fuel properties and HCCI engine performance, four main statistical conclusions were made [1]:

- At the mid-load and high-speed condition, specific fuel consumption (SFC) performance appeared statistically related to fuel aromatic and iso-paraffin content. Best SFC was associated with fuels having low aromatic and iso-paraffin content. Increases in either fuel property were associated with decreased SFC performance.
- At the mid-load and high-speed condition,  $\text{NO}_x$  emissions appeared statistically related to n-paraffin content (excluding butane) and the temperature at which 10 percent of the fuel distills. Lowest  $\text{NO}_x$  was associated with fuels having low n-paraffins and high T10. Though not completely consistent, increases in n-paraffins were generally associated with lower  $\text{NO}_x$  and increases in T10 with higher  $\text{NO}_x$ .
- At idle, CO emissions appeared statistically related to fuel aromatic and iso-paraffin content. Lowest CO was associated with fuels having high aromatics and low iso-paraffins. Increases in either fuel parameter were associated with decreased CO emission levels.
- At all speed and mode conditions, smoke appeared statistically related to aromatic content and RON. Lowest smoke was associated with low aromatics and RON of at least 75.

---

### CUSTOMER CONFIDENTIAL



At the conclusion of this study, which will hereafter be referred to as Phase I, AVL recommended that future testing be conducted with various blends of ethanol.

## 1.2. Project Objectives

In this second phase of the project, AVFL-13B, gasoline-like test fuels with varying percentages of ethanol are tested in an AVL single cylinder engine equipped with a hydraulic variable valve train (VVT) and gasoline direct injection (GDI) system. By using VVT and GDI, two different intake charge preparation modes are implemented: re-compression early injection (RCEI) and re-breathing early injection (RBEI). For each intake charge preparation mode, three engine operating conditions are investigated:

- 1.5 bar IMEP at 1000 rpm
- 3 bar IMEP at 2000 rpm
- 5.5 bar/degCA of maximum rate of pressure rise (MRPR) at 3000 rpm

For all engine operating conditions and intake charge preparation modes, the combustion phasing, represented by the 50% mass fraction burned location (MFB50), are fixed at 5 degrees after top dead center (ATDC).

This report will focus on the effect of ethanol on engine performance. The statistical effect of the volumetric ethanol content of each fuel is determined separately from the other fuel component effects. The impacts of the remaining fuel components on HCCI combustion are quantified by a multiple regression method [2, 3], in which two out of nine independent fuel properties are correlated with combustion or emission related parameters. The results of all phases of testing are included in this analysis.



## 2. Technical Methodology

### 2.1. Description of Test Plan

The start of combustion in HCCI engines is controlled by chemical kinetics, which is subjected to the intake charge temperature and pressure histories [4]. In general, the intake charge temperature and pressure are controlled by the fuel injection, external exhaust gas re-circulation (EGR) and internal residual gas for naturally aspirated engines.

Several researchers have implemented HCCI combustion successfully with port fuel injection (PFI) [5, 6]. PFI offers good fuel/air mixing; however, there is no control of the combustion phasing. Marriott et al [7] demonstrated that the combustion phasing can be controlled by the injection timing in a direct injection engine. By sweeping the injection timing from early in the intake stroke to late in the compression stroke, optimum combustion phasing over a range of intake air temperature, engine loads, and speeds was obtained.

In HCCI engines, combustion happens spontaneously leading to high energy release rates and combustion noise. It is very important to dilute the intake charge to lower the combustion rate to protect the engine. EGR is a major method used to dilute the charge [8-10]. The higher heat capacity of the exhaust gas can cause a reduction of the end-of-compression charge temperature, which would tend to retard the auto-ignition.

With a variable valve train, two major strategies were employed to obtain the residual gas to dilute the intake charge: re-compression and re-breathing. In the re-compression mode, the exhaust valves are closed early in the exhaust stroke, before exhaust TDC, to trap residual gas within the cylinder [11, 12]. In the re-breathing mode, the exhaust gas re-enters the cylinder after leaving the engine through reopening the exhaust valve during the intake stroke, which is also called internal EGR [13, 14].

In this report, both re-compression and re-breathing modes were investigated with a fully variable valve train and direct injection system. For each intake charge preparation mode, three engine speeds/loads were investigated at the fixed combustion phasing, represented by 50% mass fraction burned location (MFB50) at 5 degrees after top dead center (ATDC).

#### 2.1.1. Intake Charge Preparation

Two different intake charge preparation modes were tested in this study. The first mode is re-compression early injection (RCEI) mode, which employs early exhaust valve closing (EVC) resulting in residual burnt gas being trapped in the cylinder and re-compressed plus early fuel injection to provide a homogeneous fuel/air mixture.

The second mode is re-breathing early injection (RBEI) mode, in which the exhaust valve remains open longer than during the first mode, trapping less residual gas, and re-opens during the intake stroke to induce burnt gas into the cylinder from exhaust port. In both modes, there is only one early fuel injection event to provide a homogeneous fuel/air mixture.

The injection timings and valve timings for the two intake charge preparation modes are shown in Figure 2.1 and Figure 2.2 along with the measured cylinder pressure. The optimization of the valve timings and injection timings will be discussed later.

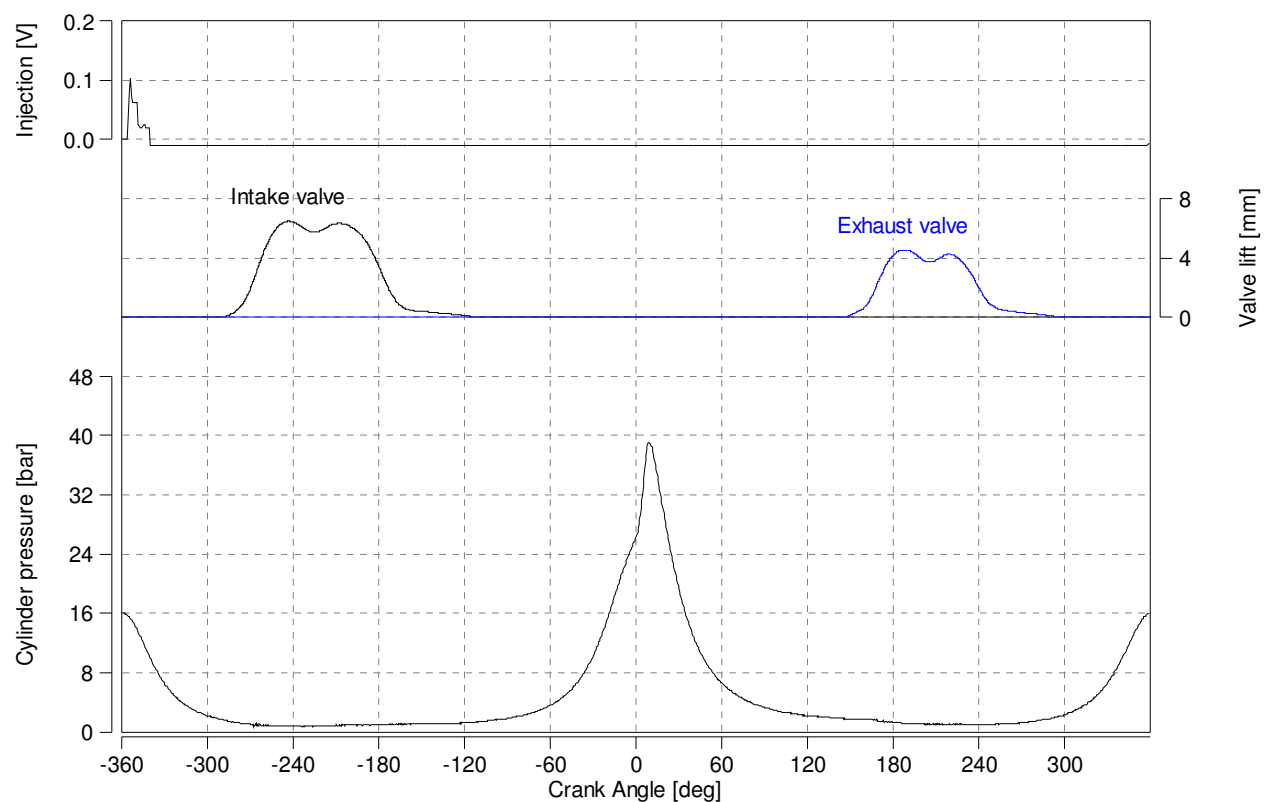


**Figure 2.1 – Injection, Valve & Cylinder Pressure Traces @ 2000 rpm, RCEI**

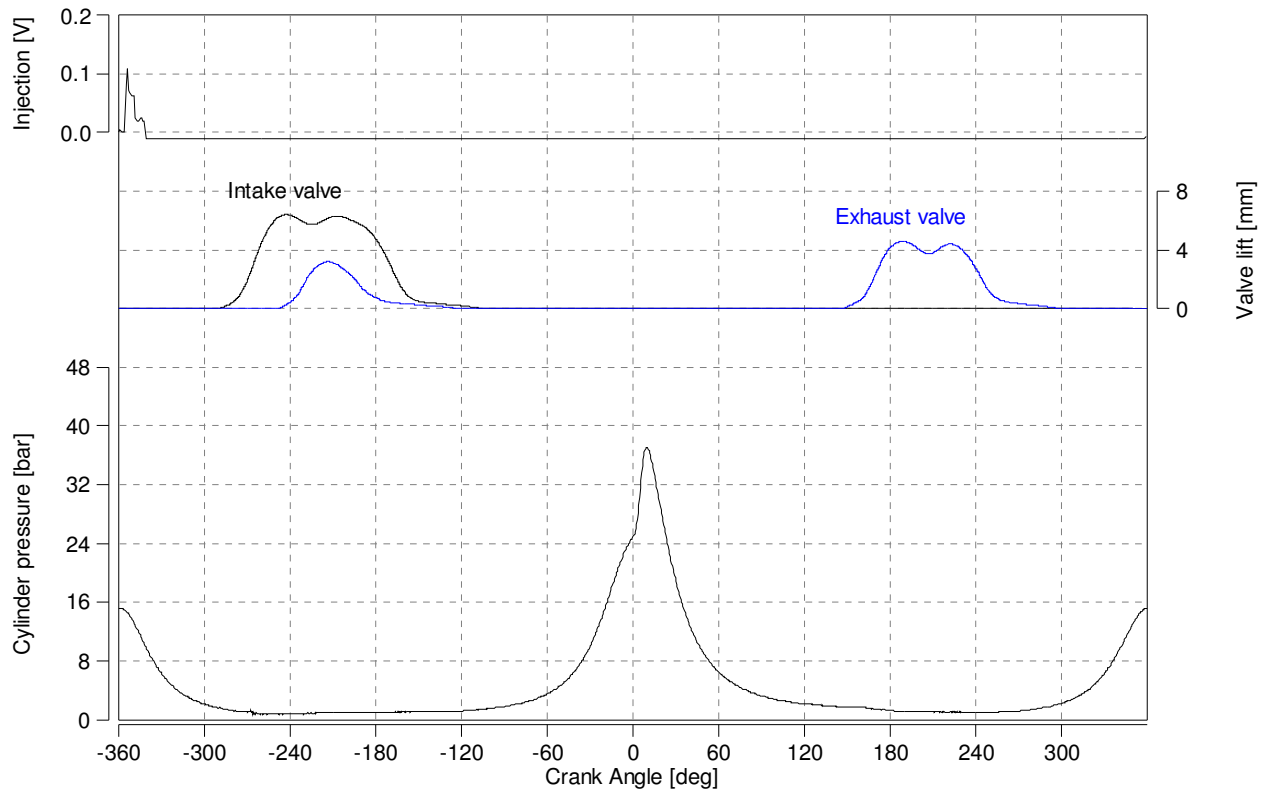


**Figure 2.2 – Injection, Valve & Cylinder Pressure Traces @ 2000 rpm, RBEI**

### 2.1.2. Engine operating conditions

Three engine operating points were investigated in this study, which are shown in Table 2.1. These three operating conditions represent, respectively: near-idle conditions, mid-speed HCCI conditions, and high-speed HCCI conditions. At higher engine speeds and loads, it is anticipated that an HCCI engine will switch to normal closed-loop spark-ignition operation.

**Table 2.1 – Engine Operating Points**

	Idle	Mid-Speed	High Speed
Speed [rpm]	1000	2000	3000
IMEP [bar]	1.5	3.0	N/A
CA50 [° ATDC]	5.0	5.0	5.0
MRPR [bar/deg]	N/A	N/A	5.5
IAT (°C)	100	25	25

For all three engine operating conditions, the combustion phasing was fixed, represented by 50% mass fraction burned location (MFB50), at 5 degrees ATDC. At 1000 rpm and 2000 rpm, the engine loads were controlled by IMEP. At 3000 rpm, the engine load was controlled by the maximum rate of pressure rise (MRPR).



## 2.2. Fuel Parameter Matrix

Fuel chemistry, especially normal paraffins, ratios of iso-paraffins to aromatics and olefins as octane components, affects both the octane ratings and octane sensitivity of blended fuels. Paraffins, especially normal paraffins, possess a unique low-temperature chemistry which can lead to knock in spark-ignited engines and can assist ignition in HCCI engines. Aromatics and many olefins do not possess this low temperature chemistry, are often rated conservatively in octane tests, and can inhibit knock in spark ignited engines to a greater extent than their octane numbers suggest. In HCCI, the goal is to enhance the pre-flame reactions of the fuel in order to ensure ignition, while allowing control of combustion phasing and rate of burning over a wide range of speeds and loads.

The relationship of these HCCI characteristics to fuel chemistry and measured octane ratings is not well understood and is also operating condition and engine design dependent. Fuels exhibiting high octane sensitivity (aromatic or olefin derived) are expected to behave differently than fuels with low octane sensitivity (paraffin derived). Refineries today are optimized to produce high octane components for spark ignited gasoline (aromatic, iso-paraffin, olefin) while minimizing low octane components (normal paraffin). Fuel volatility in the normal range for gasoline is not expected to affect HCCI mixing, although large changes in volatility such as between gasoline and distillate fuels would be expected to have an effect.

### 2.2.1. Fuel Chemistry

Based on a review of relevant literature and Oak Ridge National Laboratory (ORNL) fuels testing expertise, it is expected that HCCI combustion in a gasoline engine will be affected by fuel research octane number (RON), fuel motor octane number (MON), their average  $(R+M)/2$ , their difference  $(R-M)$ , boiling point distribution, and fuel chemistry.

Octane number is known to affect knock and pre-ignition in conventional spark ignited engines and is a basic specification for the production control of commercial gasoline. RON and MON are measured under different conditions and correlate to different types of engine operation. It is common to refer to an averaged octane number  $((R+M)/2)$  and an octane sensitivity number  $(R-M)$ . The main way of varying octane numbers and their relationship is to vary fuel chemistry.

Fuel volatility controls fuel evaporation and mixing and in conventional gasoline is varied seasonally to aid cold starting (high volatility desired) in cold weather and to prevent HC evaporative emissions and vapor lock in hot weather (low volatility desired). Volatility is controlled by a combination of the fuel boiling point distribution (T10, T50, and T90), Reid vapor pressure (RVP), and Vapor/Liquid (V/L) ratio. The boiling point distribution describes the complete fuel with minor emphasis on the high volatility components and the RVP and V/L ratio describe the highly volatile front end of the fuel in more detail. In this project, RVP was adjusted to 7 psi with the addition of n-butane for every fuel as a

---

#### CUSTOMER CONFIDENTIAL



safety precaution to ensure that an explosive mixture would not occur in the vapor space. This measure also eliminated volatility as an independent variable. However, as ethanol is blended into each base fuel, the RVP will increase accordingly. For this reason, the effect of the volumetric ethanol content of the fuel on engine performance will be analyzed separately from the other fuel composition effects.

Gasoline is composed of hydrocarbon molecules such as paraffins (normal paraffin, iso-paraffin, or cyclo-paraffin), aromatics, olefins, and oxygenated compounds such as alcohols or ethers. Fuel chemistry is not restricted except in emissions non-attainment areas, and refineries are allowed to blend as desired to maximize gasoline yield while meeting other performance specifications such as octane and volatility requirements. Other gasoline quality standards include corrosion, gum, and oxidation stability.

It is the desire of this project to correlate engine performance variables to fuel variables, both fuel properties and fuel chemistry. Table 2.2 lists the recommended properties and fuel chemistry for this study.

**Table 2.2 – Fuel Properties used for Analysis**

1	API
2	Research octane number (RON)
3	Motor octane number (MON)
4	Averaged octane number (R+M)/2
5	Sensitivity (R-M)
6	T10
7	T50
8	T90
9	% Aromatics
10	% Olefins
11	% N-paraffins
12	% Iso-paraffins
13	% All paraffins
14	% Naphthenes

### 2.2.2. Fuel Candidates

In Phase I of this project, ten fuels were blended and evaluated. A complex analysis process was used for the selection of these fuels and is described by Dr. Yuan Shen [1]. Phase II looked at one additional fuel representing intermediate chemical properties. However, the primary goal of Phase II was to examine the effects of ethanol. Therefore, based on the results of Phase I, some of the fuels were selected to be blended with varying amounts of ethanol. Phase II testing was performed in two batches which will hereafter be referred to as Phase II-a and Phase II-b. The final fuel matrix for all phases is listed in Table 2.3.

---

#### **CUSTOMER CONFIDENTIAL**



The eleven gasoline-like base test fuels were blended from four common refinery streams normally used to blend commercial gasoline: (A) reformat [about 50% aromatic], (B) alkylate [about 100% iso-paraffin], (C) cat cracker gasoline [about 45% olefin], and (D) straight run gasoline [about 100% normal paraffin] (n-paraffin). Although there are other refinery streams available for gasoline blending, the four streams selected reflect the most commonly used blend stocks in finished gasoline. The only other blending component used in the test fuels was normal butane (n-C4). Normal butane was added to bring each test fuel up to a consistent, nominal 7 psi vapor pressure. This was done as a safety precaution since some of the blends had an RVP so low that there was a concern that an explosive mixture could occur in the vapor space when using the fuels.

**Table 2.3 – Fuel Test Matrix**

	Fuel Name	Fuel Blend by Volume Percent					Total%
		A%	B%	C%	D%	EtOH%	
Phase I	A100	100.0					100.0
	B100		100.0				100.0
	C100			100.0			100.0
	B50D50		50.0		50.0		100.0
	C85D15			85.0	15.0		100.0
	B77D23		77.0		23.0		100.0
	B30D70		30.0		70.0		100.0
	A79D21	79.0			21.0		100.0
	C50D50			50.0	50.0		100.0
A33D67	33.0			67.0		100.0	
Phase II-a	C100			100.0			100.0
	C100E20			80.0		20.0	100.0
	A79D21	79.0			21.0		100.0
	A79D21E10	71.1			18.9	10.0	100.0
	A79D21E20	63.2			16.8	20.0	100.0
	A79D21E30	55.3			14.7	30.0	100.0
	A50C20D30	50.0		20.0	30.0		100.0
Phase II-b	C50D50			50.0	50.0		100.0
	C50D50E15			42.5	42.5	15.0	100.0
	C50D50E30			35.0	35.0	30.0	100.0
	B100		100.0				100.0
	B100E15		85.0			15.0	100.0
	B100E30		70.0			30.0	100.0
	B77D23		77.0		23.0		100.0
	B77D23E15		65.5		19.6	15.0	100.0
B77D23E30		53.9		16.1	30.0	100.0	

**CUSTOMER CONFIDENTIAL**



The target recipes for blending these four refinery streams to produce the eleven test fuels were determined by first using a proprietary blending model to generate a set of 56 potential test fuels where the research octane quality was set at or near three levels (92, 65 to 70, and a mid level), and the composition (aromatics, olefins, n-paraffins, and iso-paraffins) and distillation temperatures were varied over as large a range as possible. The final eleven blending recipes were then selected using an experimental-design statistical procedure that maximized the spread in fuel parameters (octane, composition, and distillation) while minimizing fuels with similar properties and statistically representing all fuel candidates. The nine fuel parameters used in the statistical analysis were:

- RON
- Sensitivity
- T10
- T90
- % Aromatics
- % Iso-paraffins
- % N-paraffins without butane
- % Butane
- % Olefins

The remaining fuel properties were excluded from the experimental design because they were highly correlated to the selected properties. The effects of the ethanol content of the fuel, designated by the letter “E” in Table 2.3, were analyzed separately.

### 2.3. Analysis Techniques

The engine parameters of interest in this study include:

- ISFC (g/kWh)
- ITE (%)
- ISNO<sub>x</sub> (g/kWh)
- ISHC (g/kWh)
- ISCO (g/kWh)
- Smoke (FSN)
- Combustion duration (degCA)
- Combustion noise (dB)
- COV of IMEP (%)
- Peak cylinder pressure (Bar)

Baseline repeatability tests were performed with indolene fuel during all project phases in order to measure test-to-test variability correlated with engine operating parameters which were measured but could not be precisely controlled. To account for variations in



operating conditions, a backward, step-wise multiple regression analysis was performed on the indolene data to develop normalization models to adjust each relevant engine parameter for every test fuel prior to further data analysis. This normalization procedure was found to reduce the overall variability in the test-fuel data. This procedure assumes that the test fuel response to minor changes in engine operating conditions is the same as is indolene response.

It was desired to perform a statistical analysis for each of the ten engine performance parameters listed previously as a function of the nine fuel parameters, excluding ethanol content, for each of the six engine test conditions (1000 rpm, 2000 rpm, and 3000 rpm each tested at the two HCCI modes: RCEI and RBEI) examined. Because of the limited number of test fuels (10) compared to the number of fuel parameters of interest (9), it was not feasible to construct a statistical model to estimate the effects of all nine fuel properties and their interactions on each performance measure. Instead, regression models were fit to all possible combinations of two fuel properties and their interaction. Separate models were fit for each of the six combinations of engine speed and mode. This approach uses four degrees of freedom for estimating model parameters and leaves six for estimating the error variances.

The model results were reviewed to identify the “best” model. The first step in this process was to identify only models with an overall F-Test p-value of 0.1 or less. These may be considered potentially explanatory of the observed variability in the performance parameter. Then these models within each speed and mode condition were ranked from lowest to highest  $R^2$  value and the two-factor model with the highest sum of ranks across the nine speed and mode conditions was identified as “best”. This method placed strong weight on a two-factor model that was both highly explanatory of observed variability (i.e., high  $R^2$ ) and consistently explanatory across all speeds and modes (i.e., high sum of ranks).

This analysis procedure was performed by Battelle, a subcontracted organization, for each phase of the project. The results of the Phase I analysis as well as a detailed description of the analysis technique used can be found in the preceding paper by Dr. Yuan Shen [1]. This paper focuses on the results of Phase II which were analyzed inclusively with the Phase I results. Further explanation of the analysis used for this phase of testing are included with the statistical results in Section 5 of this paper.

### 3. Experimental Set-up

#### 3.1. Test Engine Specifications

The engine used for all phases of this study is a single-cylinder research engine equipped with a hydraulic variable valve train and gasoline direct injection system. The geometric parameters of the engine are shown in Table 3.1.

**Table 3.1 – Engine Specifications**

Bore [mm]	90.2
Stroke [mm]	90.0
Displacement [l]	0.575
Compression Ratio	11.3
Valve Arrangement	2 Intake / 1 Exhaust
Valve Timing/Lift	Fully Variable
Fuel Injection System	GDI

The engine has two inlet ports, a tangential swirl port and a neutral filling port. The ports are designed to give a torque meter swirl ratio of 2.6 with only the tangential swirl port valve open and 0.1 with both valves open [15]. In this study, only the swirl valve was used to enhance swirl and improve combustion control. Swirl motion of the intake air helps the mixing of fuel and air at the beginning of the intake stroke, and then the mixing process stabilizes during the compression stroke. Near the end of the compression stroke, stabilized motion of the intake charge leads to lower maximum rate of cylinder pressure rise and combustion noise [16, 17]. For all experiments there was no intake-manifold throttling. The engine was run using lean air-fuel conditions and fuel pulse width was used to control the engine load.

A Sturman fully variable hydraulic valve actuation (HVA) system is used on the engine to control valve timings and lifts. It utilizes hydraulic force controlled by high-speed digital latching valves, in place of traditional mechanical camshafts, to actuate engine intake and exhaust valves. Fully variable lift, duration, and timing are independently controlled for all three engine valves [15].

A Bosch HDEV gasoline direct injector was mounted between the two intake valves in the cylinder head. The injector was controlled by a Bosch Injector Power Stage ES-HDEV1, which enables multiple injection events in a single engine cycle. Based on a previous study, the fuel rail pressure was set to 60 bar to help maintain stable combustion. This pressure was only reduced at lower engine speeds due to the minimum injection pulse width limit.

The engine is equipped with a centrally located spark plug. The spark plug is utilized to start the engine in spark-ignited mode, then transition to HCCI mode. Figure 3.1 is a picture of the engine setup in the test cell.

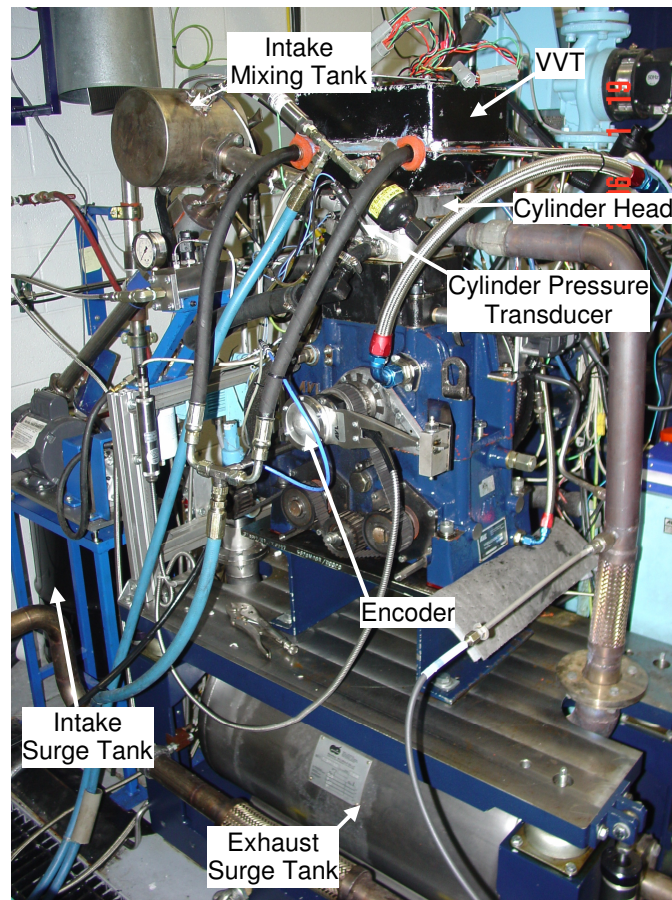


**Figure 3.1 – Engine Set-up**

### 3.2. Test Cell Configuration

AVL PUMA was installed in the single-cylinder engine test cell for dynamometer control and low speed data acquisition. In general, low speed data include temperatures, pressures, voltages, and currents. Sampling locations for each of these parameters are included in Figure 3.2 and Figure 3.3. A list of the measured parameters can be found in Appendix B.

For high speed data acquisition, the AVL Indimeter 619 was employed. The AVL Indimeter 619 is a device with 8 channels capable of 1 MHz data acquisition rates. The test cell was equipped with AVL IndiWin software which works with Indimeter 619 for high-speed real-time data analysis. All combustion related parameters, such as indicated mean effective pressure (IMEP) and crank angle of 50% mass fraction burnt (MFB50), were calculated by the software based on measured cylinder pressure, calculated volume and crank position. For this project, data was recorded every 0.5 crank angle degree.

1 Cell 3 SCE

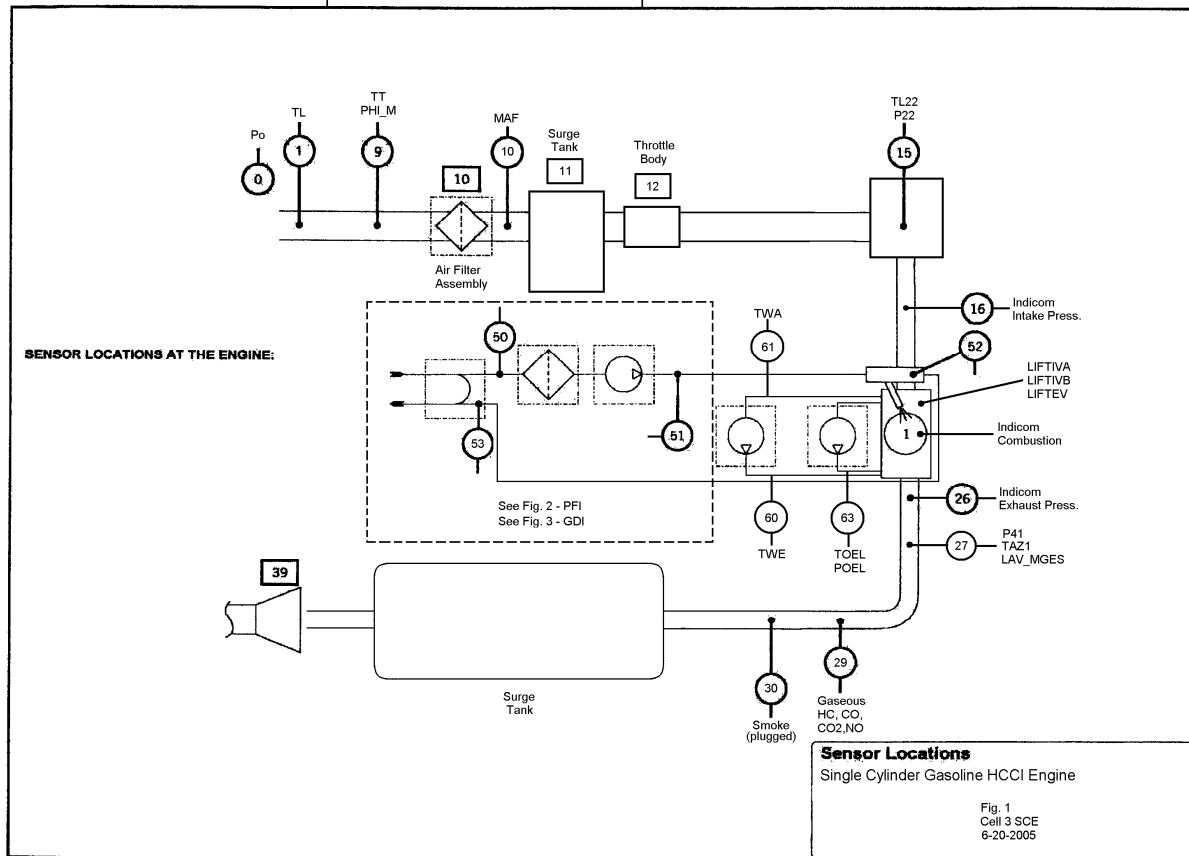
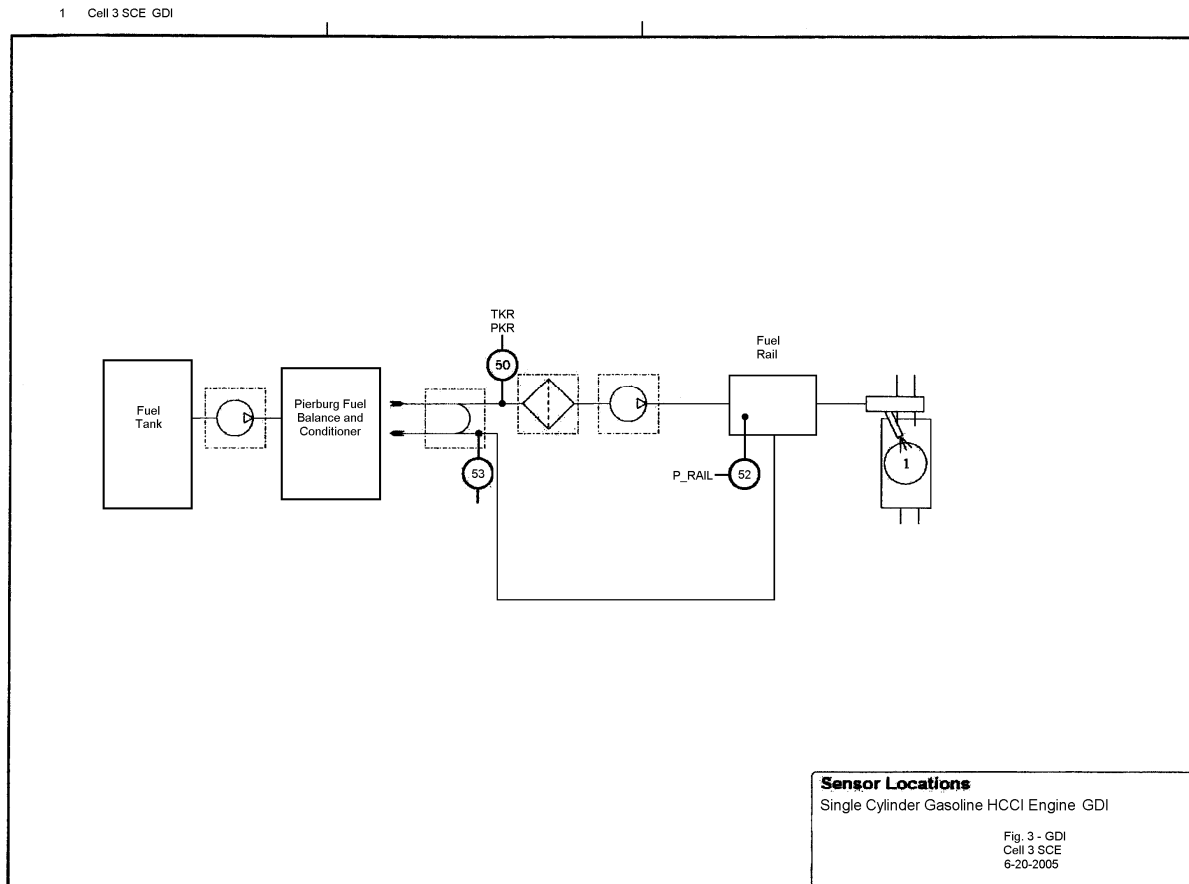


Figure 3.2 – Test Cell Set-up & Measurement Locations

An AVL CEB II raw emission bench was installed in the test cell for emission measurement. The device performs continuous measurement of HC, CO, CO<sub>2</sub>, O<sub>2</sub>, and NO<sub>x</sub>. The test cell was also equipped with an AVL Smoke Meter 415S for smoke measurement. A filtered smoke number (FSN) was reported to PUMA after each measurement, which was converted to the soot flow rate based on an empirical formula. In general, smoke emission is not a major concern for gasoline fuel based HCCI engines. However, smoke generation is of interest for gasoline direct injection combustion, especially where there are dual injections.



**Figure 3.3 – Test Cell GDI System Measurement Locations**

### 3.3. Test Procedures

During Phase II-a, seven fuels were tested from December, 2006 until May, 2007. Three indolene baseline tests were completed during this time as well. The order of testing for Phase II-a is shown in Table 3.2. During Phase II-b, nine additional fuels were tested from November, 2008 until December, 2008. Four indolene baseline tests were also completed during this time. The order of testing for Phase II-b is shown in Table 3.3.

For each fuel tested, three operating points were tested using two different intake charge preparation methods. In general, the testing was performed in the order shown in Table 3.4. Each measurement taken in the test cell represents a time average over a period of steady state operation. During Phase I and Phase II-a, a minimum of five 30-second measurements were taken for each of the six operating conditions. During Phase II-b, three 60-second measurements were taken. In both cases the measurements were averaged together for reporting purposes.

#### CUSTOMER CONFIDENTIAL



**Table 3.2 – Fuel Test Order for Phase II-a**

1	A79D21E30
2	Indolene 1
3	A79D21E20
4	A79D21
5	A79D21E10
6	Indolene 2
7	C100
8	C100E20
9	A50C20D30
10	Indolene 3

**Table 3.3 – Fuel Test Order for Phase II-b**

1	Indolene 1
2	C50D50
3	C50D50E15
4	C50D50E30
5	Indolene 2
6	B100
7	B100E15
8	B100E30
9	Indolene 3
10	B77D23
11	B77D23E15
12	B77D23E30
13	Indolene 4

**Table 3.4 – Operating Point Test Order for Each Fuel**

Run #	Engine Speed	Mode
1	2000 rpm	RCEI
2	2000 rpm	RBEI
3	3000 rpm	RCEI
4	3000 rpm	RBEI
5	1000 rpm	RCEI
6	1000 rpm	RBEI

Approximate valve and injection timings for each operating point and mode were predetermined during Phase I. These were optimized for indolene and all indolene baseline points were performed with a fixed set of timings as shown in Table 3.5. Exhaust valve closing (EVC) and injection pulse width (IPW) were the only variables adjusted to obtain the specified IMEP and combustion phasing. However, for the other fuels tested in Phase I and Phase II-a, the operator was allowed more freedom to adjust the valve and injection timings to obtain the target operating conditions. This resulted in variability in the data which was normalized using Battelle’s statistical analysis.



**Table 3.5 – Indolene Baseline Valve and Injection Timings**

Parameter	Unit	1000 rpm		2000 rpm		3000 rpm	
		RBEI	RCEI	RBEI	RCEI	RBEI	RCEI
Intake Valve Open	°BTDC	240	240	268	268	270	276
Intake Valve Close	°BTDC	164	164	160	168	160	164
Intake Valve Lift	mm	30	30	60	60	70	70
Exhaust Valve Open	°ATDC	164	164	166	166	176	178
Exhaust Valve Close	°ATDC	varies	varies	varies	varies	varies	varies
Exhaust Valve Lift	mm	2.0	2.0	4.0	4.0	5.0	5.0
Exhaust Valve Open B	°BTDC	220	0	230	0	270	0
Exhaust Valve Close B	°BTDC	180	0	180	0	170	0
Exhaust Valve Lift B	mm	1.0	0.0	2.0	0.0	2.5	0.0
Injection Angle	°BTDC	360	360	360	360	360	360
Injection Pulse Width	µs	varies	varies	varies	varies	varies	varies

During Phase II-b fuel testing, a concentrated effort was made to reduce variability in the data. For the fuels tested in Phase II-b, the valve and injection timings were fixed to the same values used for the indolene baseline tests. In addition, tolerances were specified for each targeted operating condition to help further reduce variability in the data. The target IMEP was held to a tolerance of  $\pm 0.5$  bar and the target 50% mass fraction burned location was held to a tolerance of  $\pm 1.0$  degCA. Similarly, the target MRPR was held to a tolerance of  $\pm 1.0$  bar/degCA for the 3000 rpm operating point. As stated previously, only the EVC and IPW were adjusted to obtain these targets.

The exhaust valve timing indirectly controls mass air flow and subsequently affects air-fuel ratio. HCCI operation typically requires lean operation of the engine in order to maintain low emissions. Rich operation causes a dramatic increase in carbon monoxide and hydrocarbons. Therefore, at higher engine loads, when the engine tends to run richer, air-fuel ratio was limited such that it was never less than stoichiometric.

Exhaust back pressure also has a significant effect on HCCI combustion. The amount of residual gas maintained in the cylinder at the point of exhaust valve closing will depend heavily on this parameter. Exhaust pressure was controlled using a manually adjustable valve inside the test cell. This valve was adjusted to target a relative exhaust back pressure of 40 mbar at 2000 rpm, 3.0 bar IMEP.

### 3.4. Fuel Specification

Two different batches of indolene were used for baseline testing during Phase II. The first batch was used for all baseline testing in Phase II-a and the first baseline test performed in Phase II-b. The second batch of indolene was used for the remaining three baseline tests. Analyses of both batches of indolene are contained in Appendix C along with the analyses of all fuels tested. The values for the Phase II test fuels are an average of the values measured at ConocoPhillips and Chevron laboratories. The analyses of the Phase I fuels are included for reference.

---

#### CUSTOMER CONFIDENTIAL



### 3.5. Data Quality

Several actions were taken to maintain data quality throughout the project. Engine leak-down was measured periodically and was maintained at a value less than 10%. In addition, motored-engine pressure traces were recorded at 3 engine speeds and 6 different valve timings. The peak cylinder pressure for each trace was maintained at +/- 1 bar. For each pressure trace, the valve events were also examined for consistency. This was done at the end of Phase II-a and before Phase II-b testing began. In addition, the motoring peak pressure was measured daily at 2000rpm before fuel testing commenced. Pressure trace data can be found in Appendix D. Other actions include daily emission bench calibration and daily fuel balance accuracy checks.

The indolene baseline tests also serve as a means of increasing the reliability of the data. By comparing the indolene tests over time, any trends relating to engine wear can be observed. In the case of an engine rebuild, differences in engine performance or emissions can be quantified and used to normalize the results of the other test fuels.

Figure 3.4 shows the indicated emissions and thermal efficiency results of the indolene baseline tests at 2000 rpm for Phase II-a and Phase II-b. An engine rebuild took place between these two phases and despite efforts to maintain the engine configuration, it caused a significant difference in engine performance. Indicated specific hydrocarbon (ISHC) emissions show a significant decrease between the two phases. The increase in indicated specific NO<sub>x</sub> (ISNO<sub>x</sub>) emissions from Phase II-a to Phase II-b indicate higher combustion temperatures. The decrease in indicated thermal efficiency (ITE) can be attributed to an associated increase in heat transfer to the cylinder walls. Overall, the increase in data repeatability reflects the efforts to minimize variability in Phase II-b.

The indolene baseline results for 3000 rpm can be found in Figure 3.6 and Figure 3.7. Again, lower ISHC emissions, higher ISNO<sub>x</sub> emissions and decreased ITE indicate higher combustion temperatures after the engine rebuild. The large increase in indicated specific CO (ISCO) emissions during the third RBEI indolene baseline test in Phase II-a is due to rich combustion. By limiting lambda to values of 1.0 or greater, variability in ISCO for Phase II-b was significantly reduced. However, an increase in ISCO emissions can still be seen because the last two points were relatively close to stoichiometric conditions.

Results for indolene baseline testing at 1000 rpm are shown in Figure 3.8 and Figure 3.9. Decreases in ISHC and ISCO emissions between the two phases again indicate more complete combustion caused by higher combustion temperatures. ISNO<sub>x</sub> emissions are near-zero and are therefore unaffected at this operating condition. Normally, a decrease in ISHC and ISCO would cause an associated increase in ITE. However, ITE is fairly constant, indicating that the increased heat transfer is counteracting this effect. Again, efforts to reduce data variability in Phase II-b seem to have a positive effect on data repeatability.

---

#### CUSTOMER CONFIDENTIAL

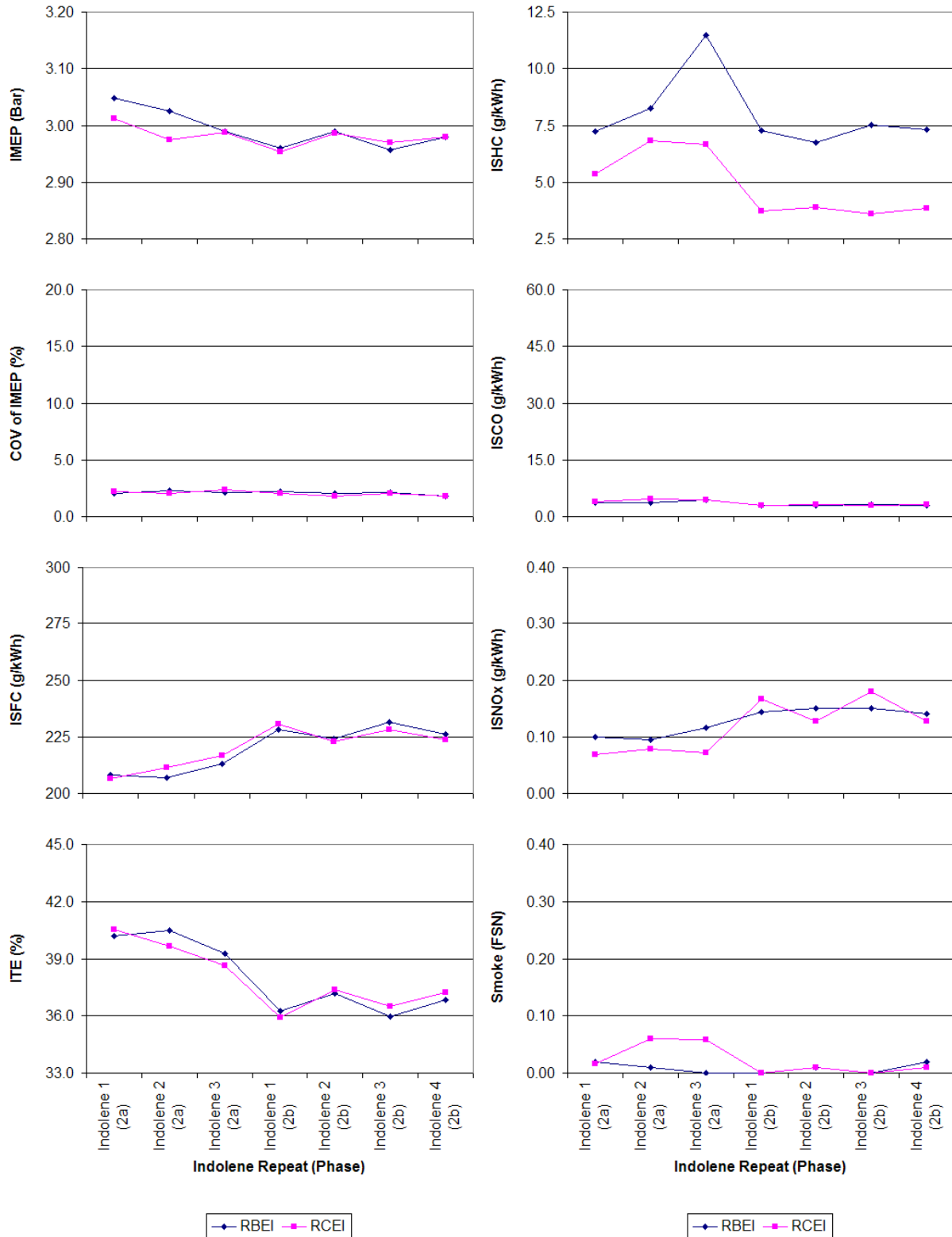


Figure 3.4 – Indolene Baseline Data @ 2000 rpm

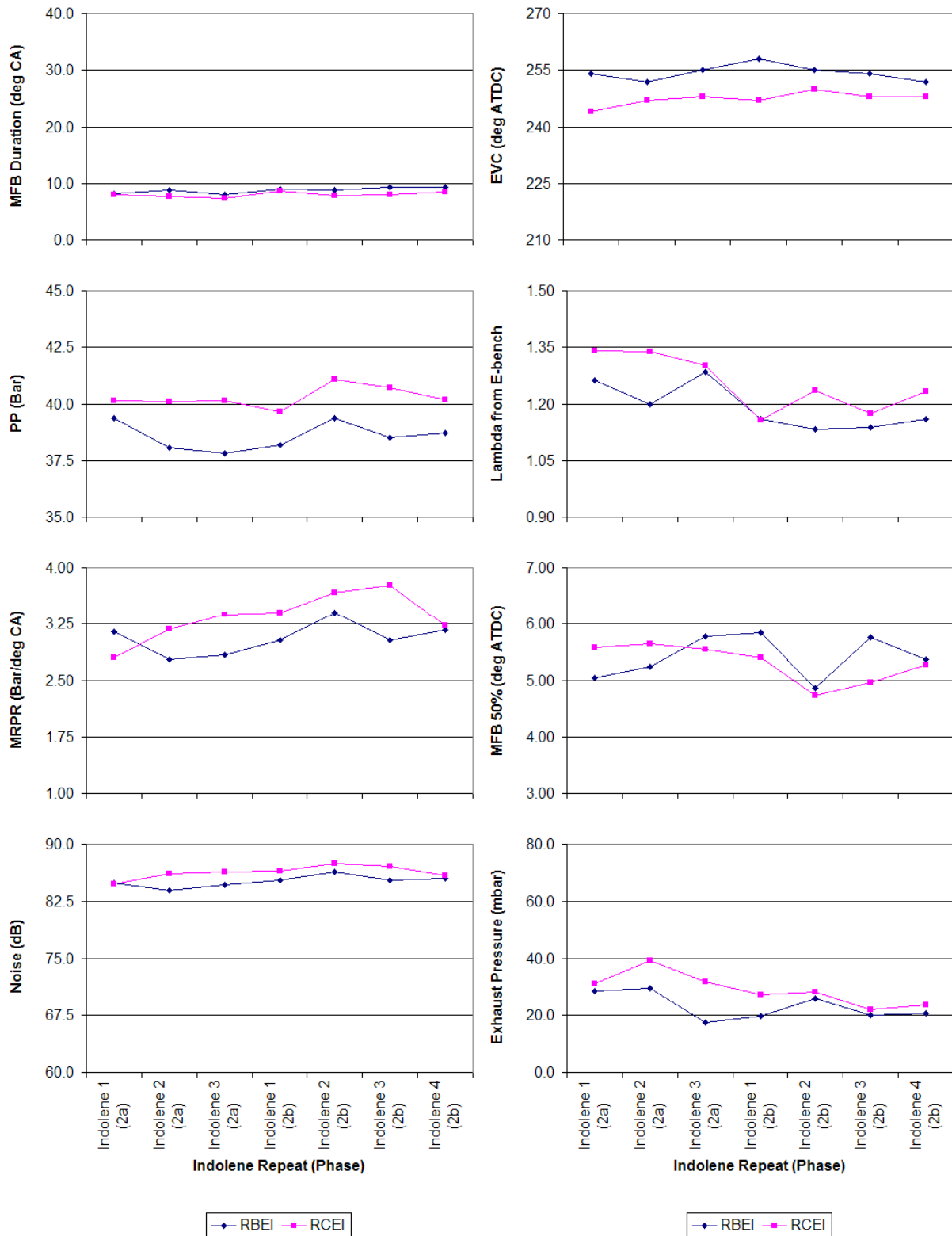


Figure 3.5 - Indolene Baseline Data @ 2000 rpm (2)

**CUSTOMER CONFIDENTIAL**

The electronic version is the only controlled copy.  
 All other copies are for reference only. Printed: 9/1/2009 4:09:13 PM  
 Page 19

CA4-prg-007 Technical Report  
 Originated: 01/01/04 Revised: 01/11/09

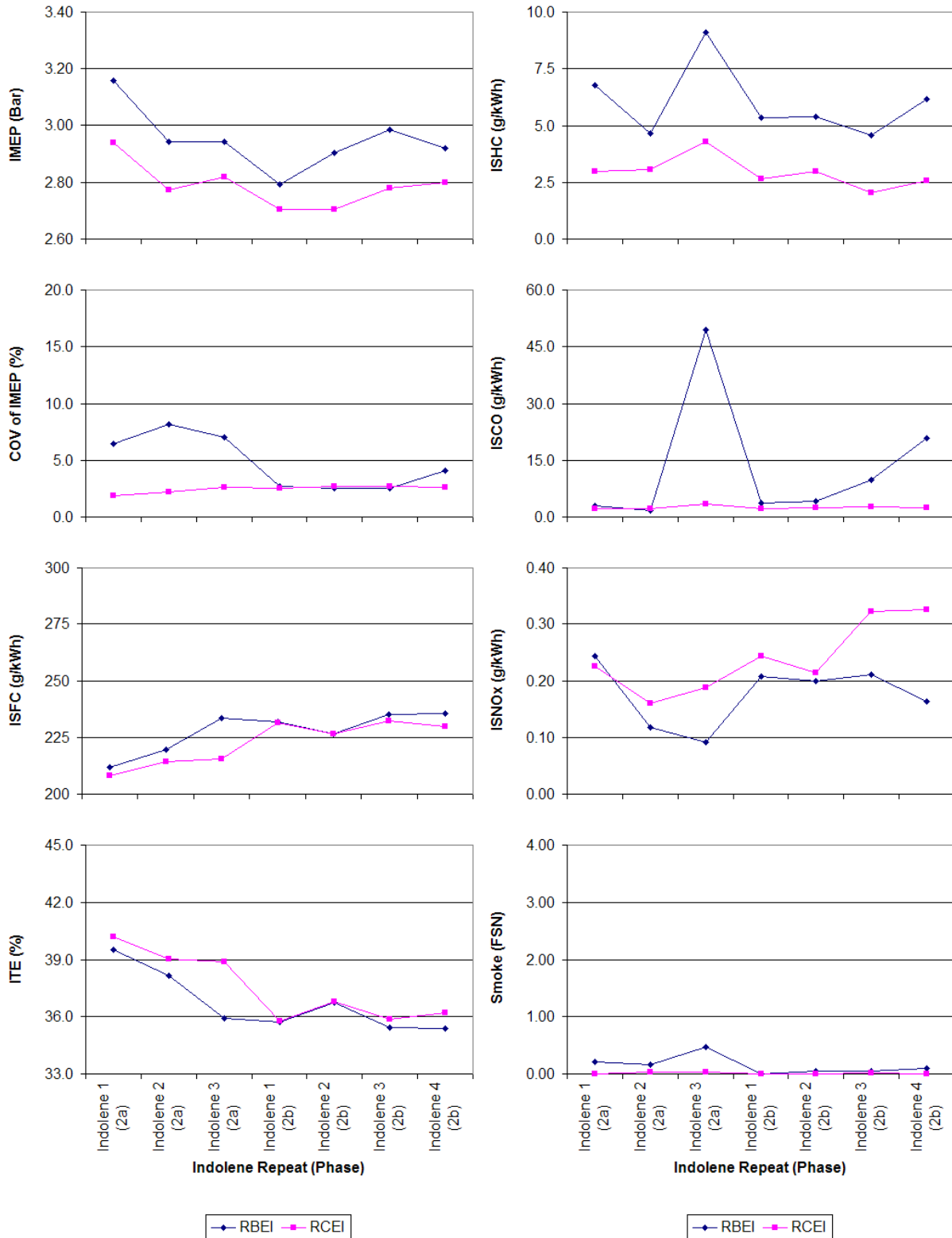


Figure 3.6 – Indolene Baseline Data @ 3000 rpm

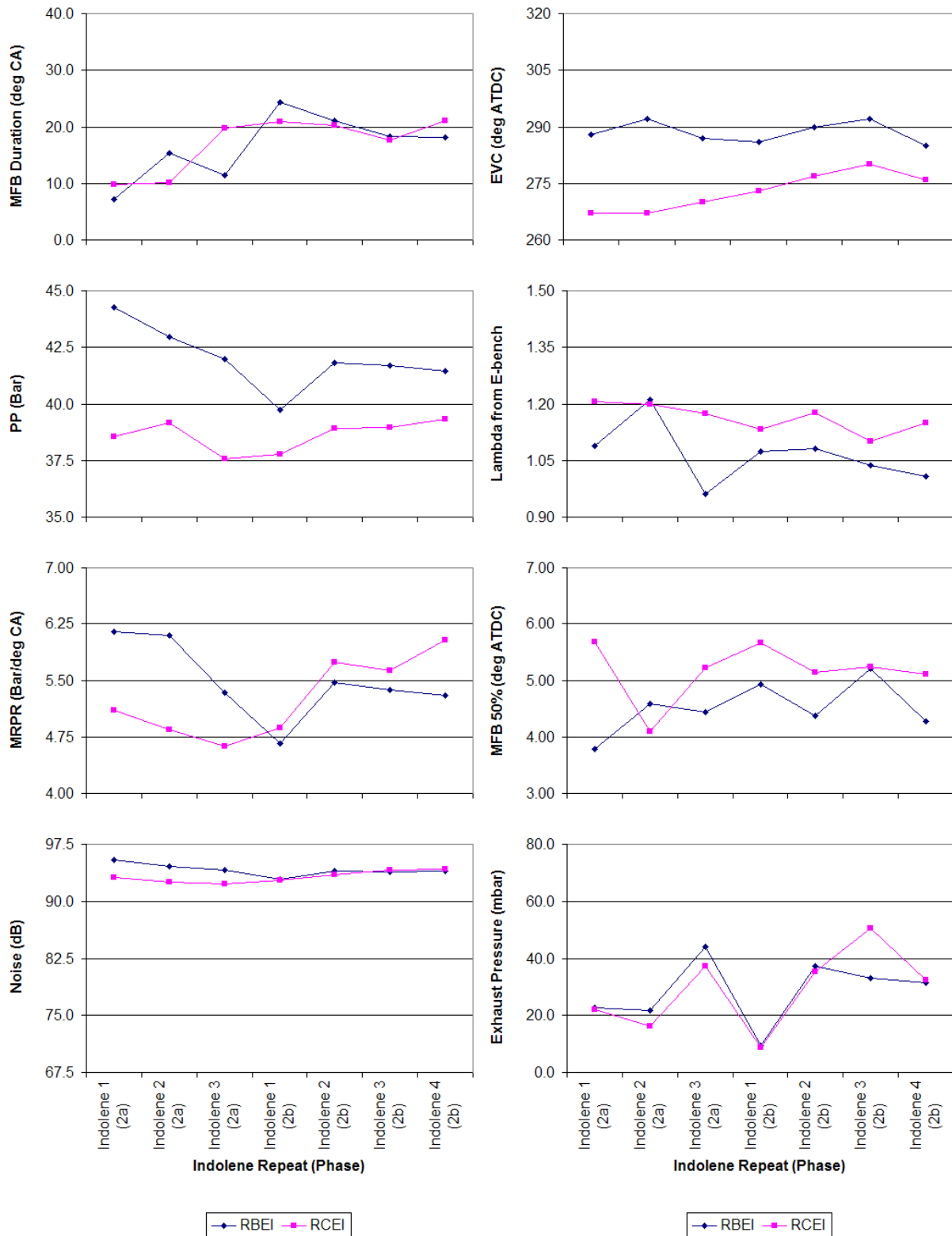


Figure 3.7 - Indolene Baseline Data @ 3000 rpm (2)

**CUSTOMER CONFIDENTIAL**

The electronic version is the only controlled copy.  
 All other copies are for reference only. Printed: 9/1/2009 4:09:13 PM  
 Page 21

CA4-prg-007 Technical Report  
 Originated: 01/01/04 Revised: 01/11/09

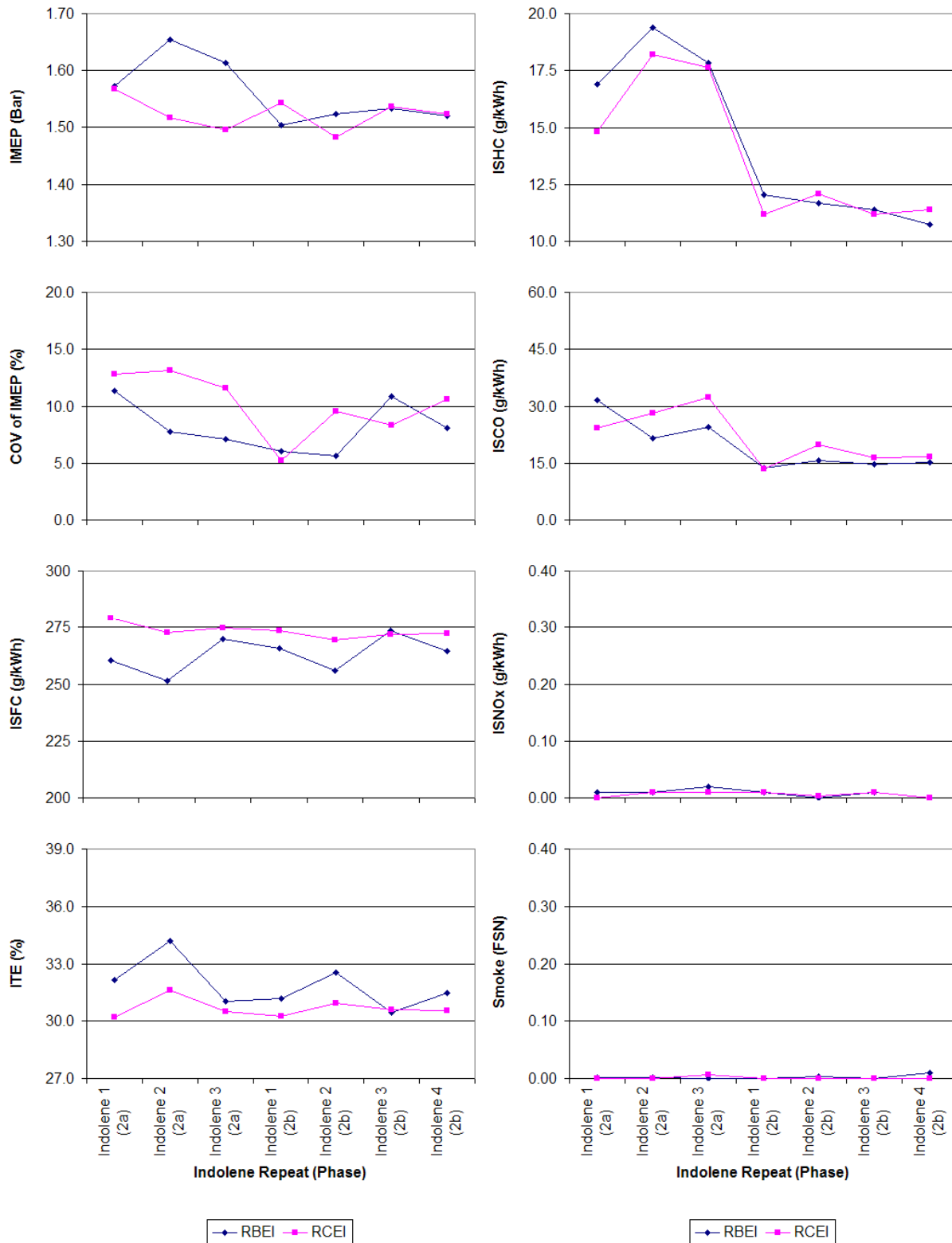


Figure 3.8 – Indolene Baseline Data @ 1000 rpm

**CUSTOMER CONFIDENTIAL**

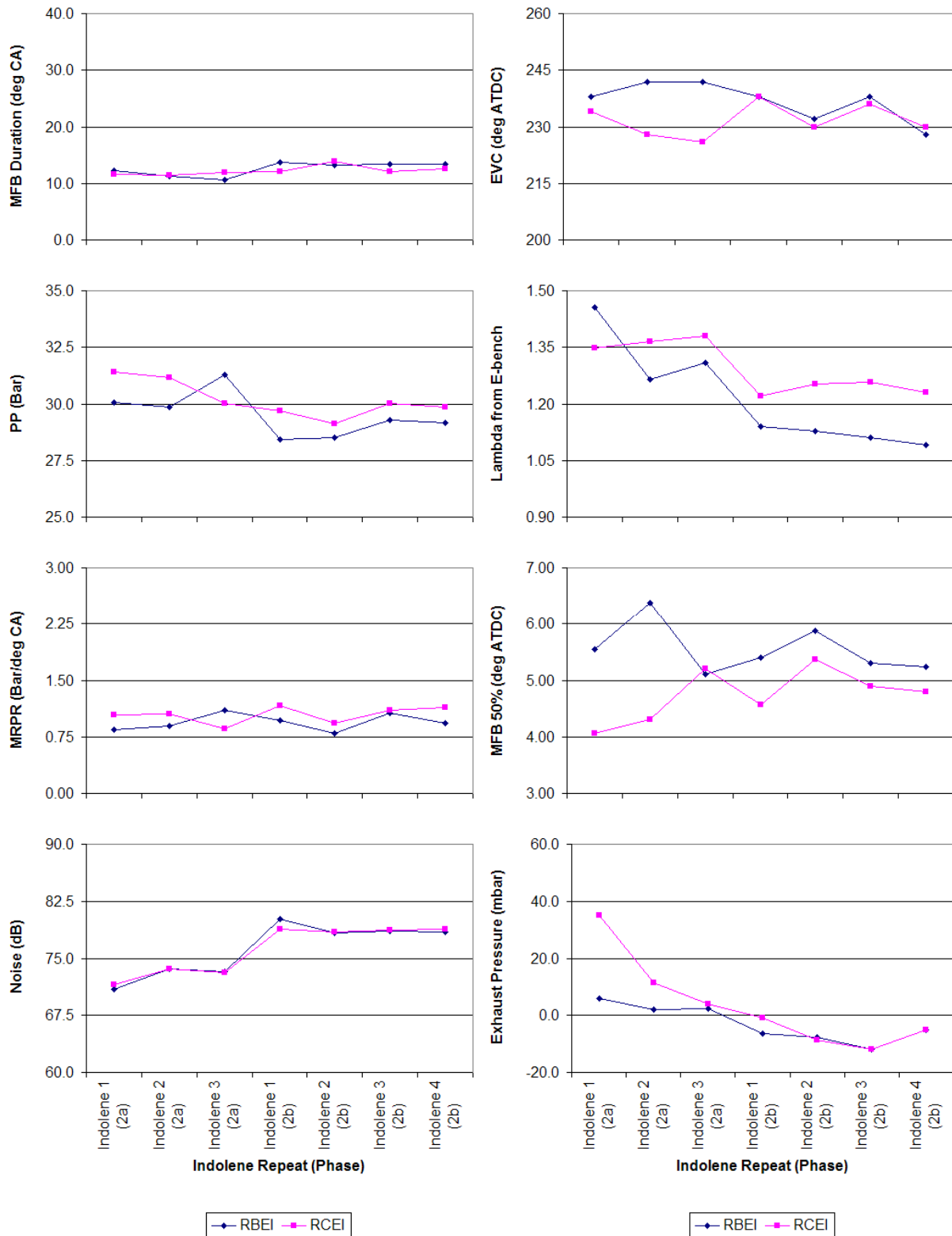


Figure 3.9 - Indolene Baseline Data @ 1000 rpm (2)

**CUSTOMER CONFIDENTIAL**

The electronic version is the only controlled copy.  
 All other copies are for reference only. Printed: 9/1/2009 4:09:13 PM  
 Page 23

CA4-prg-007 Technical Report  
 Originated: 01/01/04 Revised: 01/11/09



## 4. Test Results

Because the main focus of Phase II (AVFL-13B) was the effect of ethanol on the HCCI engine performance parameters, all the results are presented with respect to the volumetric ethanol content of the fuel. In this section an overall picture of the results is presented and a preliminary assessment of the effect of ethanol on HCCI engine performance is made. A discussion of the statistical significance of the effect of ethanol will follow in the next section along with the rest of Battelle's analytical results.

### 4.1. Test Results from Phase II-a

Figure 4.1 and Figure 4.2 show the results for the Phase II-a fuels at 2000 rpm, RCEI mode. As the percent ethanol content of the fuel is increased from 0 to 20%, the fuel consumption increases linearly due to the lower volumetric energy content of the fuel. However, the ITE increases significantly over this same range of ethanol content. The increase in thermal efficiency can be partially attributed to more complete combustion indicated by the decrease in ISHC emissions. In addition the decrease in ISNO<sub>x</sub> emissions indicates a decrease in combustion temperatures and an associated decrease in heat transfer to the cylinder walls which is beneficial to thermal efficiency. This cooling effect of ethanol has been noted in other studies performed by GM and Toyota [18, 19].

As the volumetric ethanol content of the A79D21 fuel is increased to 30% (A79D21E30), there is a large increase in fuel consumption that cannot be entirely explained by the decreased LHV of the fuel. The increase in COV of IMEP and a significant drop in the peak cylinder pressure indicate unstable and incomplete combustion. This is also illustrated by the increase in HC emissions and FSN. The relative exhaust pressure for this point was negative and inconsistent with the other points for this engine speed. The exhaust pressure is controlled manually by the cell technician and was not monitored properly on this day. A lower exhaust pressure could have a significant effect on the amount of internal residual left in the cylinder at the point of exhaust valve closing. Because the quality of HCCI combustion depends heavily on the amount of residual dilution, this effect will dominate any other effects of the fuel composition. Unfortunately, this was the case for every operating point run on this fuel blend. For this reason, this data was considered unrepresentative and this fuel blend was eliminated from the statistical analysis.

The Phase II-a results for 2000rpm, RBEI mode can be found in Figure 4.3 and Figure 4.4. The trends observed as the volumetric ethanol content is increased from 0% to 20% are similar to those seen for the RCEI mode results. However, there is more variability in the MFB 50% location and exhaust pressure. An associated variability in the peak cylinder pressure and MRPR can also be seen as a result of the differences in the amount of residual dilution and combustion timing. This variability in the engine performance leads to trends in fuel consumption and thermal efficiency that are less clear and no longer linear.

---

#### CUSTOMER CONFIDENTIAL

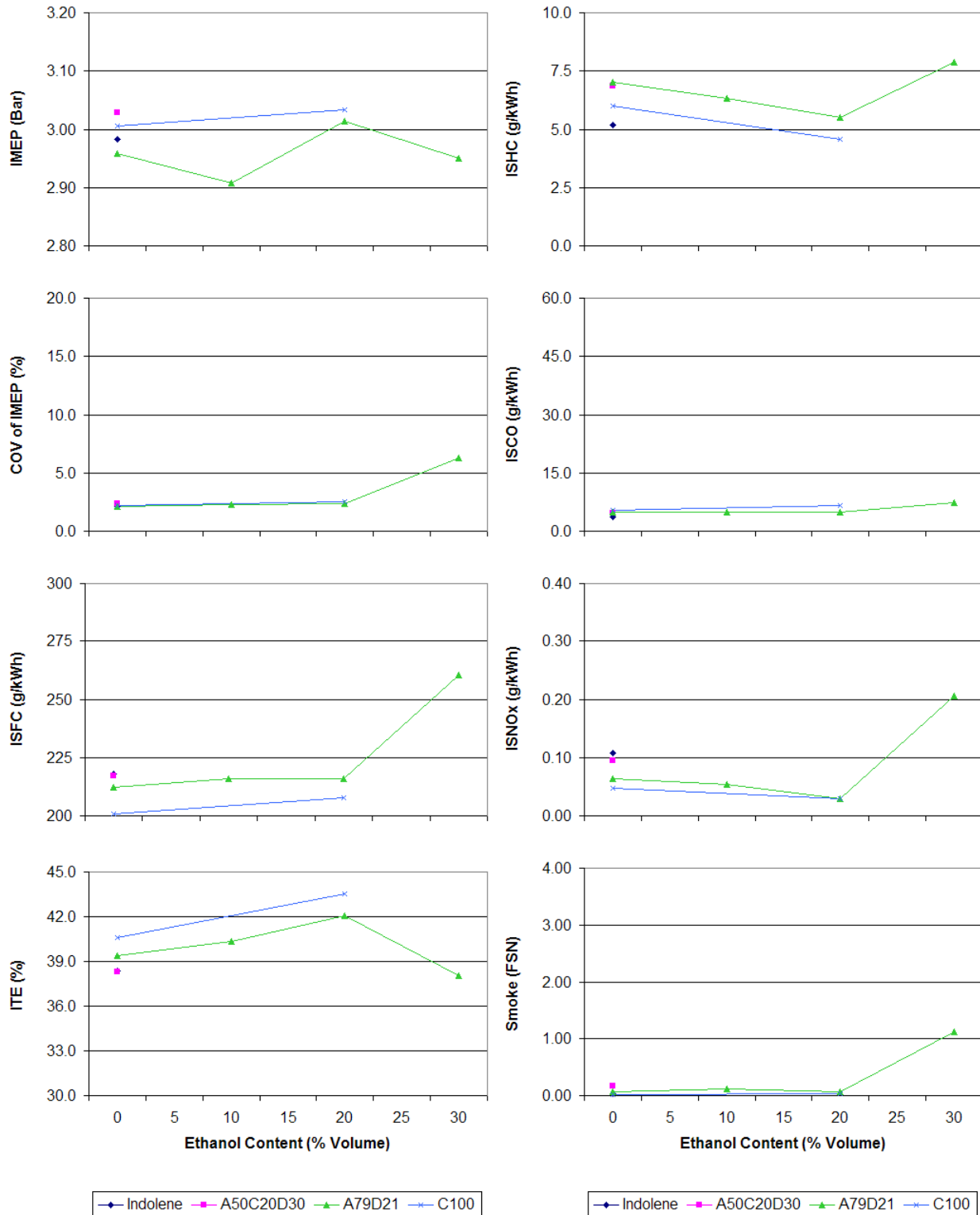


Figure 4.1 - Phase II-a Results for 2000 rpm, RCEI

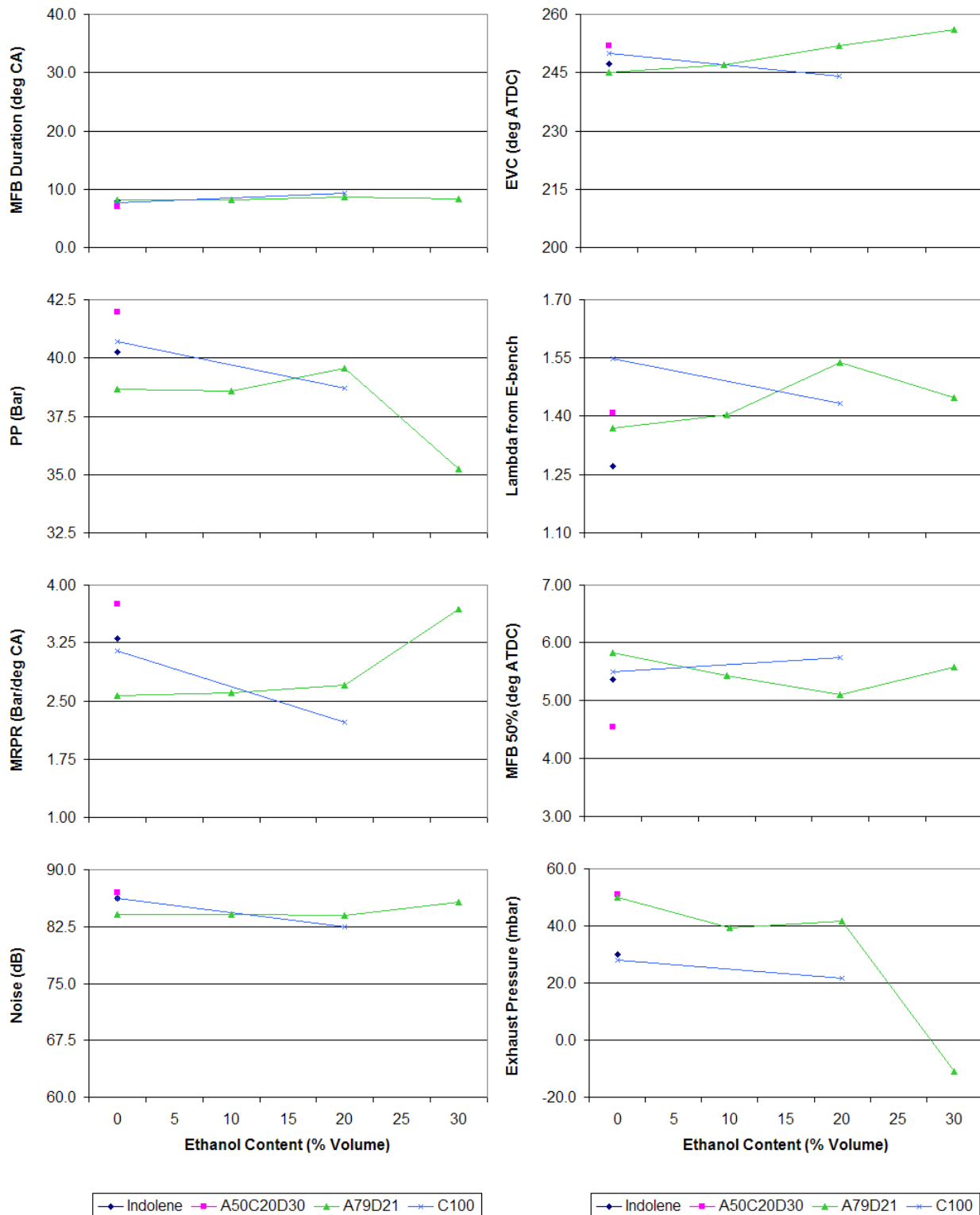


Figure 4.2 - Phase II-a Results for 2000 rpm, RCEI (2)

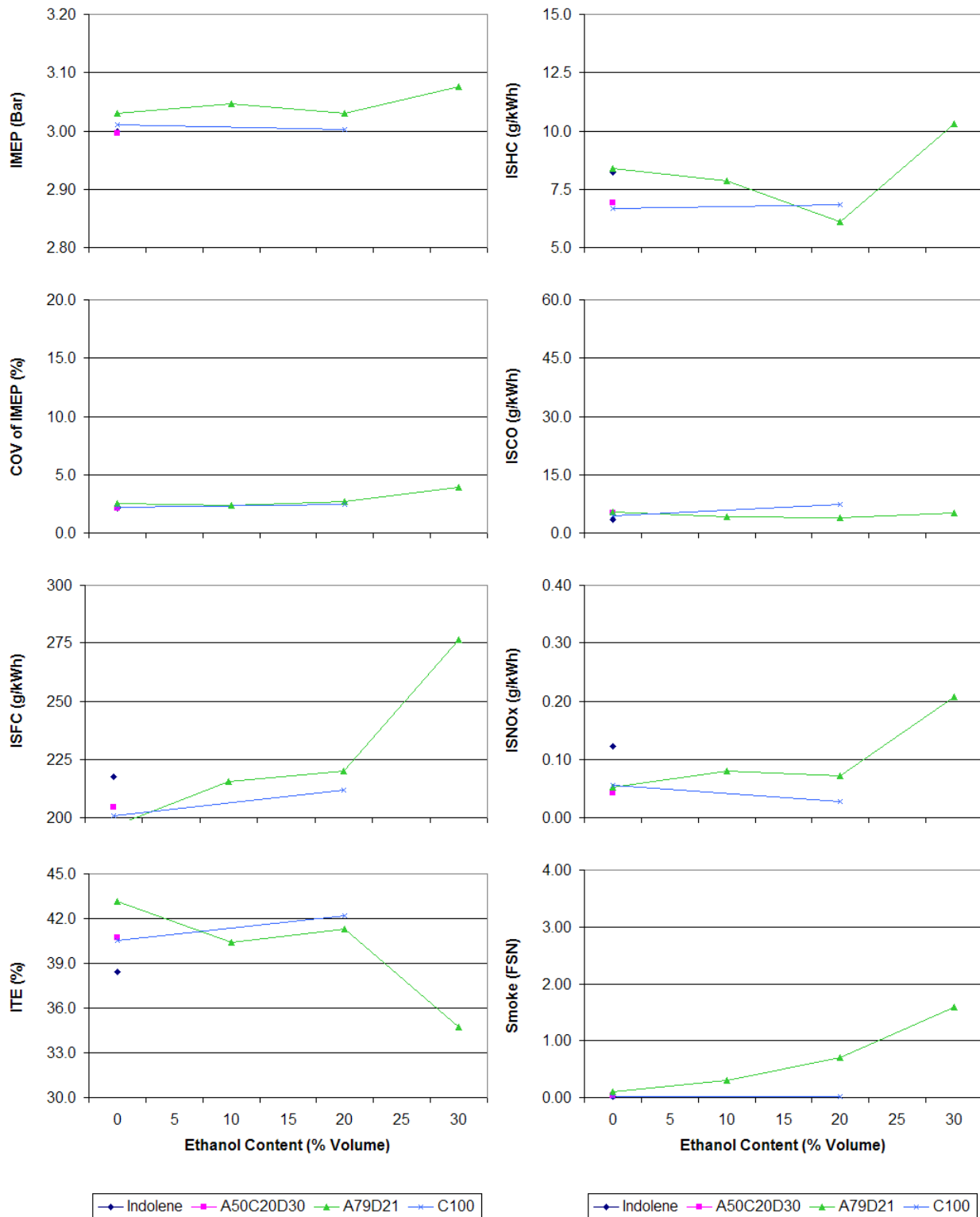


Figure 4.3 - Phase II-a Results for 2000 rpm, RBEI

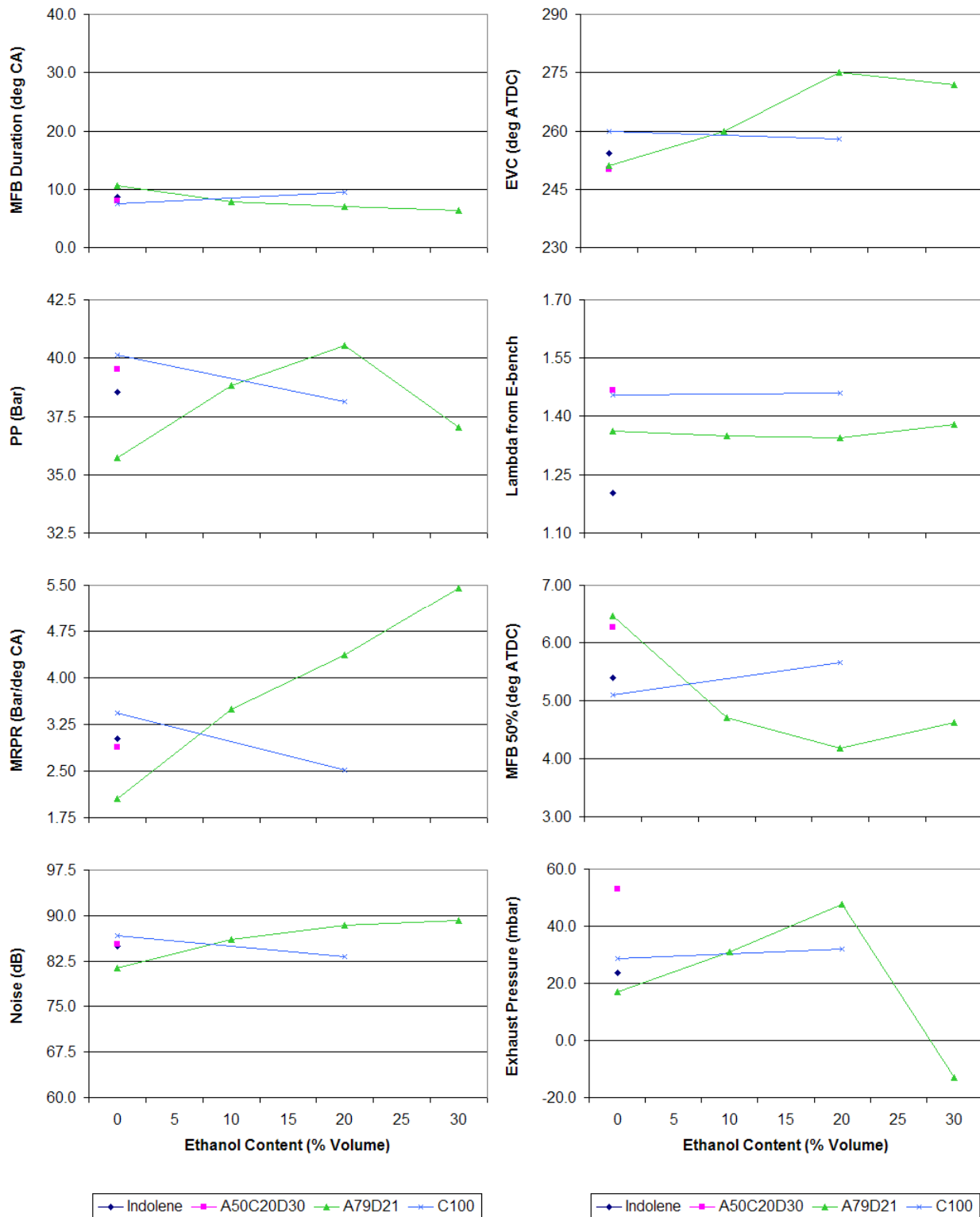


Figure 4.4 - Phase II-a Results for 2000 rpm, RBEI (2)



The Phase II-a results for 3000 rpm, RCEI and RBEI can be found in Figure 4.5 through Figure 4.8. At 3000 rpm, the MRPR is controlled instead of IMEP. This method is used because the engine tends to experience high levels of knock at this relatively high speed and load for HCCI combustion. By targeting a specific MRPR, the amount of knock can be limited to that which would be acceptable for a production vehicle despite variations in the fuel properties.

As the percent ethanol is increased, the fuel consumption and the thermal efficiency again increase as observed at 2000 rpm. However, the smaller increase in thermal efficiency in this case is mainly due to the decrease in ISHC emissions. There is no consistent trend observed in the  $ISNO_x$  emissions for either RCEI or RBEI mode. In RCEI mode, an increase in the IMEP indicates that the cooling effect of the ethanol is suppressing the knock allowing for a higher engine load for a given MRPR. In RBEI mode, there is more variation in the MRPR which makes this trend in increasing IMEP less clear. A large variation in the combustion duration is observed in both modes as well. This variation can be attributed to the fact that engine knock, indicated by high noise levels, makes the combustion duration difficult to estimate from the cylinder pressure curve. It should also be noted that the smoke levels for the A79D21 fuel blend are very high at 3000 rpm, RBEI mode. This is also true for the intermediary fuel blend, A50C20D30.

Figure 4.9 through Figure 4.12 show the Phase II-a results for 1000 rpm. In both the RBEI and RCEI modes, the COV of IMEP increases significantly as the ethanol content of the fuel is increased from 0% to 20%. In general, the fuel consumption increases as a result of the lower LHV and the loss of combustion stability. However, the fuel consumption also seems to be affected by the variability in the MFB 50% location. There is also an increase in ISCO emissions associated with the increase in COV of IMEP. ISHC emissions show no consistent trend, but vary considerably. The thermal efficiency is directly affected by this variation. In the RCEI mode, the C100 fuel exhibited very poor combustion stability. This led to high ISHC and ISCO emissions, however, the fuel consumption and thermal efficiency seem unaffected when compared to the other data plotted. The A79D21 fuel blend with no ethanol was run at a very high IMEP in comparison to the other fuels tested at this operating point. For this reason, this point was not included in the statistical analysis.

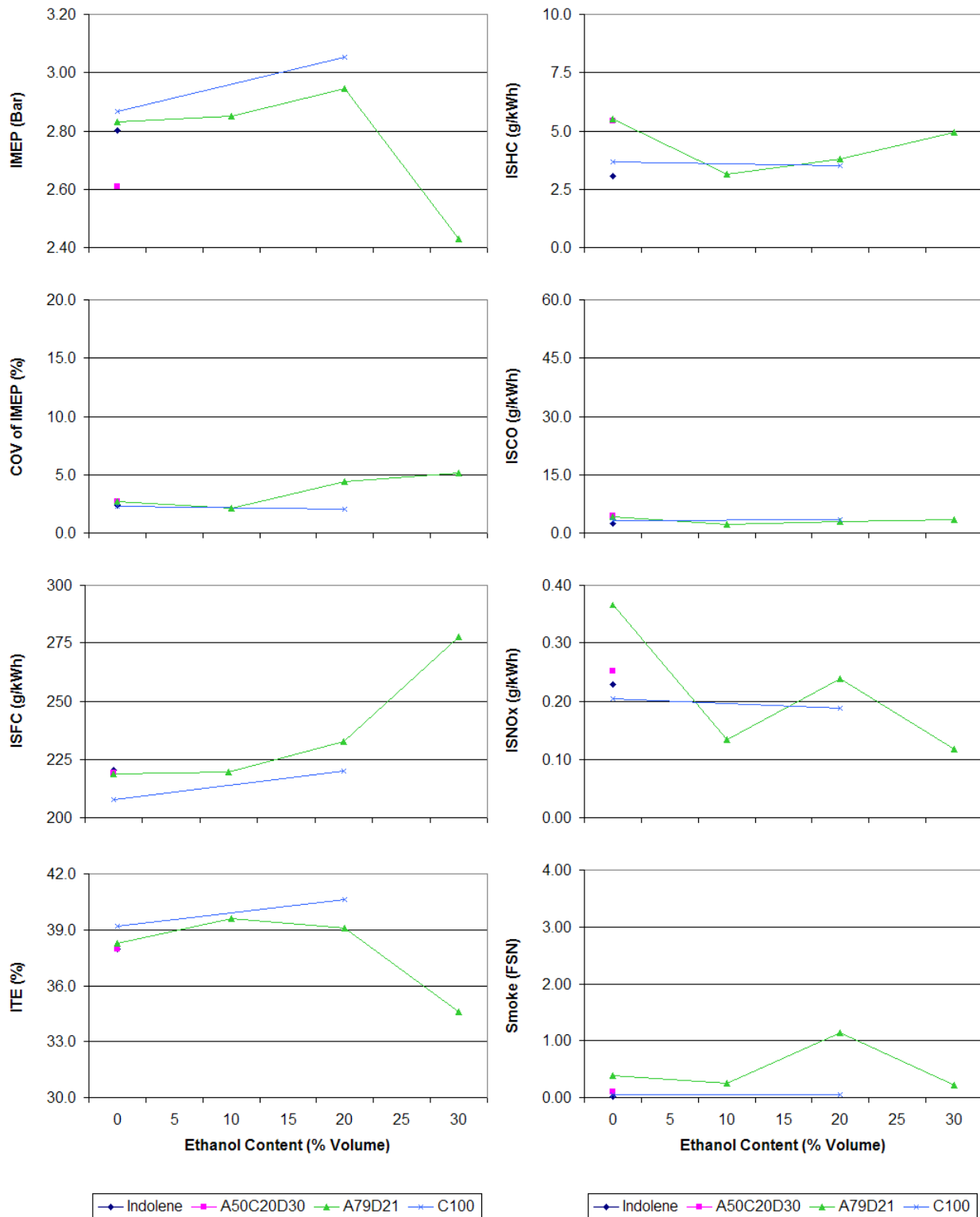


Figure 4.5 - Phase II-a Results for 3000 rpm, RCEI

**CUSTOMER CONFIDENTIAL**

The electronic version is the only controlled copy.  
 All other copies are for reference only. Printed: 9/1/2009 4:09:13 PM  
 Page 30

CA4-prg-007 Technical Report  
 Originated: 01/01/04 Revised: 01/11/09

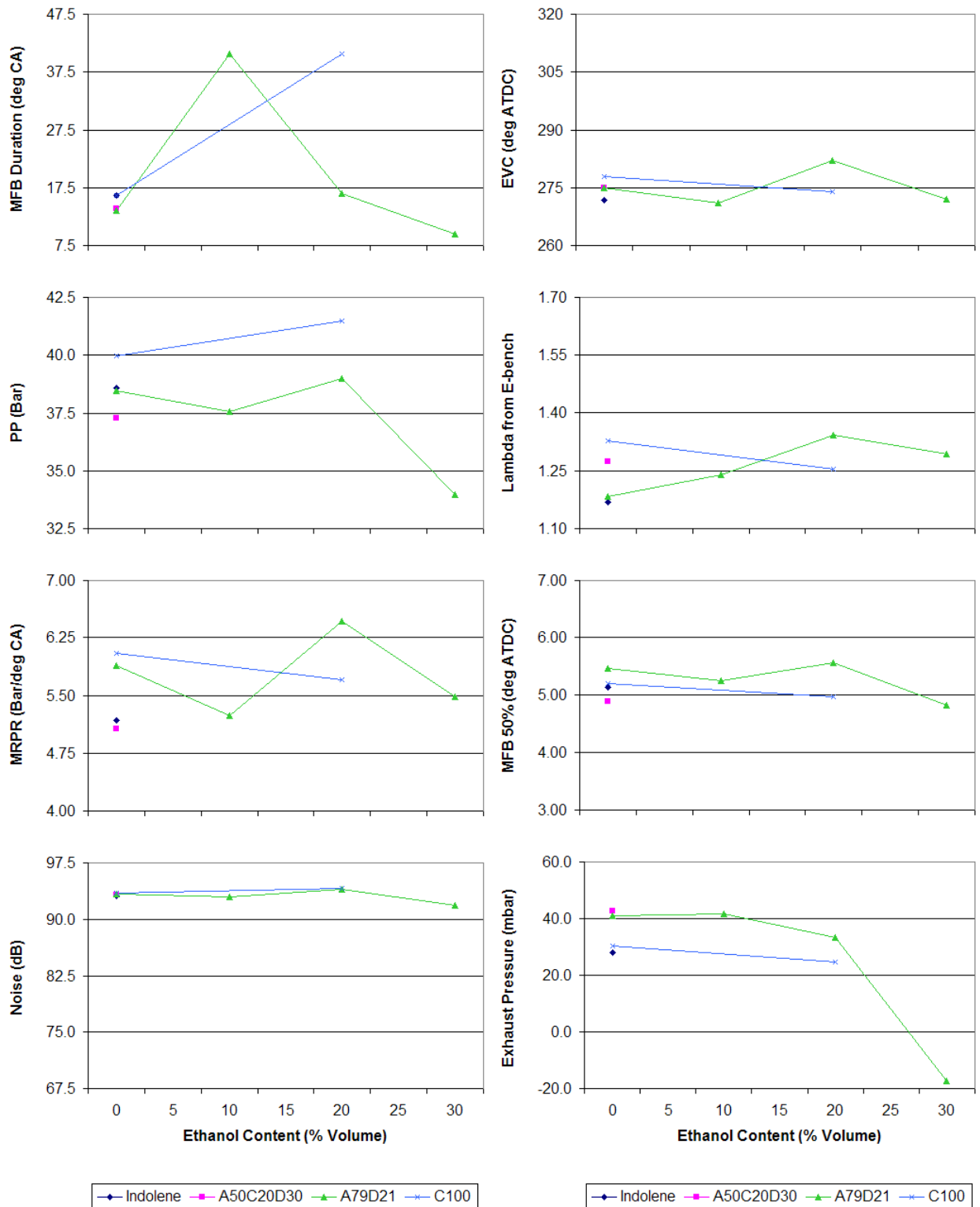


Figure 4.6 - Phase II-a Results for 3000 rpm, RCEI (2)

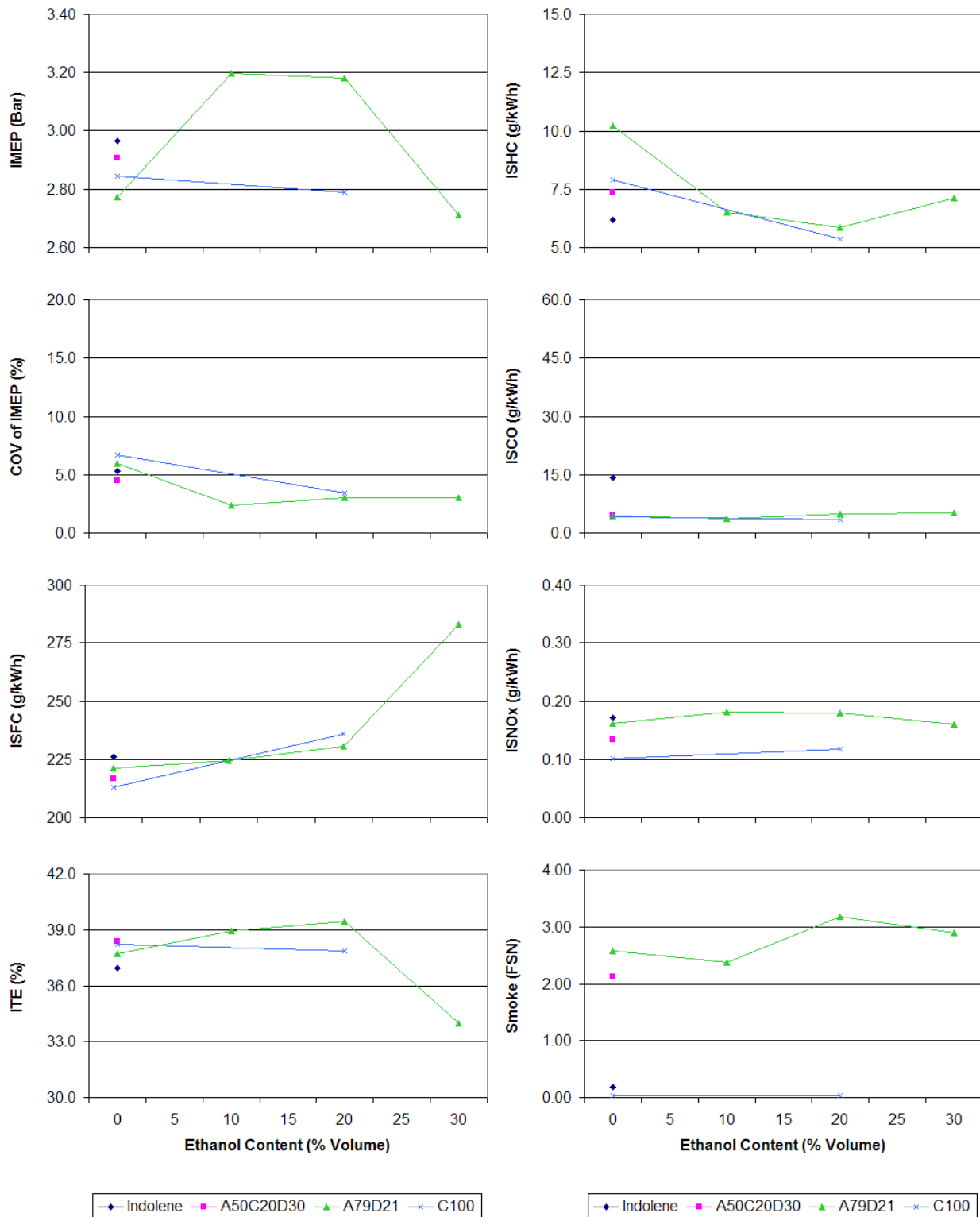


Figure 4.7 - Phase II-a Results for 3000 rpm, RBEI

**CUSTOMER CONFIDENTIAL**

The electronic version is the only controlled copy.  
 All other copies are for reference only. Printed: 9/1/2009 4:09:13 PM  
 Page 32

CA4-prg-007 Technical Report  
 Originated: 01/01/04 Revised: 01/11/09

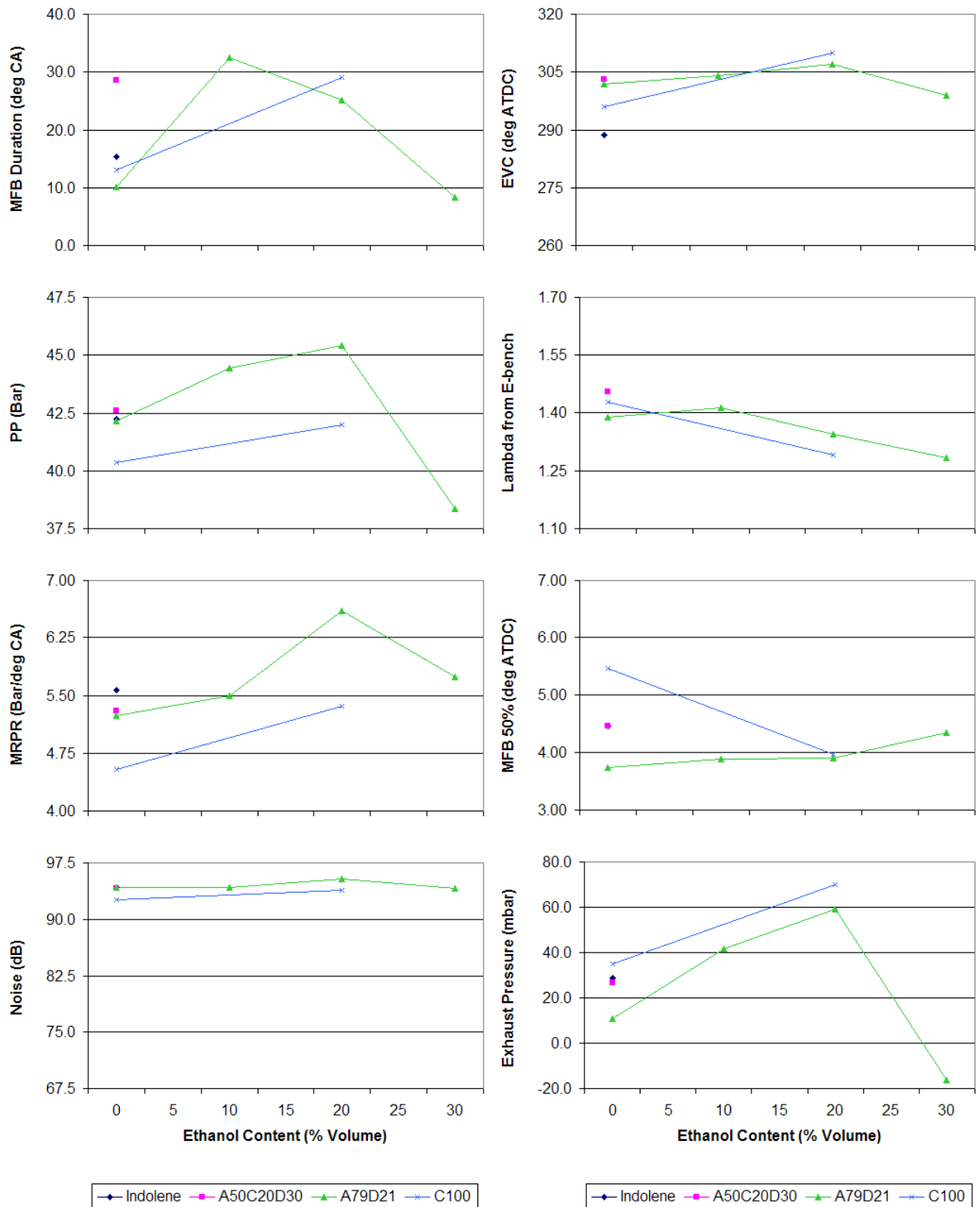


Figure 4.8 - Phase II-a Results for 3000 rpm, RBEI (2)

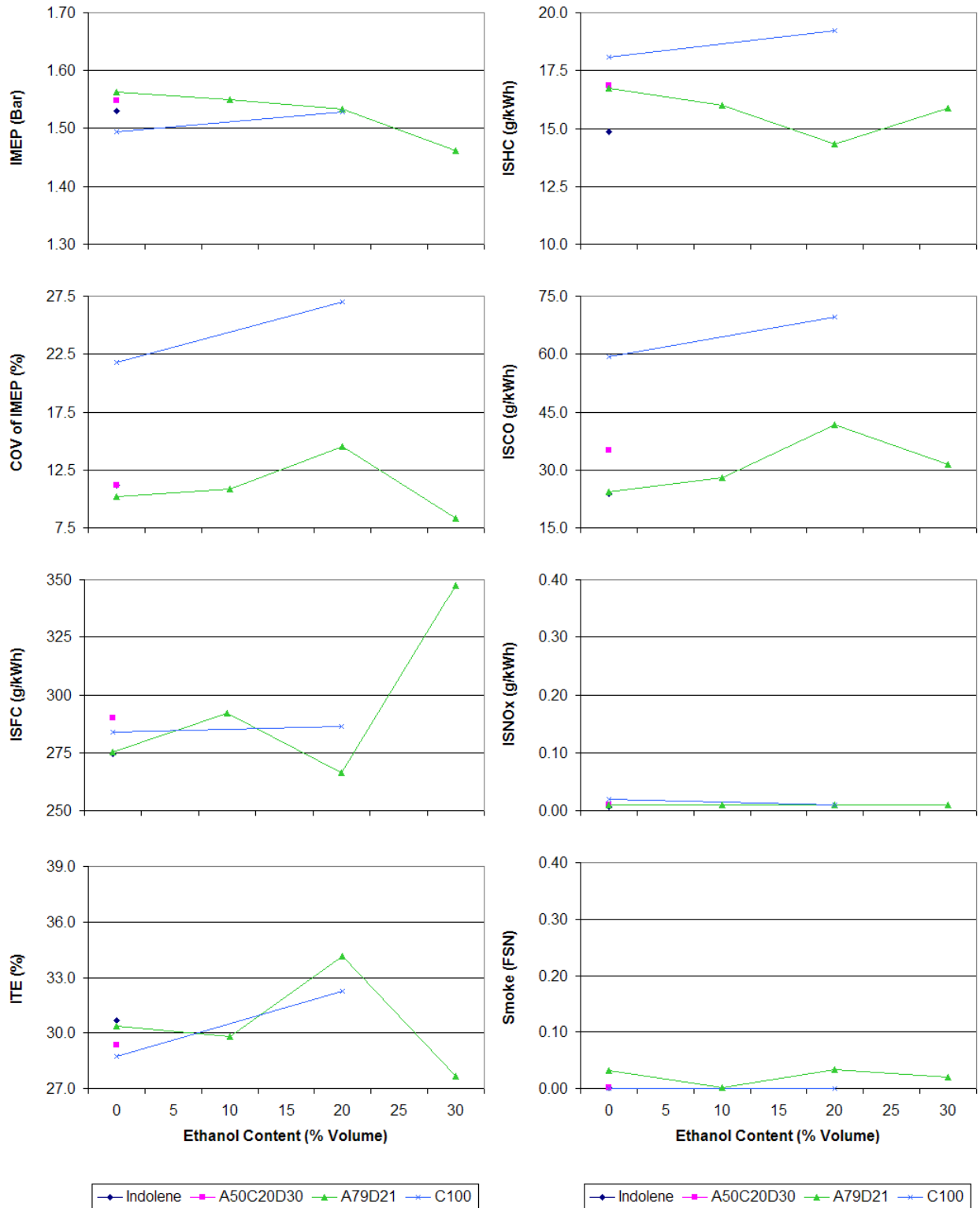


Figure 4.9 - Phase II-a Results for 1000 rpm, RCEI

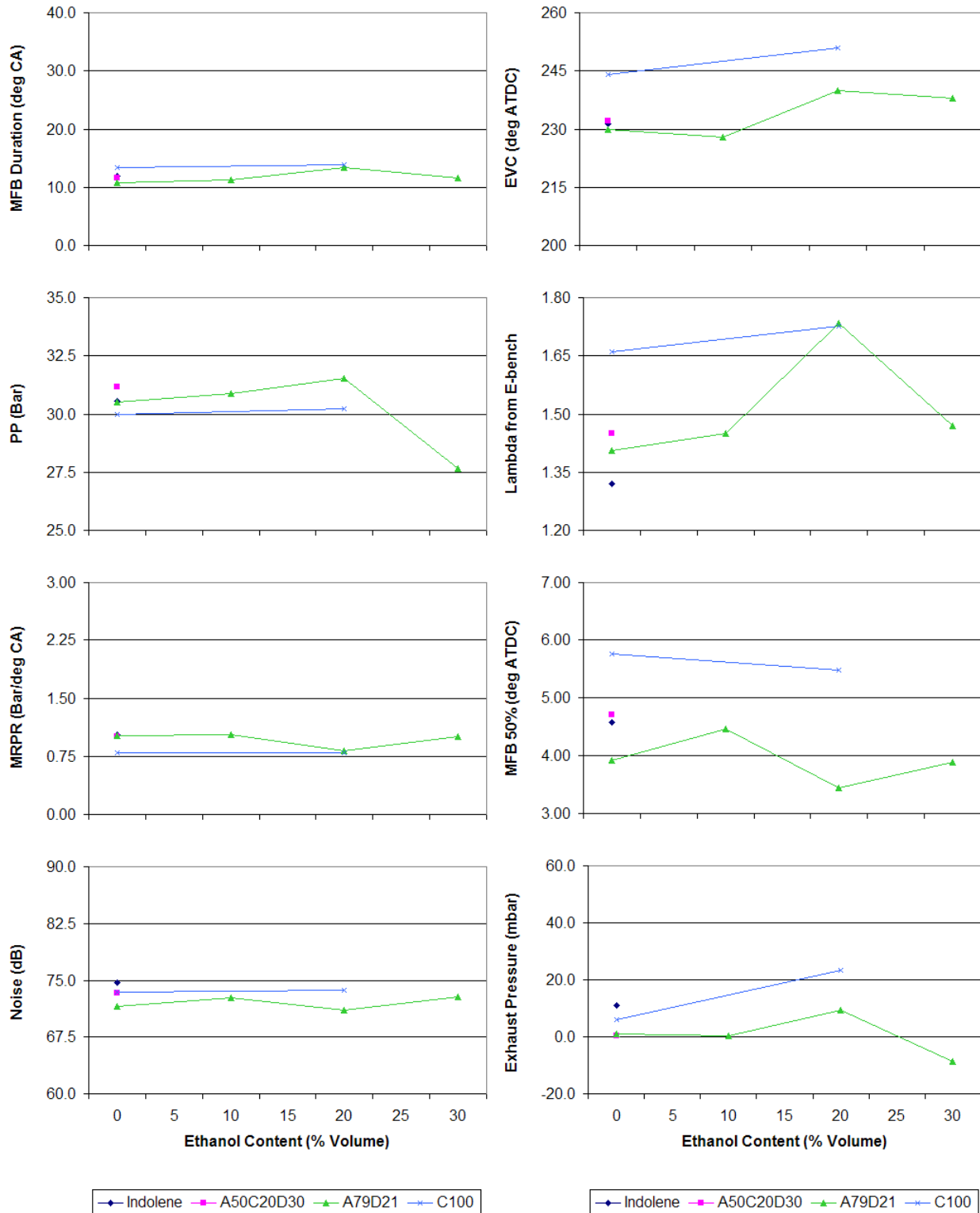


Figure 4.10 - Phase II-a Results for 1000 rpm, RCEI (2)

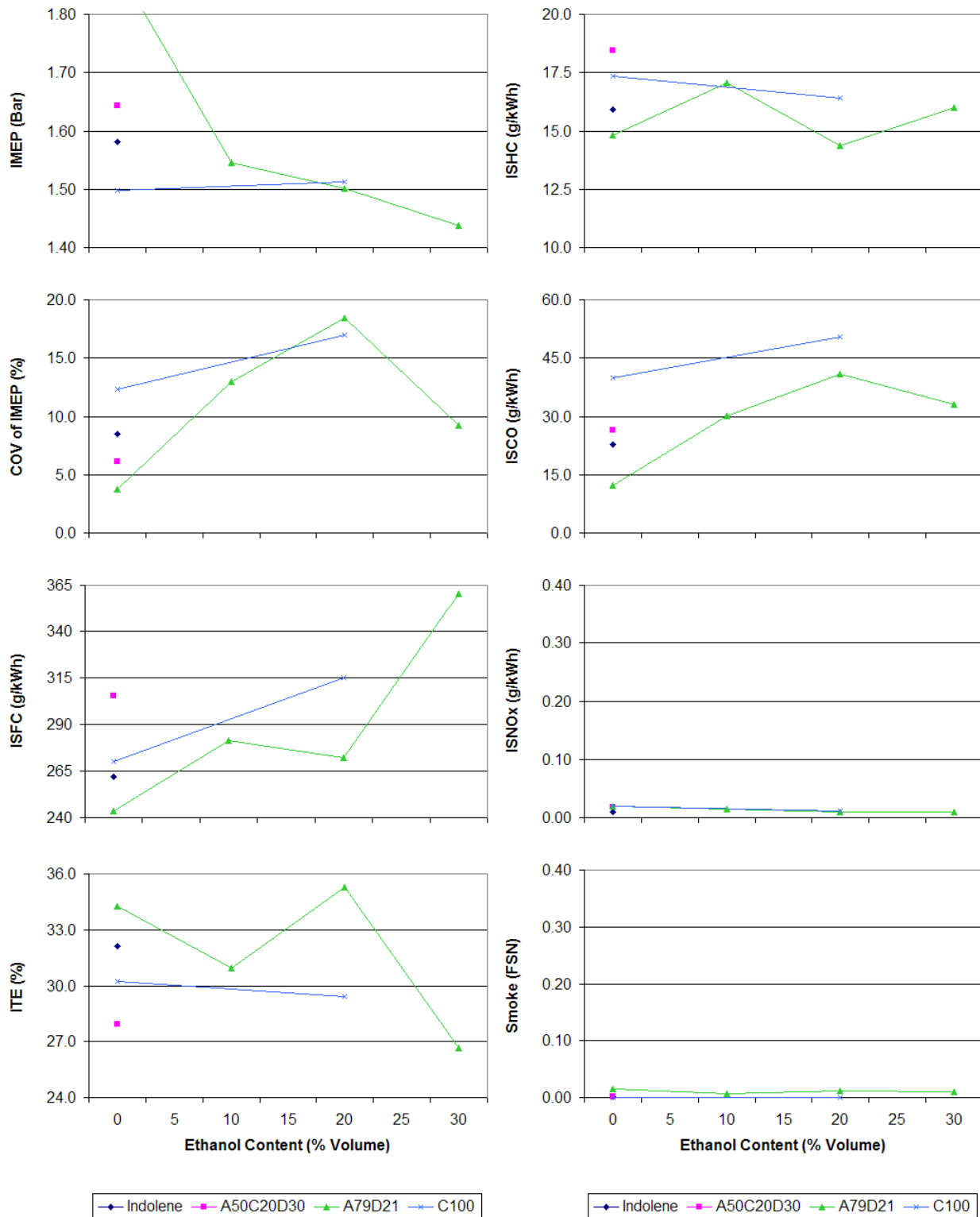


Figure 4.11 - Phase II-a Results for 1000 rpm, RBEI

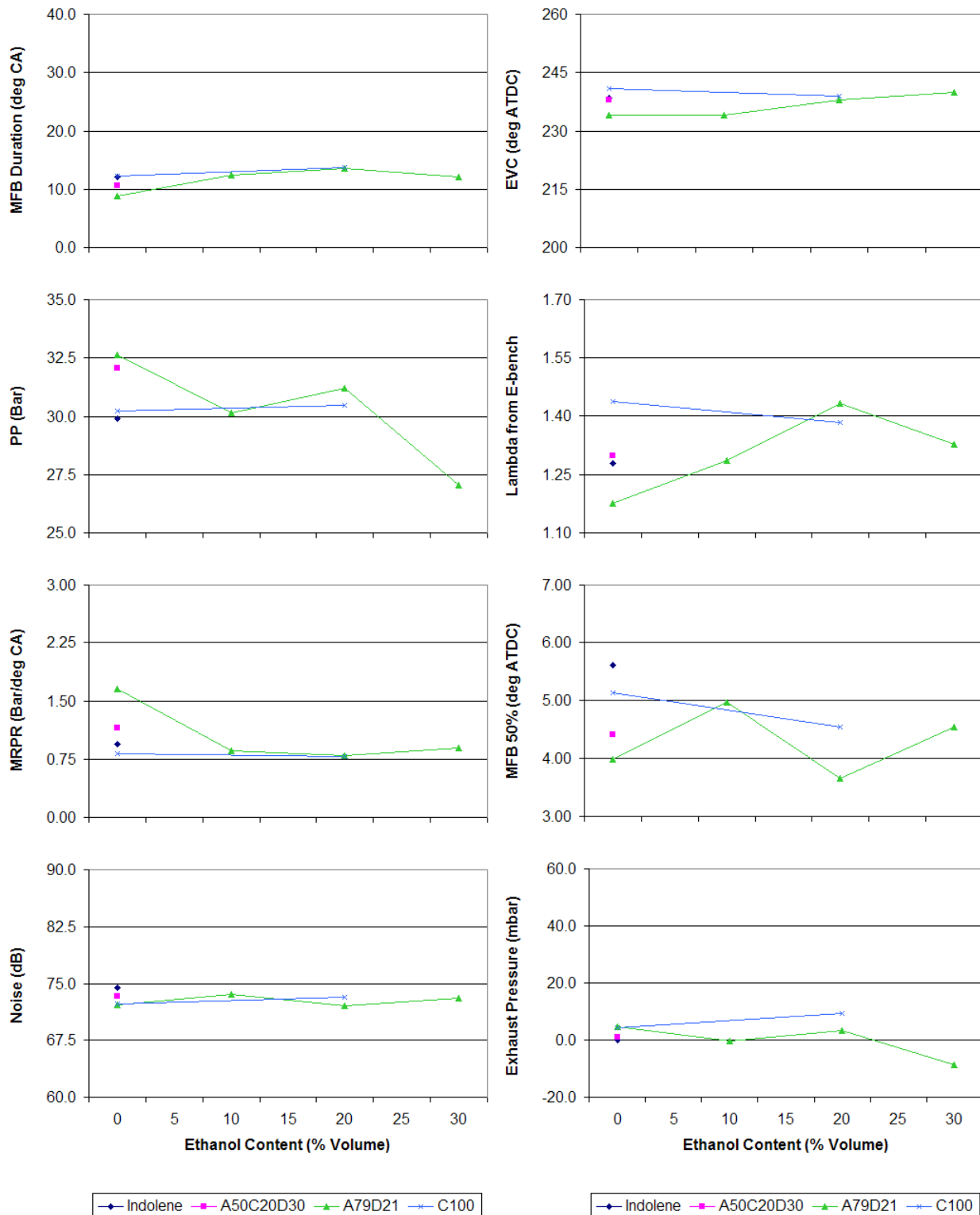


Figure 4.12 - Phase II-a Results for 1000 rpm, RBEI (2)



## 4.2. Test Results from Phase II-b

The Phase II-b results for 2000 rpm can be found in Figure 4.13 through Figure 4.16. As mentioned previously, several actions were taken to minimize variability during Phase II-b. The IMEP, the MFB 50% location and the exhaust pressure are much more consistent across the range of fuels tested. This resulted in minimal variation in peak cylinder pressure and MRPR. In addition, the ISHC and ISCO emissions show very little change across the range of fuels tested and remain constant as the volumetric ethanol content of each fuel is increased from 0% to 30%. The  $ISNO_x$  emissions, however, show a clear decreasing trend as ethanol content is increased, indicating lower combustion temperatures. Therefore, the thermal efficiency is increasing as a function of ethanol content, despite increased fuel consumption, due to reduced heat transfer losses.

The results for 3000 rpm are shown in Figure 4.17 through Figure 4.20. The MRPR, MFB 50% location and exhaust pressure are again more consistent across the range of fuels tested in Phase II-b. In the RCEI mode, the IMEP is relatively constant as the ethanol content is increased. However, this could be due to the unintentional decrease in MRPR. In the RBEI mode, there is an increasing trend in IMEP with increased ethanol content similar to that seen in Phase II-a. This indicates that the anti-knock properties of the ethanol are enabling a higher load. For both modes, the ISCO and ISHC emissions are constant with respect to ethanol content. However,  $ISNO_x$  emissions again illustrate a decreasing trend and the thermal efficiency increases. At 3000 rpm, the engine tends to run closer to stoichiometric conditions. ISCO emissions are highly dependent on air fuel ratio at lambda values less than 1.05 for this engine. This is clearly illustrated in the RBEI mode.

Figure 4.21 through Figure 4.24 show the results for 1000 rpm. At this speed and load, the combustion stability was poor and similar to that seen in the previous phase. As a result, the ISHC and ISCO emissions are high across the entire range of fuels tested. In addition, the COV of IMEP shows an increasing trend with increased ethanol content causing an associated increase in ISCO emissions. The effect of the volumetric ethanol content on  $ISNO_x$  and thermal efficiency is minimal since combustion temperatures at this operating condition are already very low. In both modes, the B77D23E30 fuel blend illustrated uncharacteristically low fuel consumption values. After reviewing the raw values for fuel flow, it was determined that aeration of the fuel contributed to an erroneous fuel measurement. For this reason, ISFC and ITE values for this fuel blend were left out of the statistical analysis.

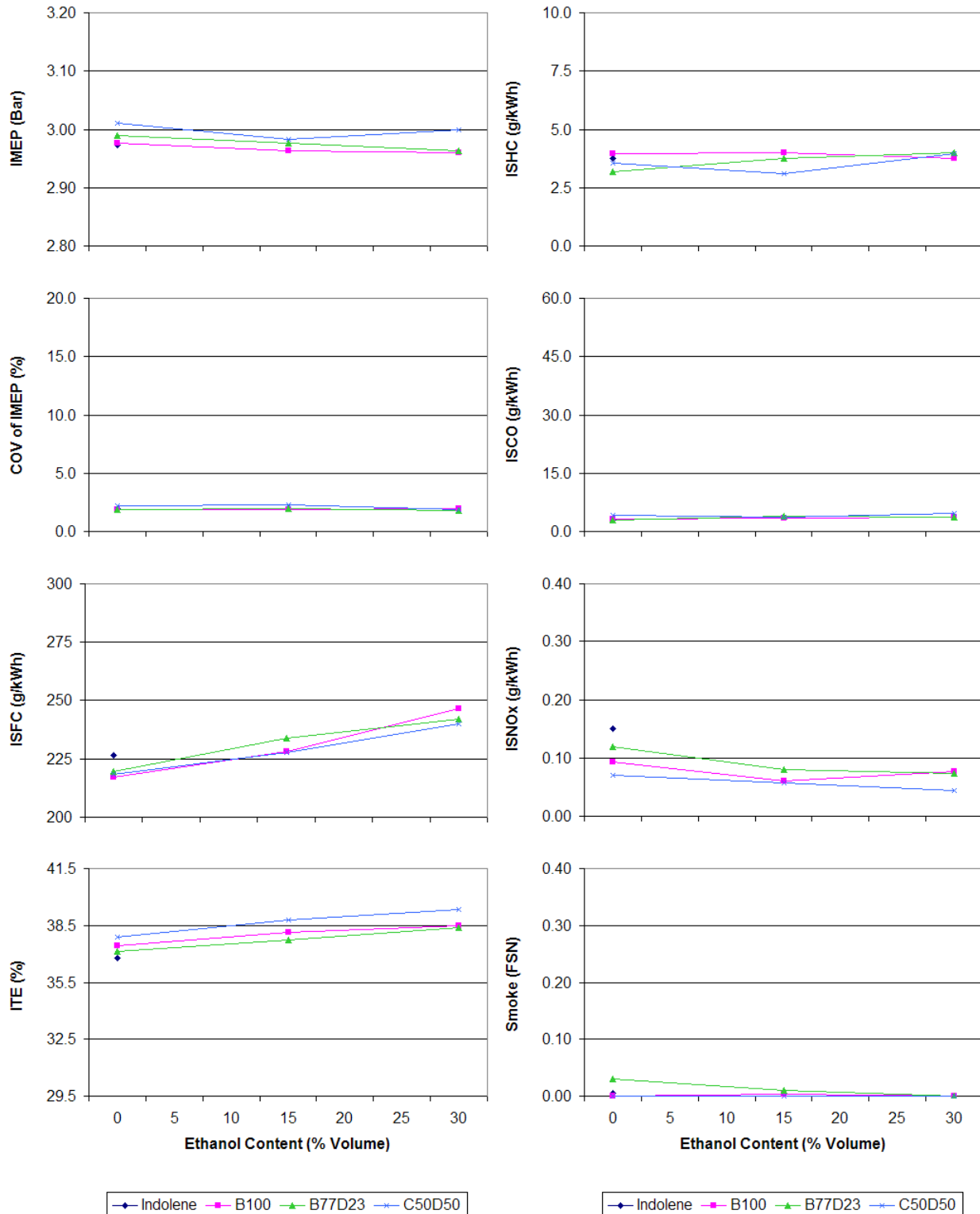


Figure 4.13 - Phase II-b Results for 2000 rpm, RCEI

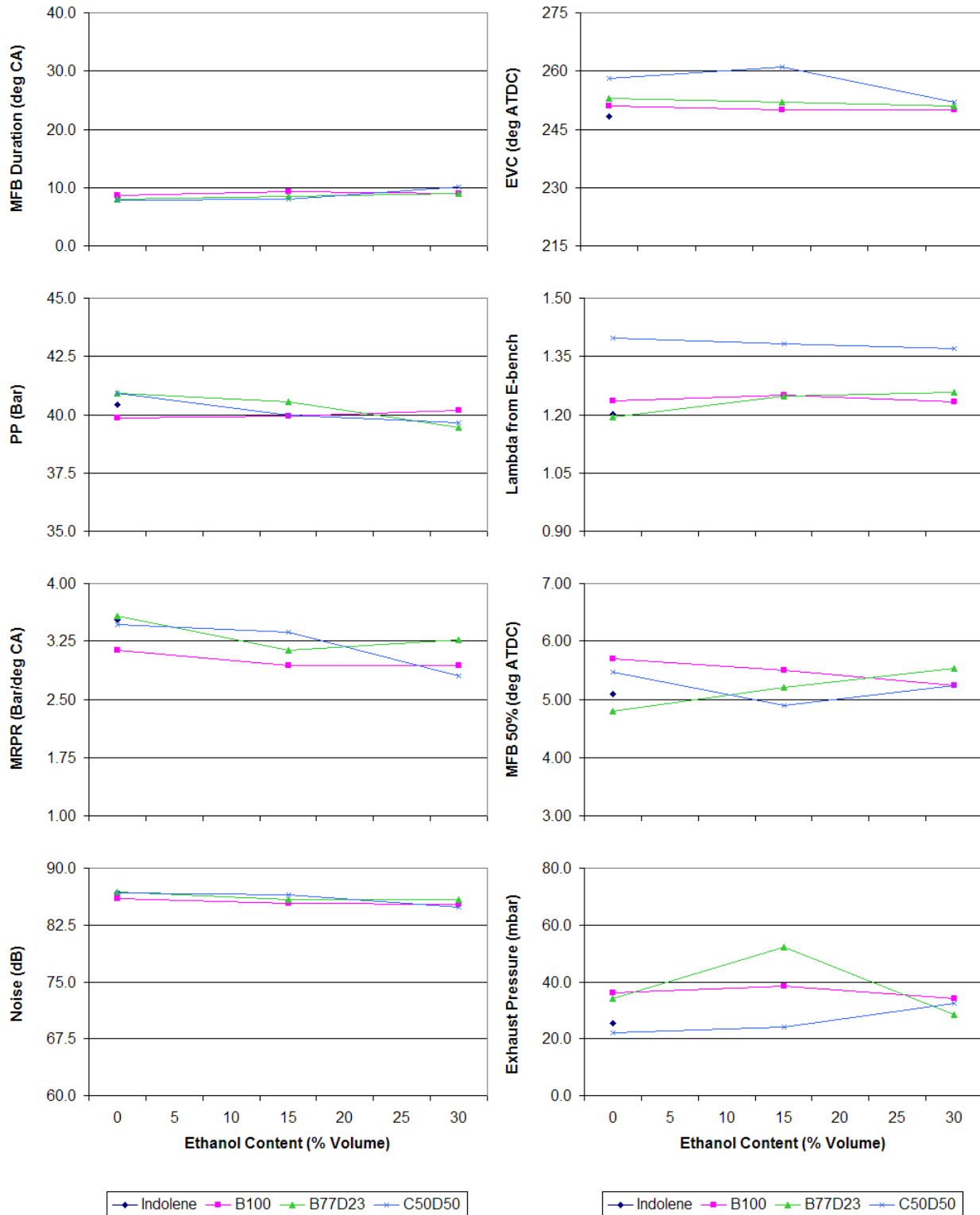


Figure 4.14 - Phase II-b Results for 2000 rpm, RCEI (2)

**CUSTOMER CONFIDENTIAL**

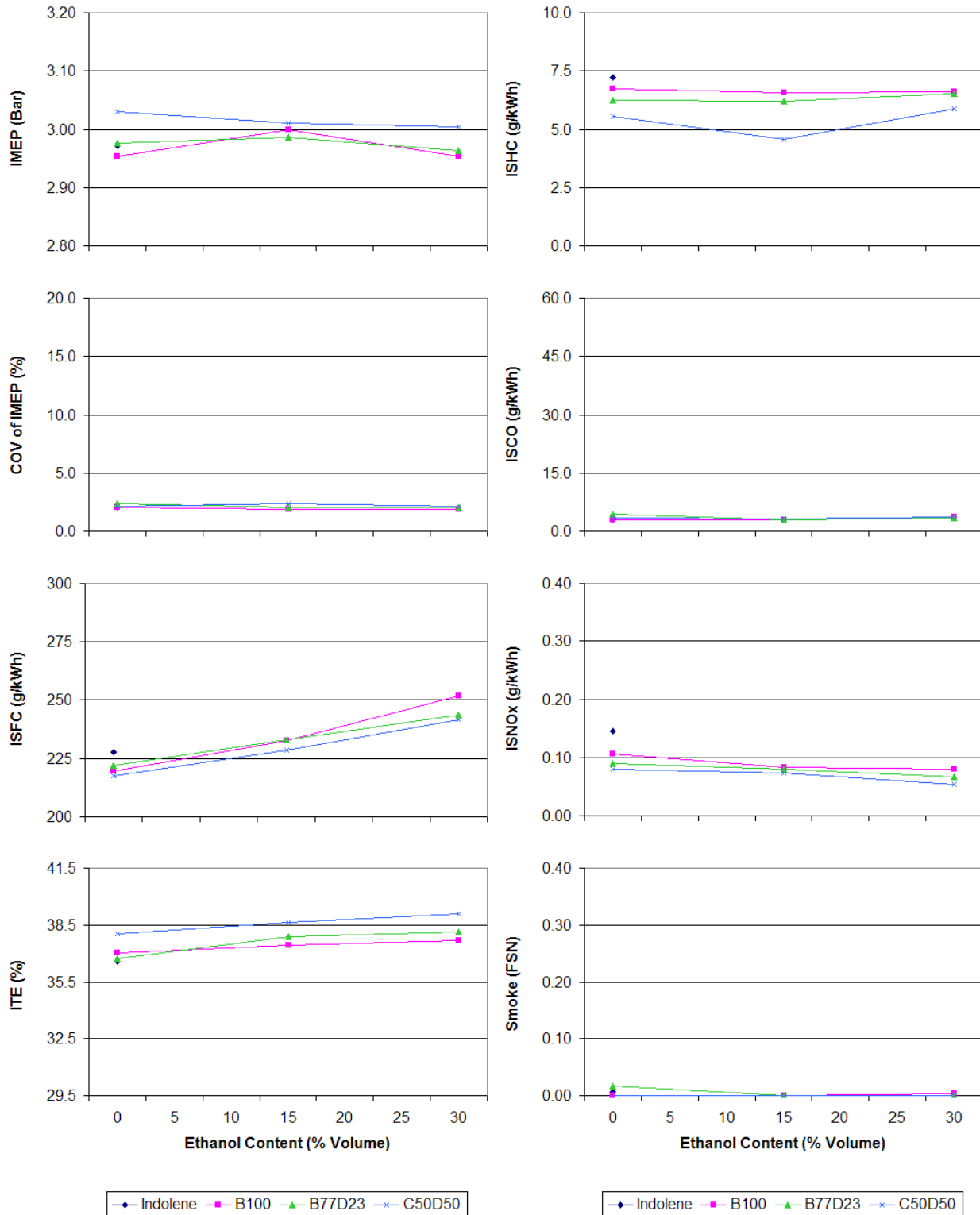


Figure 4.15 - Phase II-b Results for 2000 rpm, RBEI

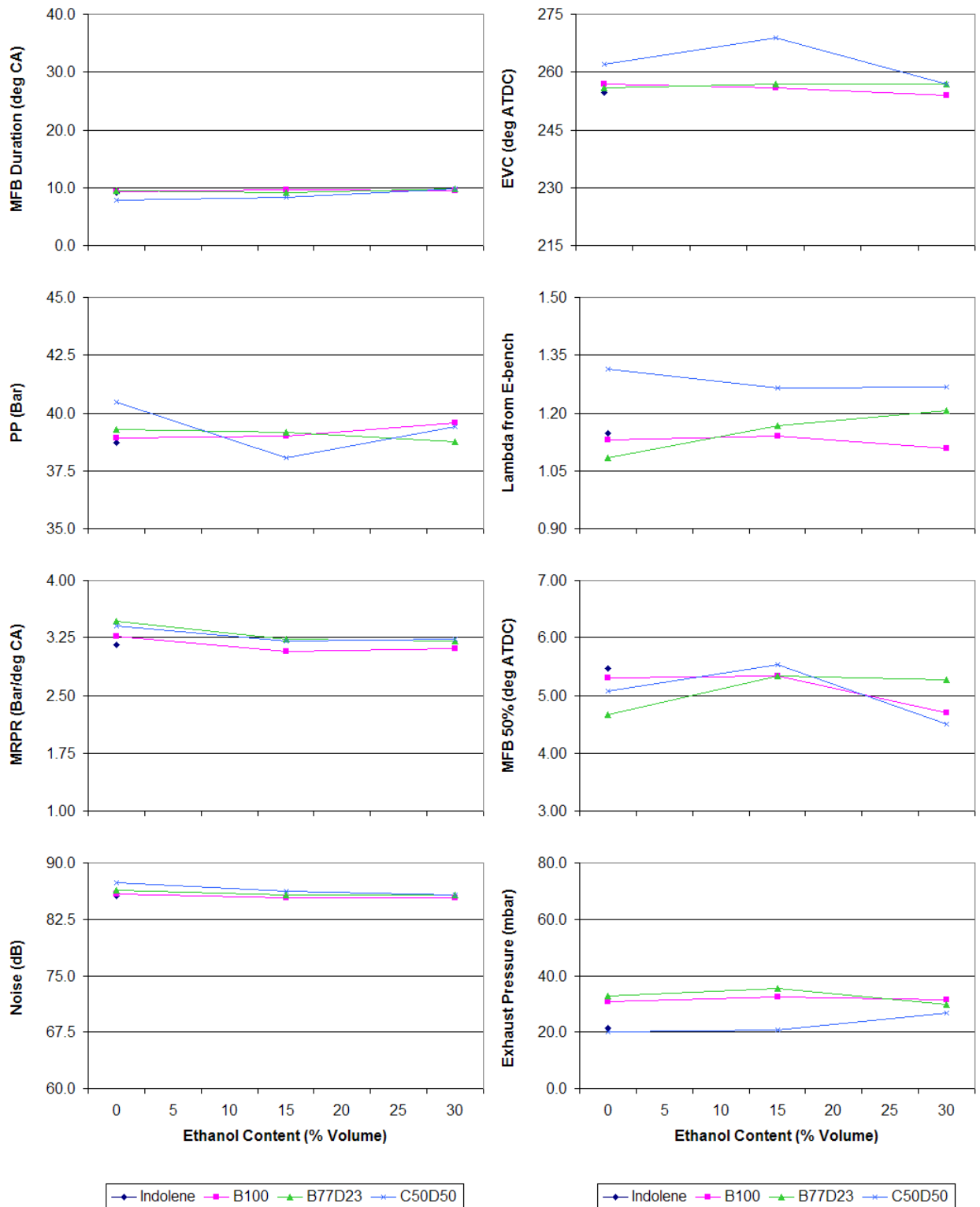


Figure 4.16 - Phase II-b Results for 2000 rpm, RBEI (2)

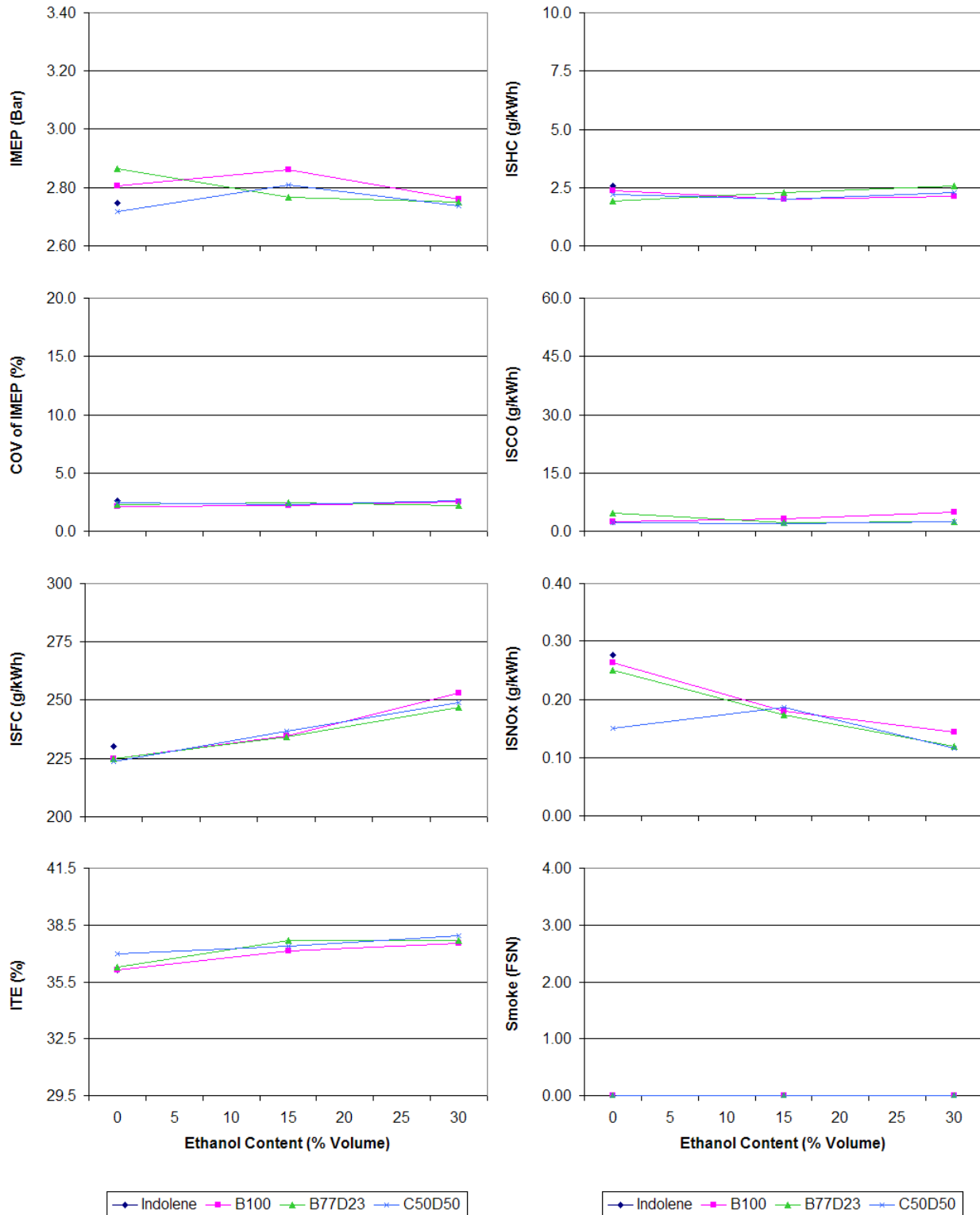


Figure 4.17 - Phase II-b Results for 3000 rpm, RCEI

**CUSTOMER CONFIDENTIAL**

The electronic version is the only controlled copy.  
 All other copies are for reference only. Printed: 9/1/2009 4:09:13 PM  
 Page 43

CA4-prg-007 Technical Report  
 Originated: 01/01/04 Revised: 01/11/09

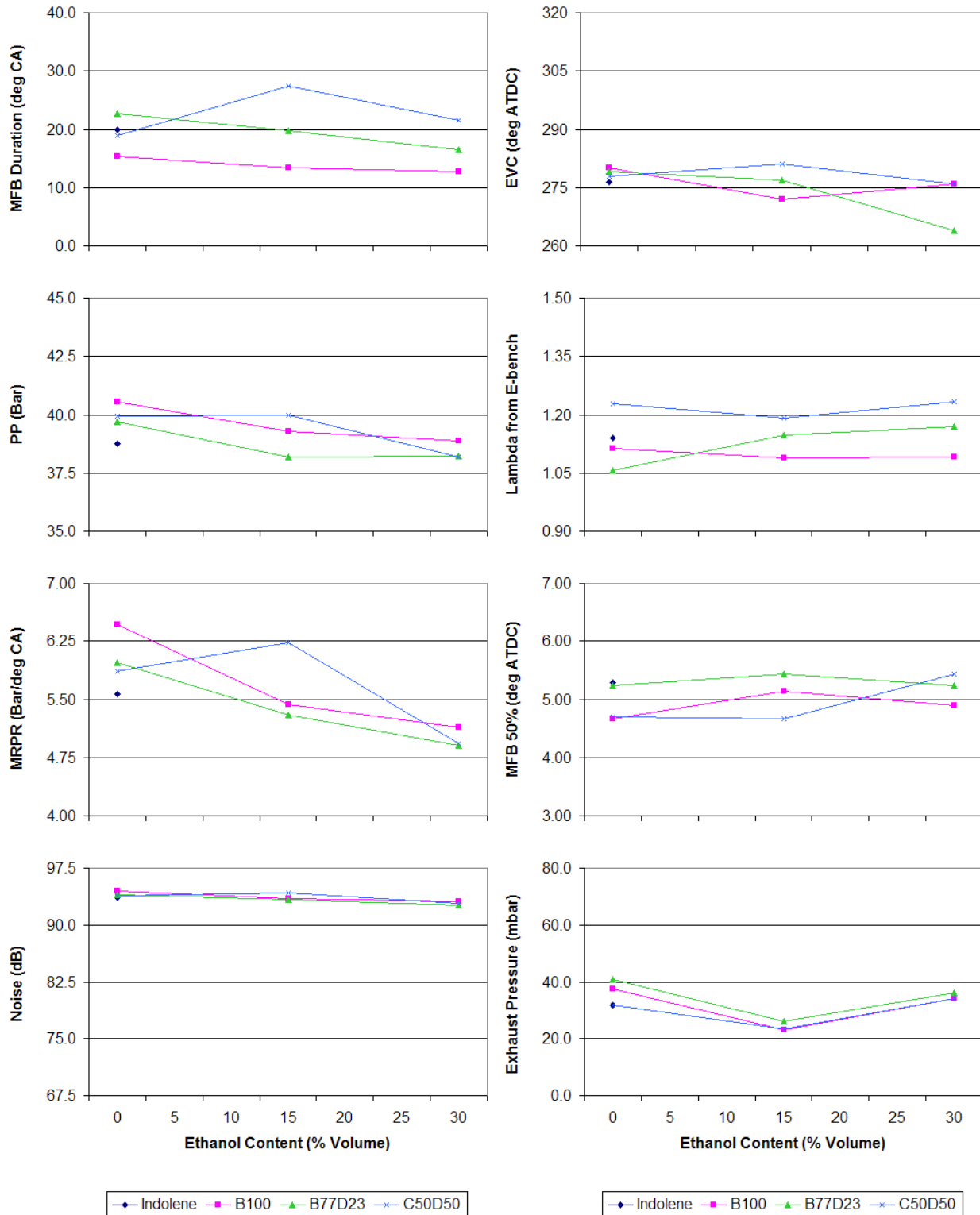


Figure 4.18 - Phase II-b Results for 3000 rpm, RCEI (2)

**CUSTOMER CONFIDENTIAL**

The electronic version is the only controlled copy.  
 All other copies are for reference only. Printed: 9/1/2009 4:09:13 PM  
 Page 44

CA4-prg-007 Technical Report  
 Originated: 01/01/04 Revised: 01/11/09

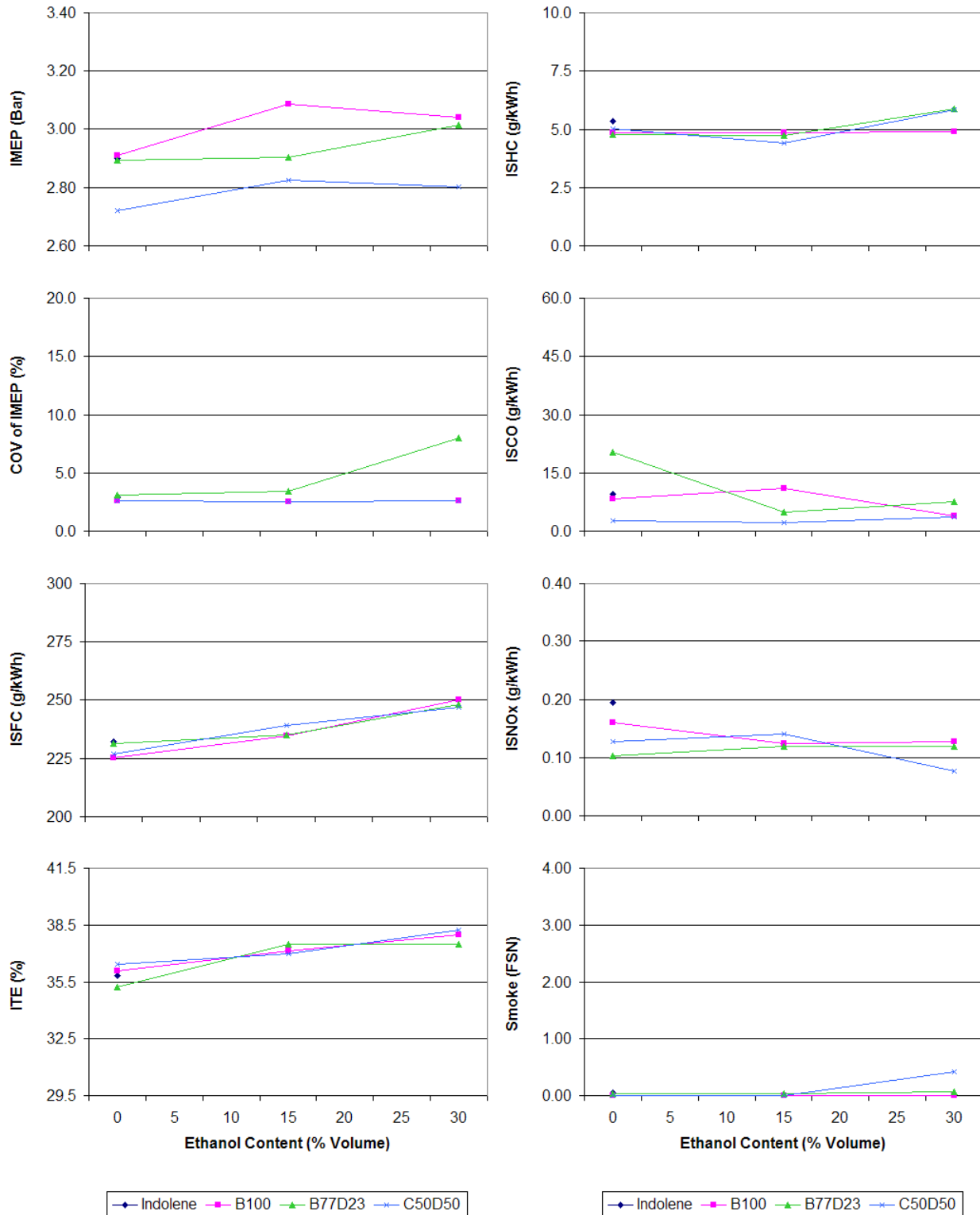


Figure 4.19 - Phase II-b Results for 3000 rpm, RBEI

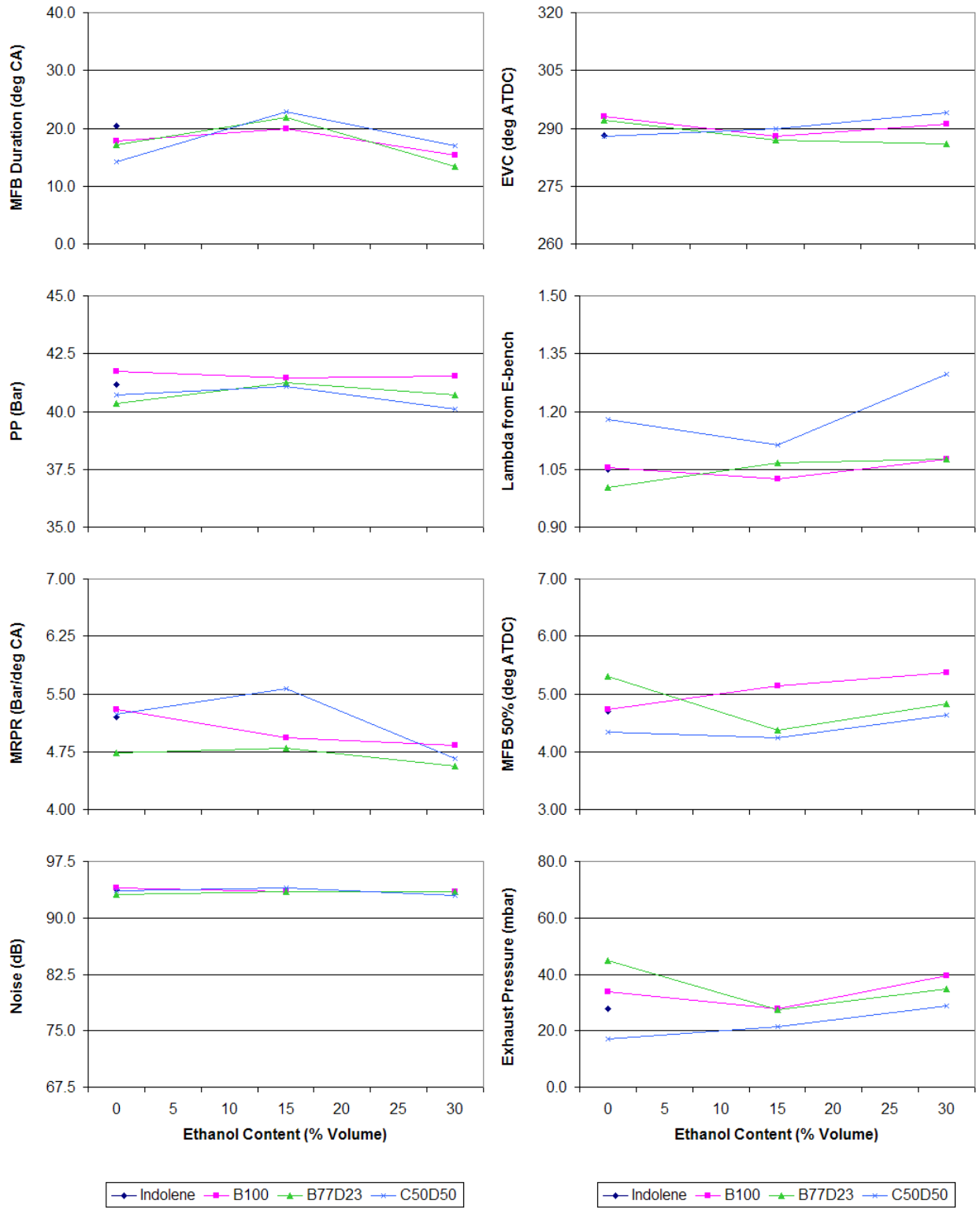


Figure 4.20 - Phase II-b Results for 3000 rpm, RBEI (2)

**CUSTOMER CONFIDENTIAL**

The electronic version is the only controlled copy.  
 All other copies are for reference only. Printed: 9/1/2009 4:09:13 PM  
 Page 46

CA4-prg-007 Technical Report  
 Originated: 01/01/04 Revised: 01/11/09

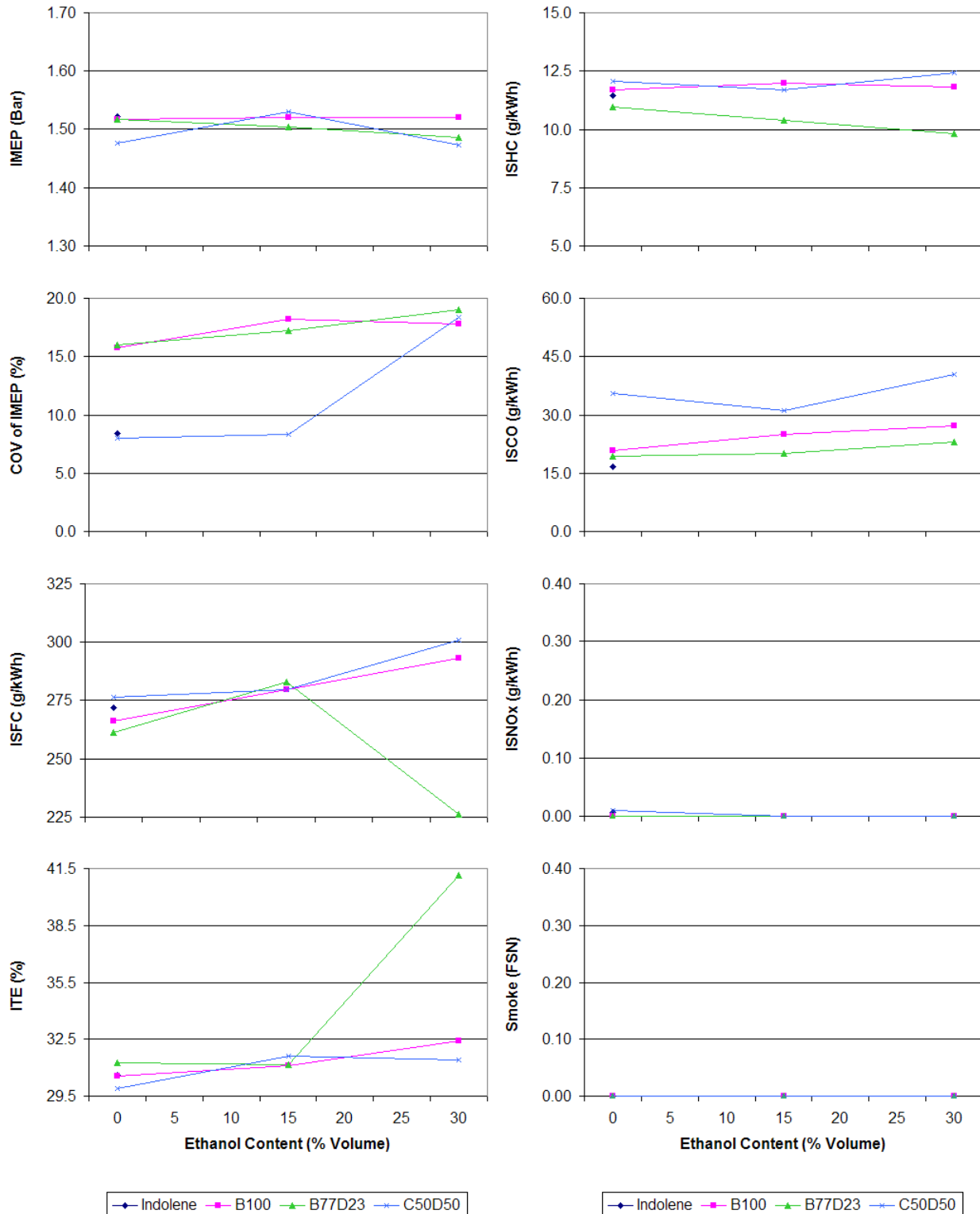


Figure 4.21 - Phase II-b Results for 1000 rpm, RCEI

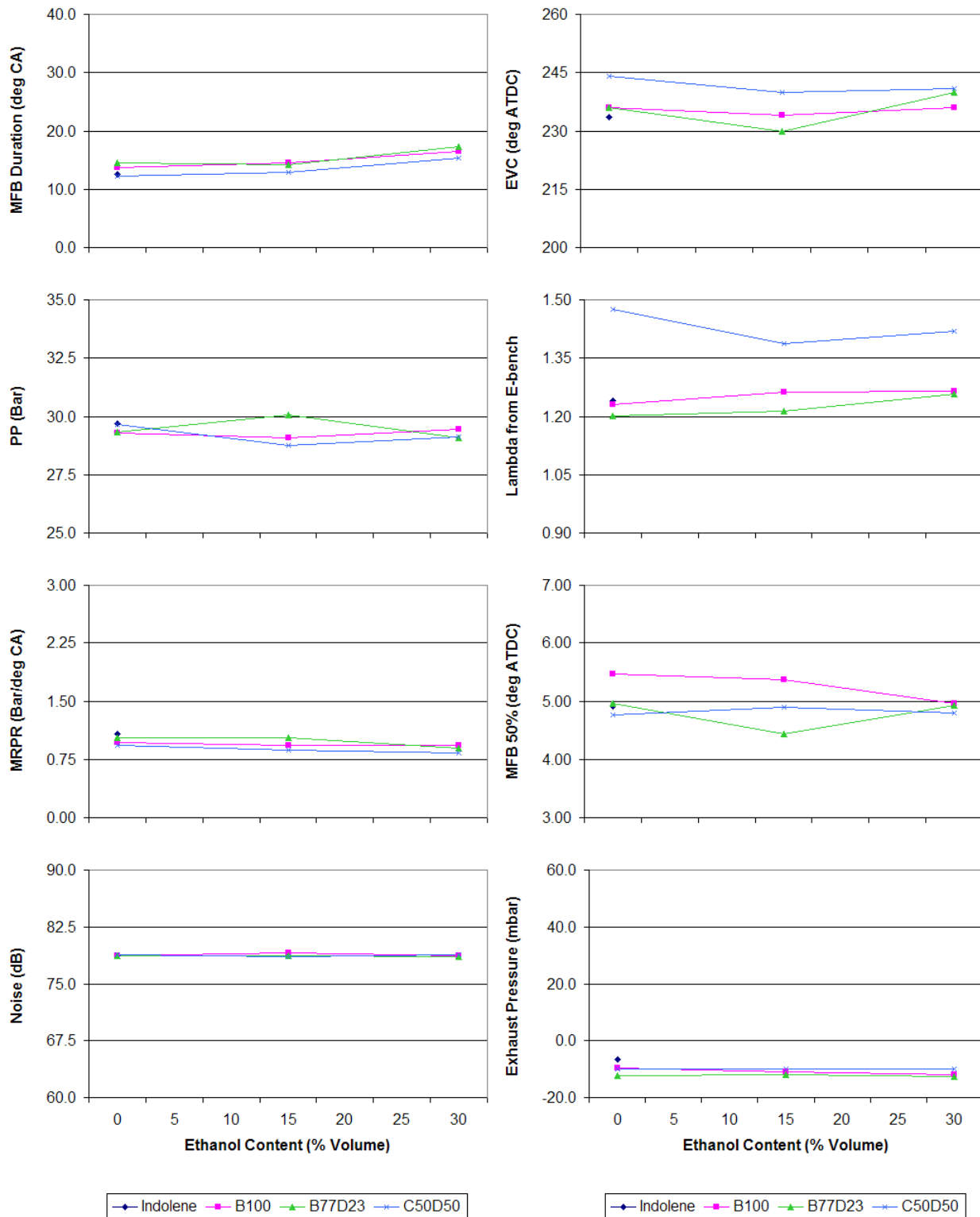


Figure 4.22 - Phase II-b Results for 1000 rpm, RCEI (2)

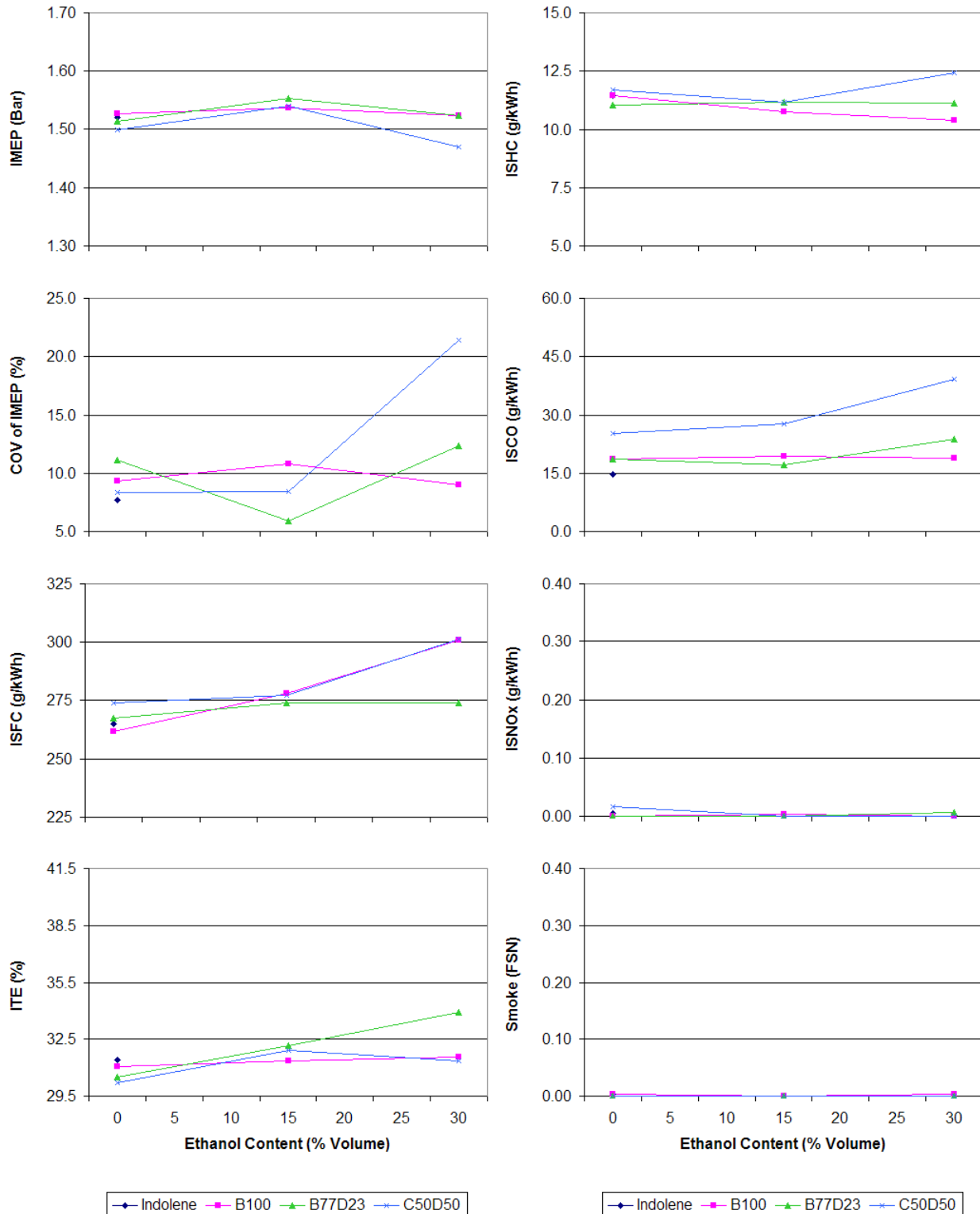


Figure 4.23 - Phase II-b Results for 1000 rpm, RBEI

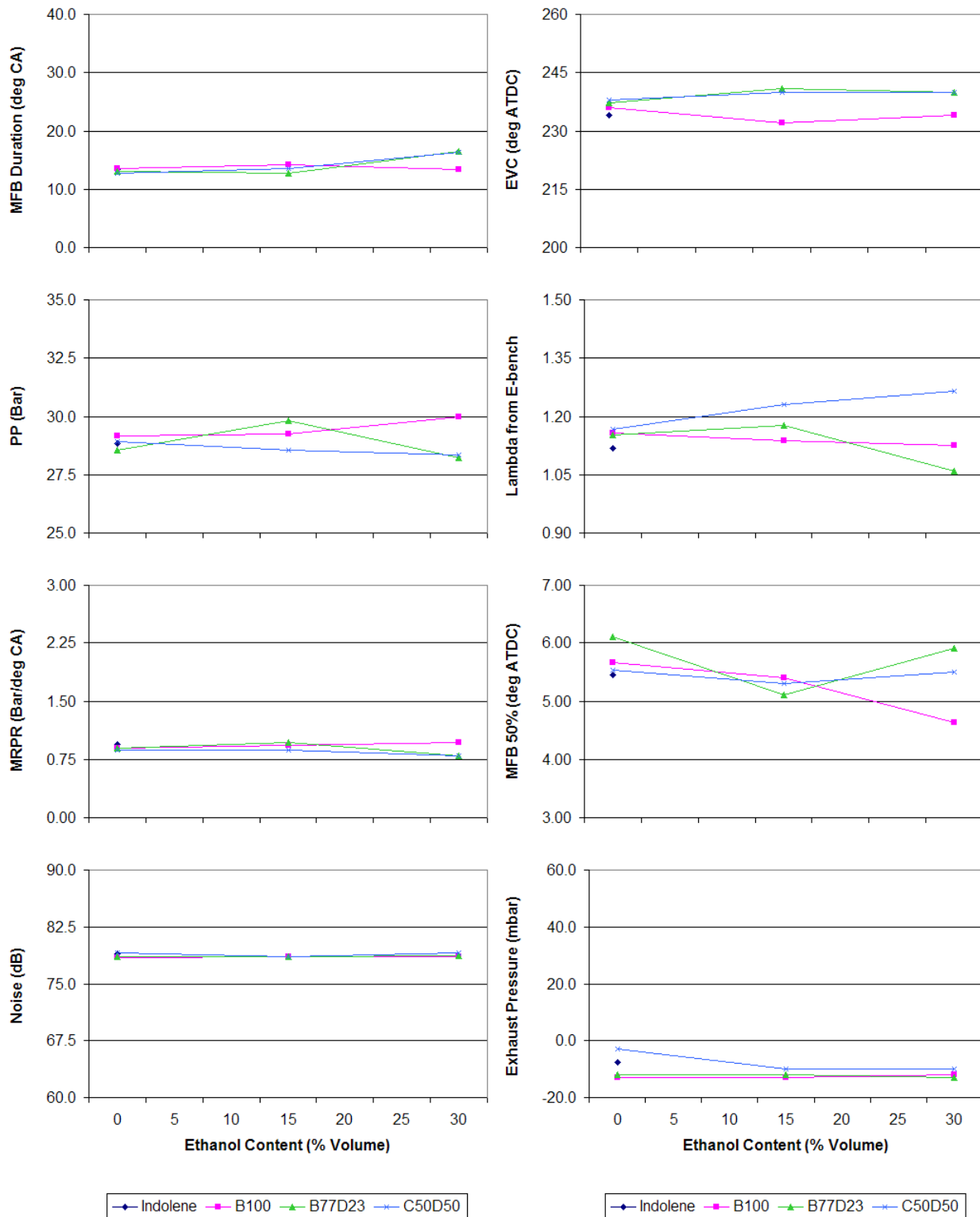


Figure 4.24 - Phase II-b Results for 1000 rpm, RBEI (2)



## 5. Statistical Data Analysis

After obtaining the engine and fuels data in this project, the data were subjected to quality reviews. The data handling process is described in Section 5.1. After assuring the quality of the data, data analysis was performed on the collected data. The methods behind this analysis are documented in Section 5.2. The final sections, Section 5.3 through 5.5, discuss the results of the three main analyses performed for the study. These were the selection of fuels, the indolene and repeat fuel test adjustments, and the regression analysis of performance parameters on fuel properties.

### 5.1. Data Handling

#### 5.1.1. Engine Test Data

Engine test data from all three test phases were incorporated into a spreadsheet, and sent by AVL to Battelle on February 2, 2009. This set of data incorporated some corrections to the data from the earlier phases of testing. This report only discusses findings relative to this new data source.

Raw data results were plotted against time and were reviewed for accuracy and completeness by the data analysis team at Battelle. This review process revealed some missing data.

- The first data measurement for Test Order 12 at 2000 rpm/RCEI was missing a filter smoke number (and indicated specific smoke).
- The first data measurement for Test Order 18 at 3000 rpm/RCEI was missing a combustion noise value.

Since the statistical analysis is ultimately performed on an average of multiple measurements, these missing values were simply excluded from the averages.

Battelle and AVL also jointly reviewed data with questionable values. This review produced several decisions about data to edit or to remove from the statistical analyses. These issues are summarized in Table 5.1.

#### 5.1.2. Fuel Properties

Another source of data for the analyses was the fuel properties. These were determined through fuel sample analysis. For Phase I, fuel property data was sent to Battelle in the form of a spreadsheet titled, "AVFL13 Fuel Analysis for Battelle - Updated 4-12-06". It was also combined with data on butane content of each fuel provided in a separate spreadsheet by AVL, "VOL% Percentage of n-C4.xls".



**Table 5.1 - Unusual Data Record Values**

Test Order	Fuel	Speed	Mode	Data Issue Identified	Resolution
21	A79D21	1000	RBEI	IMEP results average 1.9 versus target of 1.5	Point exceeds targeted operating condition; Exclude data from analysis
18	A79D21E30	1000, 2000, 3000	RBEI, RCEI	Very poor ISFC and ITE performance	Engine found to have been run at a negative exhaust pressure rendering results unrepresentative of intended target conditions; Exclude data from analysis
27	Indolene	3000	RBEI	ISCO values 10x higher than other tests of this fuel	Engine run too rich (Lambda<1); Exclude data from analysis
39	B77D23E30	1000	RBEI, RCEI	ISFC results do not reflect expected progression from 0 and 15% ethanol blends	Fuel measurement believed to be inaccurate; Exclude only ISFC and ITE results from analysis
Various	Various	1000	RBEI, RCEI	Measured NO <sub>x</sub> values were recorded as less than 0	All ISNO <sub>x</sub> values for such points were set to 0 and used in analysis

For Phase II-a, the fuel properties were sent as the file, “fuel\_data\_avfl-13b\_080107.xls.” The Phase II-a testing included two fuels that were also tested in Phase I, as well as four ethanol blends. When reviewing the Phase II-a fuel properties, several important issues were uncovered. The issues and their corresponding resolution were:

- The C100 and A79D21 fuels tested in both Phase I and Phase II-a did not show identical fuel property results. Since the fuel properties were determined from separate samples of each fuel, it was decided to associate the fuel properties with the corresponding phase of testing.
- The A79D21 and A50C20D30 fuels tested in Phase II-a were found to contain small amounts of oxygenates (ETBE, ETOH, and MTBE), the measure used to determine ethanol content for the Phase II-a ethanol blends. The ethanol content for these two fuels was included in the statistical analysis.
- The measured ethanol content for the C100E20, A79D21E10, A79D21E20, and A79D21E30 fuels varied from the 20, 10, 20, and 30 percent, respectively, that were targeted for each ethanol blend. The analyzed ethanol content was considered to be the actual result and was used for the statistical modeling.
- Indolene fuel properties were only determined in Phase I. It was assumed that the indolene fuel properties were the same in Phase II-a as in Phase I.

**CUSTOMER CONFIDENTIAL**



For Phase II-b, the fuel properties were sent as the file, "Fuel Data - AVFL13B 2nd fuel set b.xls" on February 10, 2009. These data were provided by Bill Cannella of Chevron. They represent an average of the values measured by ConocoPhillips and Chevron laboratories. Issues related to the Phase II-b fuel properties included:

- Fuels C50D50, B100, and B77D23 tested in Phase II-b were also tested in Phase I. As with the repeat fuels from Phase II-a, the fuel properties of the Phase II-b repeats were slightly different than they had been in Phase I, so the performance results for each of these fuels is associated with the corresponding fuel properties in the phase where it was tested.
- Indolene fuel properties were determined separately for the first indolene run in Phase II-b and for the final three indolene runs in Phase II-b. The indolene properties were similar to each other and to the properties from Phase I.

The information from the Phase I, Phase II-a, and Phase II-b fuel property spreadsheets used in the statistical analysis is provided as Appendix C.

## 5.2. Data Analysis Methods

The following section provides discussion of the methods used in the final analysis. This is divided into separate discussions of the indolene and repeat test fuels adjustments, and the regression analysis on the final adjusted results.

### 5.2.1. Indolene and Repeat Fuel Test Adjustments

Indolene fuel was run several times throughout the testing. Five other test fuels (A79D21, B100, B77D23, C100, and C50D50) were run one time in each of two different test phases. The measured performance parameter results for these repeated tests of common fuels showed some variability that could be correlated with attaining the desired controlled engine conditions. For example, each fuel test involved setting an engine speed, controlling the crank angle for 50% fuel burn, and achieving a target engine load (for the 1000 and 2000 rpm tests) or maximum rate of cylinder pressure rise (for the 3000 rpm tests). While it was possible to control the engine speed very precisely, there was more variability in the acceptable fluctuations of the other control parameters. Additionally, other uncontrolled conditions (i.e. ambient temperature, shifts in engine operation) may impact the performance of an engine on a particular test.

It was hypothesized that some of the observed variability in test fuel results may have been due to variation in attaining the controlled engine conditions and in the engine operation itself over time. It was therefore suggested that the test fuel results be normalized to a consistent set of control conditions. The repeated tests of indolene and other fuels throughout the test period provided an opportunity to make approximate corrections for variability in the test conditions or the engine operation. To do so, the following procedure was followed:

---

### CUSTOMER CONFIDENTIAL



1. For each performance parameter, the average repeat fuel test performance  $\bar{y}_{ij}$  was calculated for each of the  $i$  repeat fuel tests and each of the  $j$  engine operating modes. This yielded  $i \times j$  data points.
2. A multiple regression model was fit to the repeat fuel data with the  $\bar{y}_{ij}$  as the response variable and a set of predictors that included:
  - a. Engine operating mode (Mode) with a value of 1 for RBEI, and 0 for RCEI
  - b. The engine test phase (with Phase I as the reference)
  - c. The fuel (with indolene as the reference)
  - d. MFB 50% Location (MFB\_50)
  - e. IMEP at 1000 and 2000 rpm or MRPR at 3000 rpm
  - f. The interaction of d and e
  - g. The intake air temperature (IAT)
3. Factors a through c were automatically modeled. Backward, stepwise regression was employed for factors d through g to reduce the model to the smallest set of significant predictors. This process was done by successively eliminating the predictor with the highest p-value greater than 0.05 (i.e., least significant) for the F-test of the Type III sum of squares for that factor. This continued until only factors with a p-value of 0.05 and below remained. The final result of this step was an equation:

$$\hat{Y}_I = \hat{\beta}_0 + \hat{\beta}_1 * Mode + \hat{\beta}_2 * Phase + \hat{\beta}_3 * Fuel + \hat{\beta}_4 * MFB\_50 + \hat{\beta}_5 * IMEP \text{ (or MRPR)} + \hat{\beta}_6 * MFB\_50 * IMEP \text{ (or MRPR)} + \hat{\beta}_7 * IAT$$

where the  $\hat{\beta}_4$  through  $\hat{\beta}_7$  terms equal zero for the non-significant predictors

4. The relationship between the predictor variables and the responses as observed in the indolene and repeat fuel tests was used to adjust the test results of the test fuels as follows:

---

**CUSTOMER CONFIDENTIAL**



$$z'_k = z_k * \frac{\hat{Y}_{I_{ref}}}{\hat{Y}_{I_{act}}}$$

where

$z'_k$  is the adjusted value of a measured parameter for a particular test fuel at replicate  $k$

$z_k$  is the unadjusted value of a measured parameter for a particular test fuel at replicate  $k$

$\hat{Y}_{I_{ref}}$  is the predicted Phase I, indolene response at the mode of the test fuel data point and at the target control values of  $MFB_{50} = 5$ ,  $IMEP = 1.5$  (1000 rpm) or 3 (2000 rpm), or  $MRPR = 5.5$  (3000 rpm), and  $IAT = 25\ C$

$\hat{Y}_{I_{act}}$  is the predicted indolene response at the test phase and mode of the test fuel data point and the observed control values for the  $z_k$  test fuel data point

The final result of this adjustment process are performance results consistent with a reference set of engine operating conditions ( $MFB_{50}$ ,  $IMEP$ , and  $IAT$ ) and a single test phase.

### 5.2.2. Analysis of Engine Performance versus Fuel Composition and Properties

Once the final data, contained in Appendix E, were obtained and adjustments were made to a common operating condition per the procedure above, the performance data for the test fuels were ready to be modeled as a function of the fuel properties.

For each of the six engine test conditions (1000 rpm, 2000 rpm, and 3000 rpm each tested for RBEI and RCEI) in Phase I, Phase II-a, and Phase II-b, ten performance parameters were examined:

- Indicated specific fuel consumption (ISFC)
- Indicated thermal efficiency (ITE)
- Indicated specific  $NO_x$  emission (IS $NO_x$ )
- Indicated specific hydrocarbon emission (ISHC)
- Indicated specific carbon monoxide emission (ISCO)
- Indicated specific smoke (IS $_{SMK}$ )
- Combustion duration
- Coefficient of Variance (COV) of  $IMEP$
- Noise
- Peak cylinder pressure

---

#### CUSTOMER CONFIDENTIAL



Additionally, the engine control parameters crank angle at EVC, MRPR (1000 and 2000 rpm only) and IMEP (3000 rpm only) were evaluated because of their potential to impact the performance parameters.

The performance data were modeled using the averages of the multiple condition-adjusted data points at each speed and mode. The averages were selected, rather than modeling the individual data values, because the averages represent a more robust measurement of the steady state engine operation, and because modeling transients within an engine run were not of interest in this evaluation.

The ten fuel properties of interest as predictors were:

- RON
- Sensitivity
- T10
- T90
- % Aromatics
- % Iso Paraffins
- % Normal Paraffins without C4
- % Butane
- % Olefins
- % Ethanol

At this point, two separate statistical analyses were performed: One for the effect of ethanol content and one for the remaining nine fuel properties in fuels without ethanol. Since ethanol was only blended into a subset of the original ten test fuels, the statistical analysis of the effects of ethanol are best treated separately, since including them in the primary analysis would confound the effects of the five ethanol blended fuels and the effects of ethanol itself.

#### 5.2.2.1. Ethanol Modeling

Five base fuels (A79D21, C100, C50D50, B100, and B77D23) were tested in Phase II with varying amounts of ethanol content. Each was originally tested in Phase I with no ethanol. A79D21 and C100 were subsequently retested in Phase II-a with no ethanol and then with ethanol blends (10, 20, and 30 percent for A79D21 and 20 percent for C100). C50D50, B100, and B77D23 were retested in Phase II-b with no ethanol and then each with 15 and 30 percent ethanol blends. The net result of this testing was a set of 20 fuel tests, spanning five different starting fuel types.

For each performance parameter, the mean adjusted data for the fuel tests was fit to three separate statistical models, each with a random effect for the five fuel types (assumed to be normally distributed with mean 0). The base model had no other factor. The second model had an additional linear, fixed effect, for the percentage of ethanol.

---

#### **CUSTOMER CONFIDENTIAL**



The third model had both linear and quadratic, fixed effects, for the percentage of ethanol. The models were fit in SAS® v9.1.3 using the PROC MIXED procedure and the maximum likelihood solution type.

The negative of twice the log-likelihood (-2LL) of the three separate models was compared. If the -2LL from the second model was more than 3.84 (corresponding to a  $X^2$  with one degree of freedom) less than the base model, a significant linear effect was concluded. A further comparison was made for the -2LL reduction of the quadratic model relative to the linear model, with the quadratic model being concluded if more than 3.84 less than the linear mode. If the linear model was not found to be significant, a separate comparison was made between the quadratic model and the base model (this time with a comparison to a  $X^2$  with two degrees of freedom=5.99), with the quadratic model being concluded if the -2LL was more than 5.99 less than the base model. If the procedure above yielded no significant differences, it was concluded that there was insufficient evidence to conclude either a linear or quadratic relationship between the performance parameter and ethanol content.

Following the model selection procedure above, the most appropriate model was fit again using the PROC MIXED procedure in SAS® v9.1.3, but with the restricted maximum likelihood method. This provided the estimates for the coefficients of the best relationship to ethanol content.

#### 5.2.2.2. Other Fuel Properties

The ten test fuels in Phase I were selected to be representative of the design space of the nine fuel properties originally of interest. In Phase II-a, two of the original ten fuel types (A79D21 and C100) were tested again. Three of the original ten fuel types were tested again in Phase II-b (C50D50, B100, and B77D23). These base fuels were from unused drums that were blended in Phase I. For Phase II-b, drums of the same base fuel were mixed together in a tank and re-drummed to ensure no drum-to-drum variation. These repeat tests provided additional information about the original design matrix for fuel tests. Phase II-a additionally included one new fuel (A50C20D30) that filled some gaps in the design matrix for fuel properties. Taken together, these 16 fuel tests provided the basis for the evaluation of effects with fuel properties. Note that since ethanol was only blended into a subset of the original ten test fuels, the statistical analysis of the effect of ethanol are best treated separately, since including them in the primary analysis would confound the effects of the five ethanol blended fuels and the effects of ethanol itself.

At the first phase of the evaluation, where there were ten distinct fuel formulations, it was decided to limit analysis to regression models with two fuel property factors and their interaction. This was motivated by the fact that models with greater numbers of factors did not leave enough degrees of freedom to properly estimate random variability. The additional fuel tests available at the conclusion of Phases 2a and 2b raise the total fuel tests to 16, but only 11 of these are distinct formulations. Therefore, it was decided

---

#### **CUSTOMER CONFIDENTIAL**



to perform the same two factor with interaction regression analysis for the combined Phase I, 2a, and 2b data as was done at the conclusion of Phase I.

Regression models were fit for each performance parameter as a function of each possible combination of two fuel properties and their interaction. With nine fuel properties, this resulted in 36 unique models of a performance parameter as a function of the nine fuel properties. For each of these models, the following data were tabulated:

- The correlation coefficient ( $r^2$ ) for the model – the degree to which this model explains the overall variability seen in the data
- The mean square error – the remaining variation unexplained by the model
- The coefficients for each of the regression parameters and the corresponding p-values for whether they were significantly different from zero. The coefficients were for the intercept of the model, the first fuel property, the second fuel property and the interaction (i.e., product of the two fuel properties).

The models were fit in SAS® v9.1.3 using the PROC GLM procedure.

After fitting and documenting all possible models, the results were reviewed to try to identify a “best” model. In most cases, this was the two-factor model that was most effective at explaining the observed variability in performance results across all speed and mode operating conditions. A ranking approach was utilized for this process, whereby each model was reverse ranked from poorest to best, relative to the others within a speed and mode condition (highest rank = 36, lowest rank = 1). The six speed and mode rankings for each two-factor model were summed, and the model with the highest sum of ranks was deemed the best. In a limited number of cases, this process was modified (i.e. when results from certain speeds and modes were not meaningful).

### 5.3. Fuel Selection Analysis Results

#### 5.3.1. Phase I

Battelle’s report, “Selection of Representative Fuels for Testing in CRC Project AVFL-13, Fuel Chemistry Impacts in Gasoline HCCI”, [August 15, 2005] provides a detailed description of the methodology and final recommendations for a set of candidate fuels. These recommendations were ultimately adopted by CRC and the following set of fuels (in order) was evaluated in the first phase of testing:

- A100 (A)
- B30D70 (G)
- A79D21 (F)
- B77D23 (I)



- B100 (B)
- C85D15 (K)
- C50D50 (J)
- C100 (C)
- B50D50 (H)
- A33D67 (E)

The fuels were defined so that the name indicated the target relative percentage of each of the four component blend stocks. For instance, B30D70 was targeted to be made up of 30% blend stock B and 70% blend stock D. The letters in parentheses after the fuel are the unique plotting symbols associated with each of the fuels in the results.

Although not one of the ten selected test fuels, the blend stock “D” fuel is referenced in some of the results and is identified with the letter “D”. The letter “E” was added later to indicate the target volumetric percentage of ethanol.

Indolene was a fuel used in the testing to perform an initial evaluation of the test engine’s ability to run in HCCI and subsequently run periodically throughout the testing as a means of establishing repeatability of engine performance results. In Phase I, it was run before A100 at all speed and mode combinations tested, as well as before B77D23 and C50D50 at all the 2000 and 3000 rpm test conditions. It is identified with a plotting symbol of “O”.

### 5.3.2. Phase II-a

In a second phase of testing, CRC AVFL expanded the fuels to be studied through the addition of seven fuel tests. To assure traceability with the first phase of testing, two of these fuels, C100 and A79D21, were the same formulation as a fuel tested in Phase I. To study the effects of ethanol on engine performance, four ethanol-blended fuels were created; a planned 20 percent ethanol for C100, and planned 10, 20, and 30 percent ethanol for A79D21. Finally, a seventh fuel was selected that provided an intermediate olefin content, since the fuels in Phase I were all either less than 3% or greater than 18% in olefins. The final set and ordering of Phase II-a fuels tested were:

- A79D21E30 (S)
- A79D21E20 (R)
- A79D21 (Phase II-a) (P)
- A79D21E10 (Q)
- C100 (Phase II-a) (M)
- C100E20 (N)
- A50C20D30 (L)

For the 1000 rpm, RCEI test condition, the A79D21 test fuel results from Phase II-a were excluded from analysis because the indicated mean effective pressure

---

#### **CUSTOMER CONFIDENTIAL**



(approximately 1.9) was judged by AVL to be too high compared to the targeted value of 1.5. The entire set of A79D21E30 test fuel results were ultimately removed when it was discovered that they had been run at a negative exhaust pressure.

In Phase II-a, testing was also completed with indolene fuel. These tests were performed before A79D21E30, before A79D21E20, before C100 and after A50C20D30. For the 3000 rpm, RBEI mode, indolene testing was performed after A50C20D30, but the data were later removed when it was judged that the very low air-fuel ratio (below 1) for the run was not representative of other indolene tests and normal engine operation. The indolene fuel used in Phase II-a was not chemically analyzed, so no fuel properties are available for it.

### 5.3.3. Phase II-b

The final set of fuel tests consisted of nine additional test fuels; three test fuels repeated from Phase I as well as a 15 and 30 percent ethanol blend of each. The fuel test order was:

- C50D50 (T)
- C50D50E15 (U)
- C50D50E30 (V)
- B100 (W)
- B100E15 (X)
- B100E30 (Y)
- B77D23 (Z)
- B77D23E15 (&)
- B77D23E30 (#)

In Phase II-b, testing was also completed with indolene fuel. These tests were performed before C50D50, before B100, before B77D23 and after B77D23E30. The indolene fuel properties for the first test in Phase II-b were analyzed and are represented by the plotting symbol "\*\*\*". The fuel properties for the final three runs of indolene in Phase II-b were determined separately and are represented by the plotting symbol "+".

An important aspect of the fuel selection analysis was the degree to which the set of fuel properties were jointly represented by the selected fuels. One tool in evaluating this issue was pairwise plots of the values of the fuel properties. Figure 5.1 to Figure 5.6 show the pairwise plots incorporating Phase I fuels (shown in red), Phase II-a fuels (shown in blue), and Phase II-b fuels (shown in green) for the original nine fuel properties of interest and ethanol. Indolene properties are also shown, but these are an exception to the color coding convention. The three available sets of indolene fuel properties (Phase I, first run of Phase II-b, and last three runs of Phase II-b) are all



shown in black. The pages are laid out so that they read from top to bottom and left to right of a triangle showing all 45 unique combinations of pairs of the 10 fuel properties.

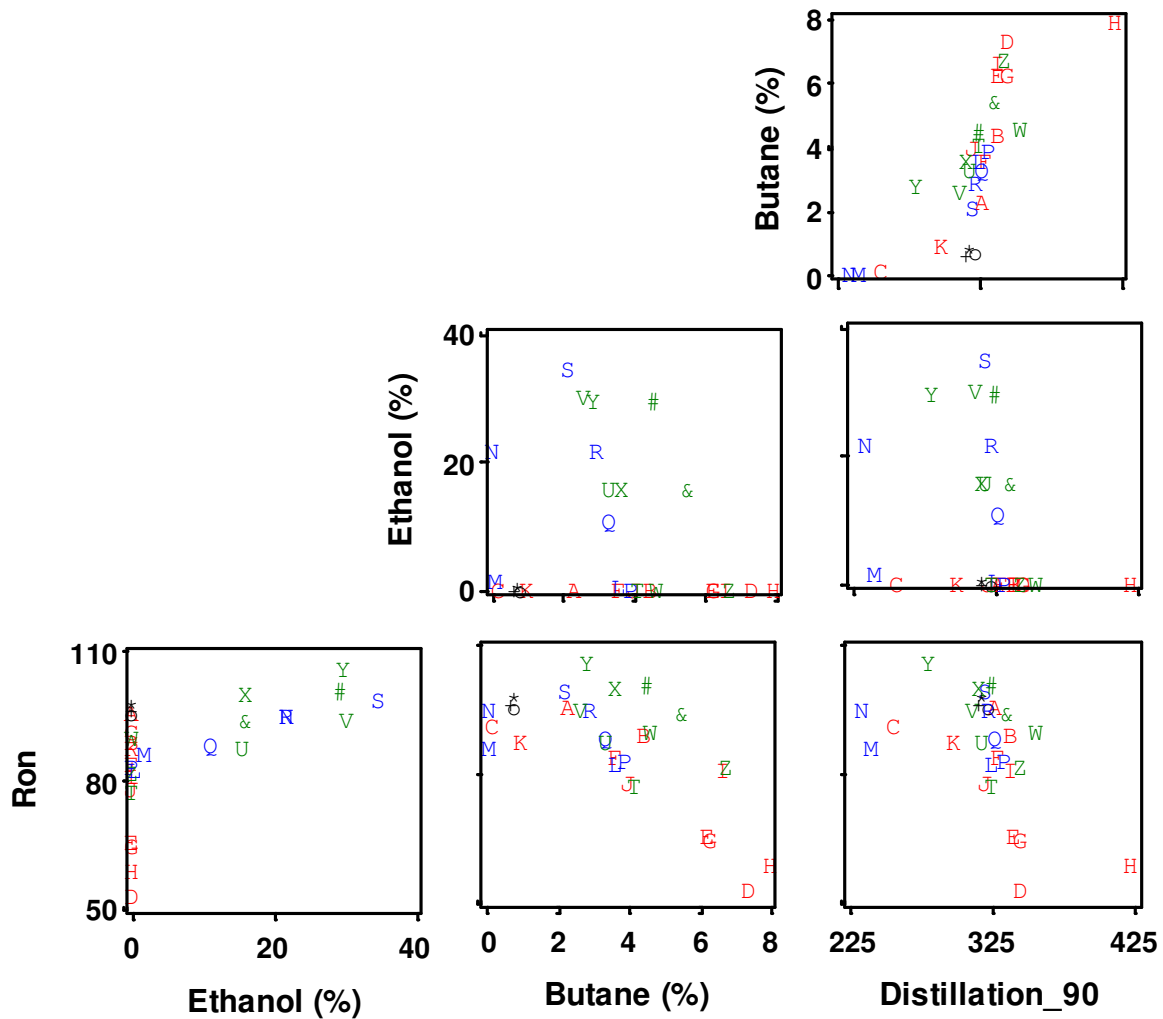


Figure 5.1 - Pairwise Fuel Properties for Phase I and Phase II

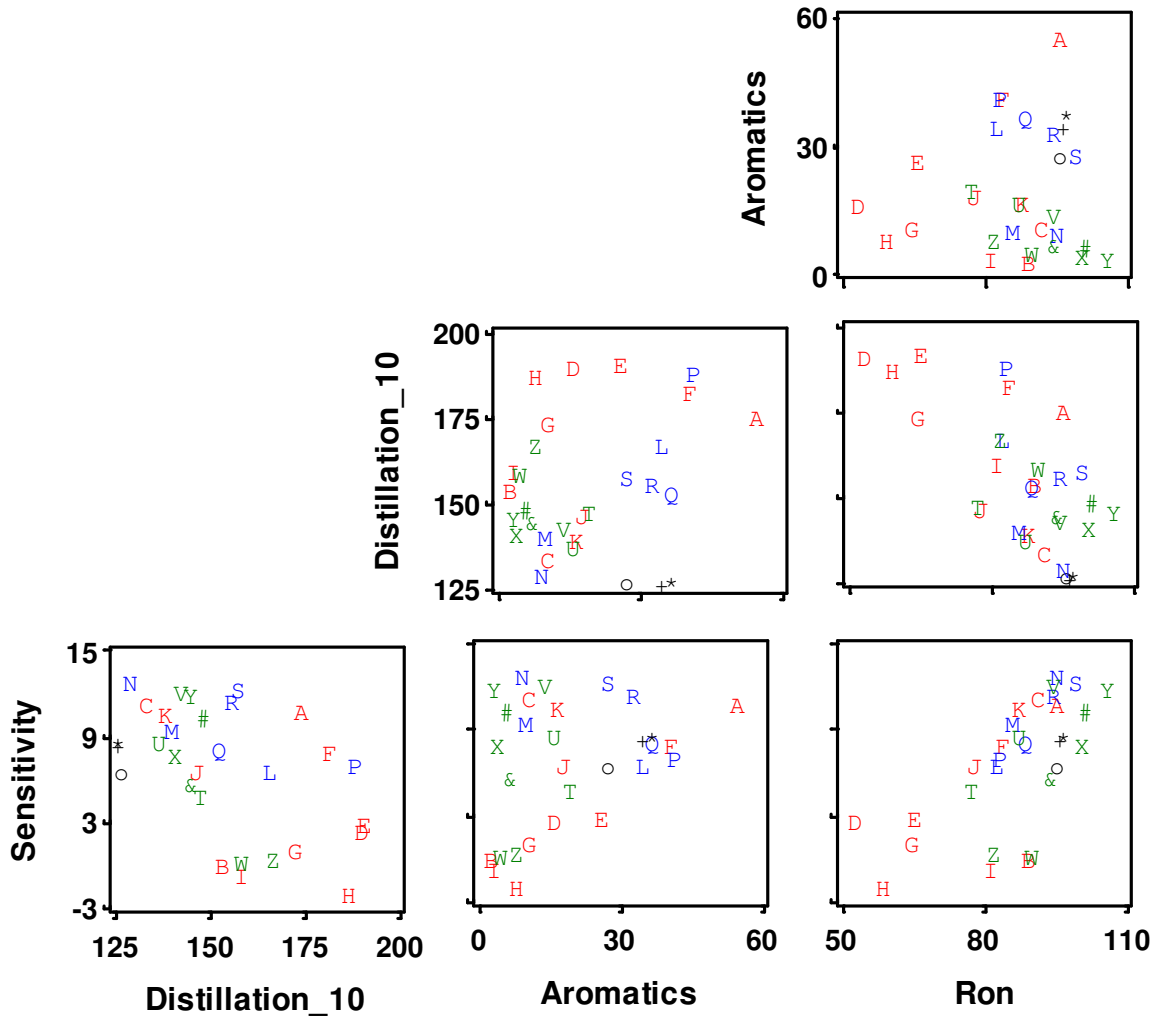


Figure 5.2 - Pairwise Fuel Properties for Phase I and Phase II (2)

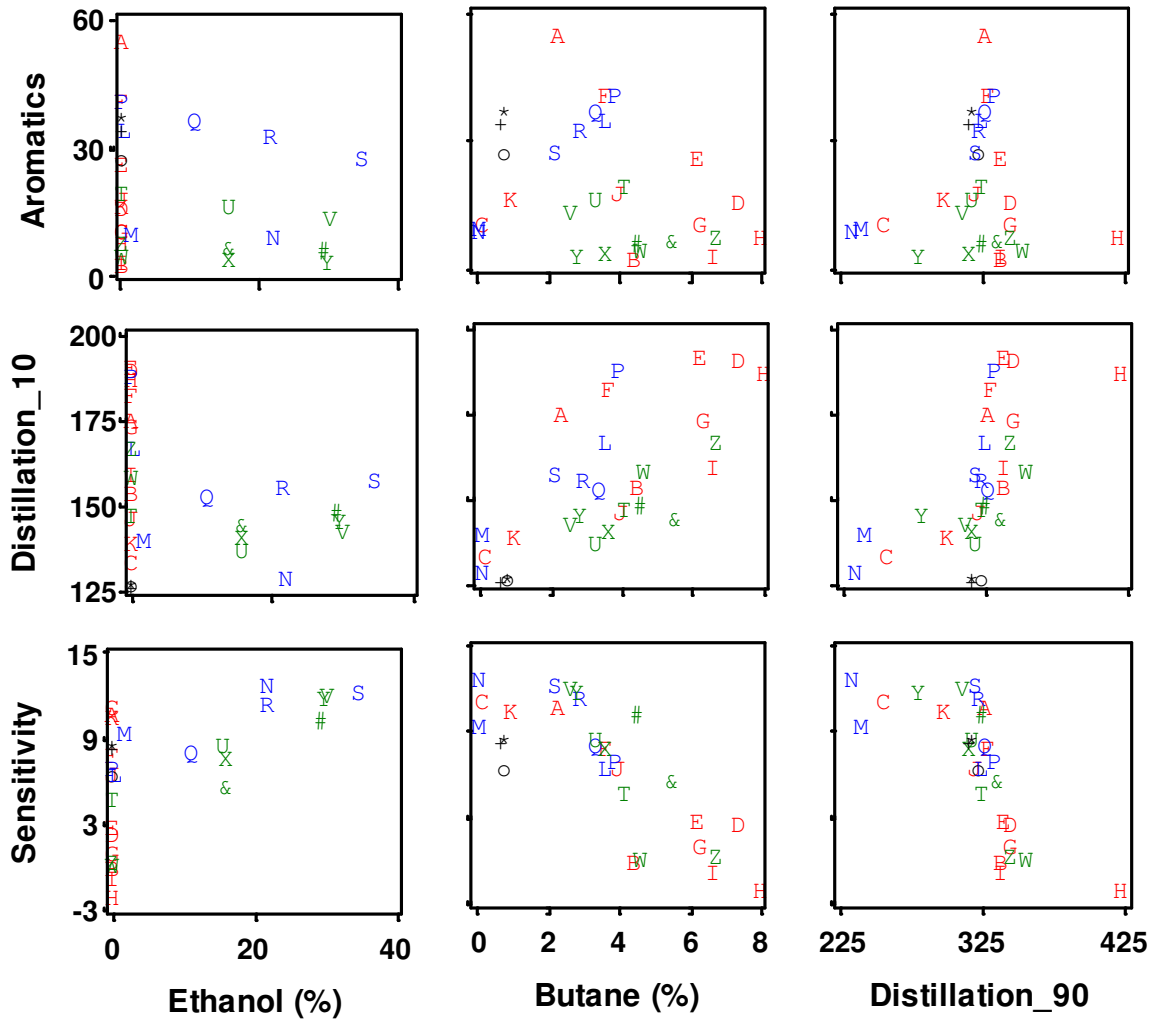


Figure 5.3 - Pairwise Fuel Properties for Phase I and Phase II (3)

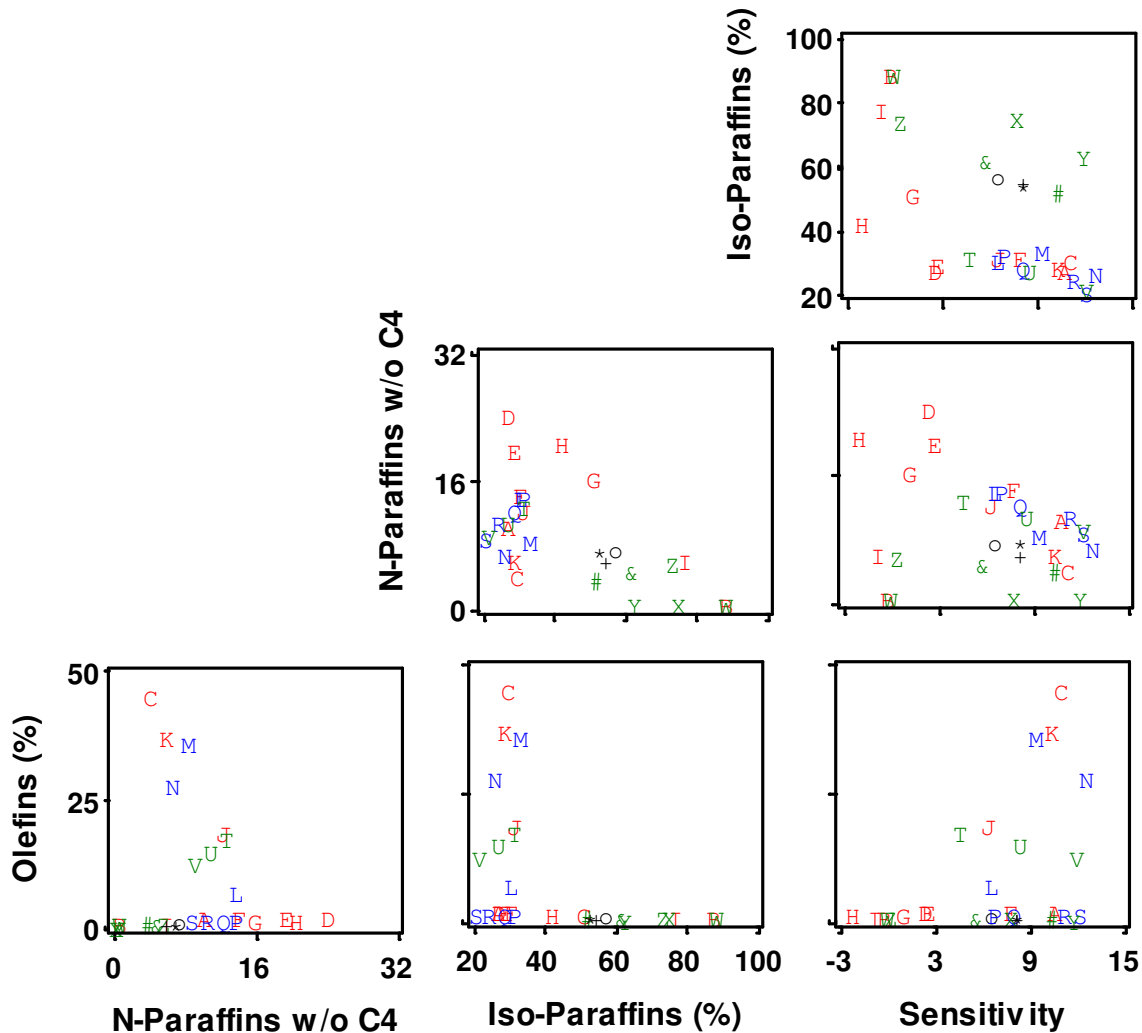


Figure 5.4 - Pairwise Fuel Properties for Phase I and Phase II (4)

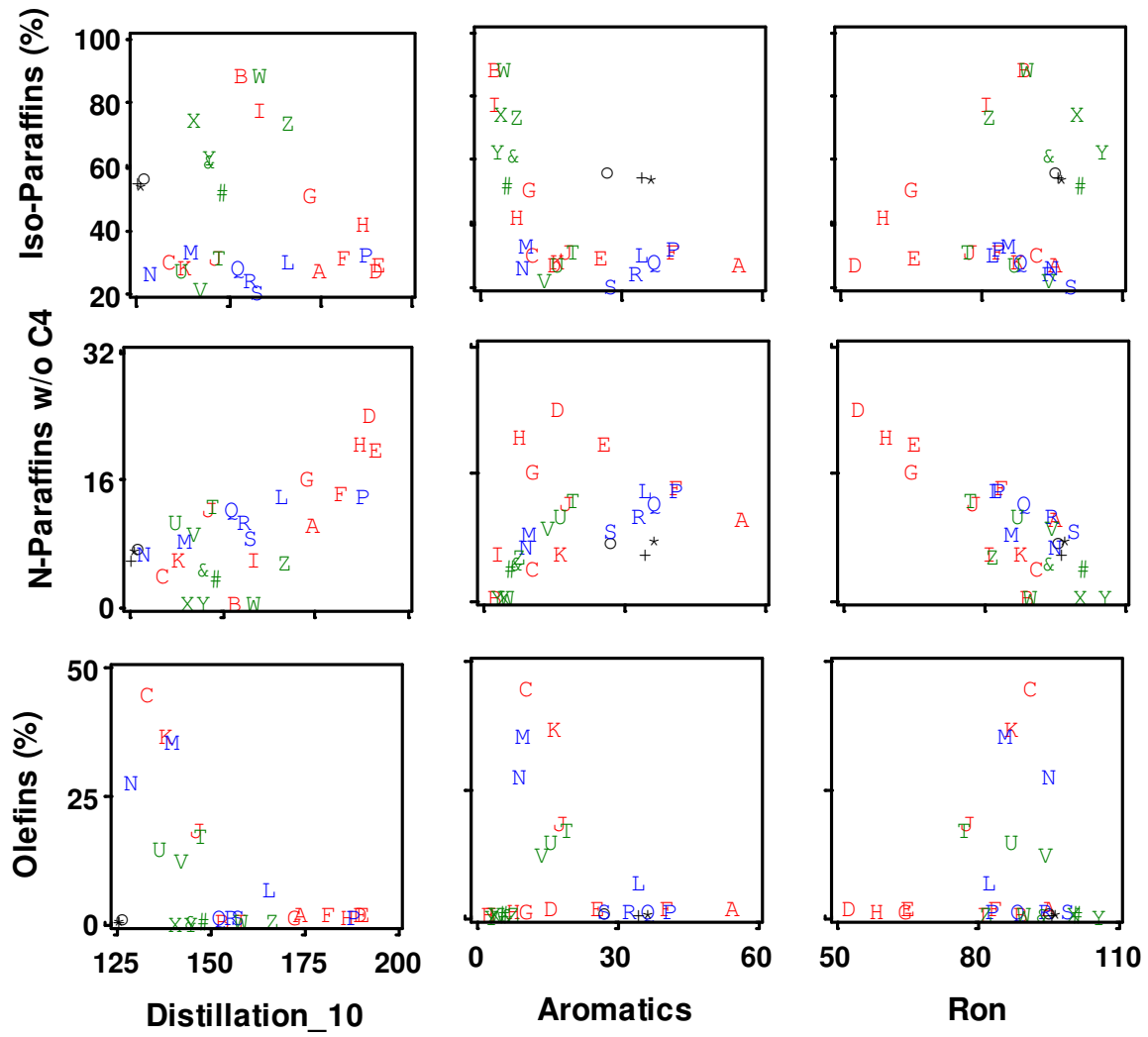


Figure 5.5 - Pairwise Fuel Properties for Phase I and Phase II (5)

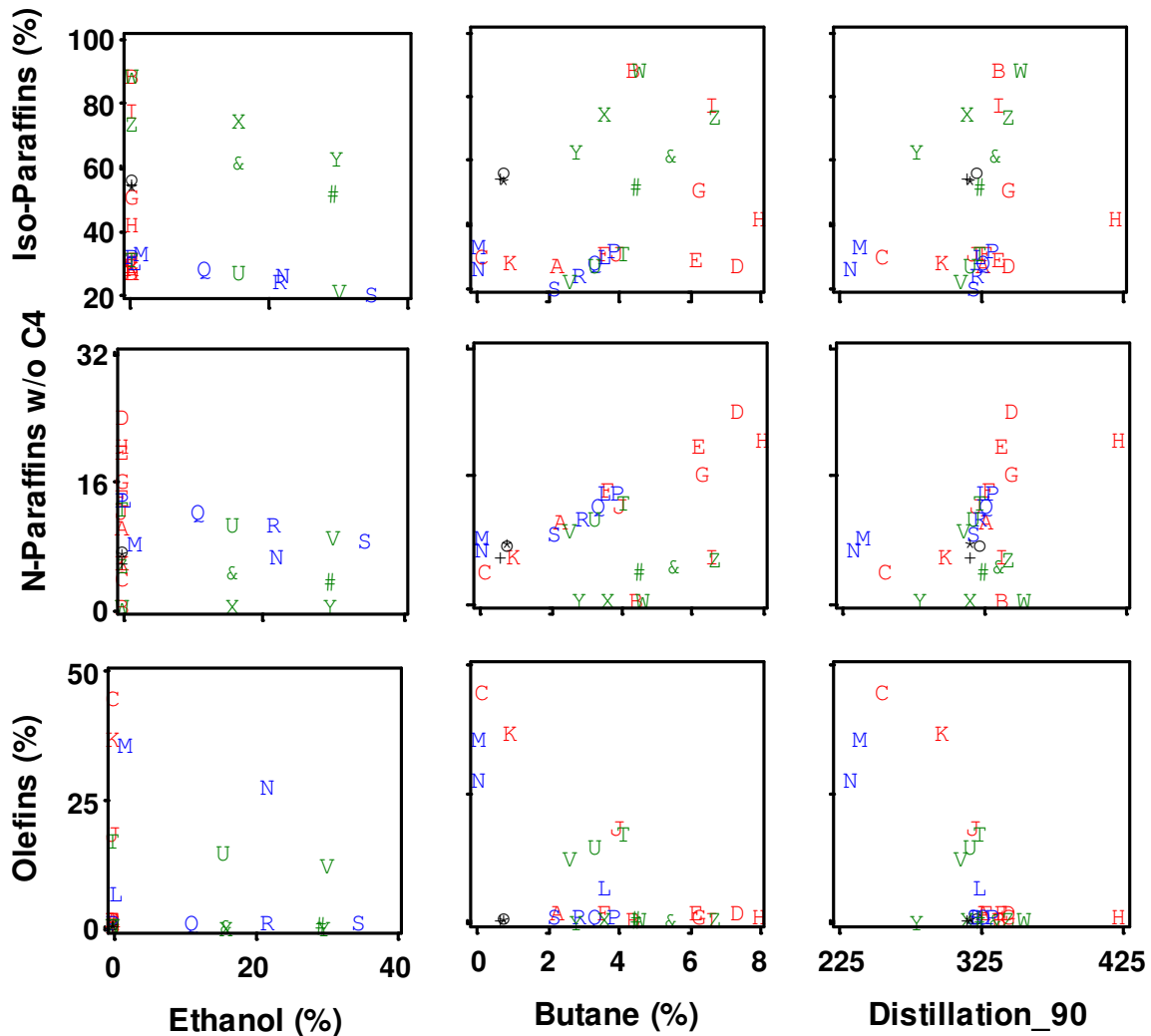


Figure 5.6 - Pairwise Fuel Properties for Phase I and Phase II (6)

#### 5.4. Indolene and Repeat Fuel Test Adjustments

Following the methodology outlined in Section 5.2.1, measured performance parameter results for the combined set of Phase I, Phase II-a, and Phase II-b data were normalized to a common set of operating conditions determined by the combined set of indolene and repeat test fuel results.

In evaluating the adjustments, an issue was found where indolene or repeat fuel measurements reached a very low air-fuel ratio (i.e., close to or less than 1) and



resulted in significant increases in hydrocarbon and CO levels. As documented in Table 5.1, the final indolene run in Phase II-a was removed from all analysis because of anomalously low air-fuel ratio. However, several other fuel tests had low air-fuel ratio values that were judged to be legitimate, but which nevertheless caused significant hydrocarbon and CO increases. To prevent skewing of the adjustment process, 3000 rpm indicated specific hydrocarbon data for air-fuel ratios below 1 were excluded from the process of determining repeat fuel adjustments. Similarly, indicated specific CO values greater than 5.0 (all occurring at low air-fuel ratios) were also excluded. With the exception of indolene, these data were not excluded from having the indolene and repeat fuel test adjustments applied to them and from subsequent use in the final statistical analysis.

Table 5.2 shows the regression equations that were developed from the repeat fuel tests. It also provides information on the test-to-test variability of the performance parameters. These indolene and repeat fuel adjustments were very important in reducing observed variability in the parameters from phase to phase. The Phase II-b testing was completed after an engine rebuild, and several of the key performance parameters appeared to shift significantly in Phase II-b relative to the earlier test phases.

The final two columns of Table 5.2 contain estimated coefficients of variation (estimated “standard deviation” of unexplained variability divided by the mean parameter value). The first of the two columns shows the repeatability result with only the mode and fuel type adjustments. For example, the value of 35.7% for indicated specific  $\text{NO}_x$  at 2000 rpm means that the standard deviation of repeat test fuel measurements adjusted to a common fuel (indolene) and mode (RCEI) are approximately 36% of the mean of these adjusted fuel results. The second of the two columns shows the same coefficient of variation after taking into account the variability that can be explained by the engine control and test phase variables. For the 2000 rpm,  $\text{NO}_x$  example, the coefficient of variation drops from 36% to 21%. The results in the two columns illustrate that parameters vary considerably in the proportional test-to-test variability within the indolene and repeat fuel tests. The coefficients of variation vary from less than 1% to almost 300%. Small values represent more “repeatable” results from test to test for a particular fuel.



**Table 5.2 - Normalization of Measured Response Variables**

Response Variable	Speed	Regression Coefficients for Modeling Indolene and Repeated Fuels Testing												Approximate Test-to-Test Variability for Repeated Fuels Tests Coefficient of Variance (%)		
		Intercept	Mode 1 RBEI	Phase 2a	Phase 2b	Fuel (A79D21)	Fuel (B100)	Fuel (B77D23)	Fuel (C100)	Fuel (C50D50)	MFB_50	Pressure	MFB_50 * Pressure	TL22	Only Mode Fuel Adjustment	Full Model
BI	1000	416.72	-4.14	18.20	12.65	5.75	-5.32	1.77	-0.84	0.24		-104.78			2.97	2.19
	2000	-664.69	-0.60	2.94	16.24	1.65	-6.05	-5.54	-11.66	-7.35	205.95	300.11	-70.37		4.07	1.79
	3000	327.67	2.17	0.23	14.87	4.82	0.64	0.96	-6.52	-5.77	-20.69	-20.10	3.64		4.06	2.01
ITE	1000	92.34	0.42	-1.64	-1.52	-1.13	0.08	-0.70	-0.83	-0.29	-14.72	-39.02	9.60		3.34	2.30
	2000	225.26	0.16	-0.52	-2.92	0.23	0.11	0.21	1.71	1.23	-42.70	-63.68	14.60		4.09	1.97
	3000	45.09	-0.40	0.60	-2.60	-0.77	-0.54	-1.15	0.41	1.00			-0.23	4.12	2.20	
I_PNOX	1000	0.01	0.00	0.00	-0.01	0.00	0.00	0.00	0.00	0.01					60.67	51.45
	2000	0.08	0.00	0.00	0.05	-0.02	-0.02	-0.03	-0.04	-0.06					35.66	21.27
	3000	-0.04	-0.06	0.05	0.08	0.06	-0.02	-0.02	-0.04	-0.07		0.04			29.99	20.95
I_PHC	1000	10.65	0.04	0.15	-6.17	-0.61	-0.16	0.22	0.05	-0.20	1.32				21.82	7.48
	2000	29.09	2.69	-0.85	-2.34	-0.14	-1.12	-0.45	-0.96	-1.10	0.67	-10.13		0.17	20.03	10.25
	3000	4.01	3.27	-0.22	-1.77	1.04	-0.42	-0.17	-0.09	-0.14					24.03	17.69
I_PCO	1000	94.23	-3.20	-1.63	-15.16	-2.89	-0.05	2.73	19.99	12.82	3.25	-51.48			29.21	11.88
	2000	136.44	-0.20	-0.31	-0.78	0.33	-0.48	0.44	0.65	0.37	-24.84	-46.48	8.52	0.13	16.14	8.99
	3000	2.39	0.40	0.38	0.36	0.64	-0.19	1.43	0.49	0.02					22.22	21.95
I_PSMK	1000	0.00	0.00	0.00	0.00	0.00	0.00	0.00	0.00	0.00				0.00	89.99	62.40
	2000	0.00	0.00	0.00	0.00	0.00	0.00	0.00	0.00	0.00					100.23	87.44
	3000	-0.29	0.04	-0.01	-0.01	0.13	-0.03	0.00	-0.01	0.00				0.01	284.84	277.59
MFB_Duration	1000	13.17	0.22	-1.83	-0.12	-0.32	0.03	0.09	1.45	-0.06					7.91	5.33
	2000	119.16	0.80	-0.23	0.65	0.13	0.00	0.04	-0.08	-0.47	-22.33	-39.01	7.80		8.48	5.05
	3000	-5.12	-0.56	1.21	10.10	-0.32	-4.16	-0.80	0.84	-2.75			0.58		41.13	18.19
VPI	1000	50.81	-0.53	1.43	-1.98	-1.78	3.43	3.43	5.40	-0.21		-26.41			27.05	23.63
	2000	2.29	0.26	-0.26	-0.40	0.01	-0.23	-0.27	0.26	0.61					24.06	23.22
	3000	2.97	1.44	0.66	-0.86	-0.27	-0.60	-0.58	0.60	0.16					36.39	33.61
Noise	1000	74.28	0.16	-1.63	4.63	-1.29	-0.89	-0.70	0.04	0.07					3.74	0.97
	2000	-99.12	-1.14	-0.65	0.16	-0.24	0.02	0.16	0.80	0.58	35.90	64.77	-12.52		1.29	0.77
	3000	88.11	0.69	0.24	0.37	0.17	0.01	0.10	-0.21	-0.23	-0.17	1.05			0.75	0.31
CYPMX	1000	26.76	-0.17	1.68	0.70	-0.38	0.10	0.16	0.15	-0.24	-0.69	3.63			2.86	1.09
	2000	-53.95	-1.59	1.19	1.45	-0.48	0.21	0.06	0.90	0.51	15.26	33.56	-5.57		2.27	0.99
	3000	32.74	2.71	1.63	1.22	-0.44	0.00	-0.06	0.06	-0.45	-0.60	1.45			2.93	1.04
ExtClose	1000	153.11	2.50	-1.12	1.67	1.25	0.47	0.10	10.80	6.22		51.82			1.98	1.68
	2000	243.63	5.94	3.42	6.38	-1.81	-1.54	0.46	4.69	4.71					1.53	1.00
	3000	251.61	17.13	5.76	8.27	4.60	0.28	0.70	6.71	3.65		2.63			1.87	1.31
PI	3000	1.87	0.18	0.06	-0.03	-0.06	-0.05	-0.04	-0.07	-0.11	0.06	0.11			3.39	2.74
PR_CYP	1000	1.37	-0.01	0.13	0.17	-0.12	-0.01	0.00	-0.14	-0.12	-0.10				10.85	7.23
	2000	6.05	-0.33	-0.24	0.01	-0.08	0.03	0.12	0.12	-0.02	-0.49				11.50	7.20

Note: Mode 2-RCEI and Indolene fuel are references (i.e., no adjustment). Pressure is PI for 1000 and 2000 rpm, PR\_CYP for 3000 rpm

**CUSTOMER CONFIDENTIAL**



The Pressure adjustment in Table 5.2 denotes the variable IMEP for the 1000 and 2000 rpm conditions since IMEP is a control parameter for these conditions. Similarly, the Pressure adjustment is the variable “MRPR” for the 3000 rpm conditions, where MRPR is a control parameter. Note that the regression equations here adjust for operating mode within speed by normalizing to RCEI. This also assumes that the effects of other variables (e.g., MFB\_50, IMEP, MRPR, or IAT) are consistent between modes within a speed.

One important limitation of this analysis is that the relationships derived from indolene and other repeat fuel test results are applied to every observed test fuel result. Therefore, the method supposes that the magnitude, direction, and significance of observed relationships in indolene and the repeat test fuels would also hold for each of the other non-repeated test fuels.

### **5.5. Analysis of Engine Performance versus Fuel Composition and Properties**

The final results for both the ethanol and the remaining fuel property statistical regression analyses are presented in this section.

The ethanol results consist of a set of six plots (one for each speed and mode condition) for each performance parameter. The plots show the measured and condition-adjusted performance results for each of the ethanol test fuels (as well as their “zero ethanol” base fuels) as a function of ethanol content. If a statistically significant linear or quadratic relationship was found for ethanol content, this relationship is drawn as a line on the plot. Below the plots, a table provides the coefficients for the intercept, linear (if applicable), and quadratic (if applicable) terms of the statistical models.

The results for the best two-factor with interaction statistical model are shown in tabular form for each of the performance parameters. For a select subset of parameters of most interest, the results are also shown in a graphic format using contour plots. Each of these is discussed below.

For each performance parameter, a table is presented that shows the two-factor regression results resulting from the best  $r^2$  model(s). Each line of this block of the table contains the following values:

- Speed – 1000, 2000, or 3000 rpm
- Mode – 1, or 2, denoting RBEI, or RCEI, respectively
- Predictor Variables
  - P1 – the first fuel property predictor variable
  - P2 – the second fuel property predictor variable

---

#### **CUSTOMER CONFIDENTIAL**



- Model Coefficients
  - Intercept – Intercept of the fitted regression function
  - P1 – coefficient on the value of the first fuel property predictor variable
  - P2 - coefficient on the value of the second fuel property predictor variable
  - P1\*P2 - coefficient on the interaction (product of the first and second fuel property predictor variables)
- Standard Deviation – The mean square error of the fitted model
- RSquare – the  $r^2$  of the model or the percentage of the observed variability explained by the model
- Overall Model p-Value – Probability associated with the F-test that the variability in results attributable to the model could be due to random chance. A low value ( $<0.1$ ) indicates the model effectively explains variability in observed results.

The model coefficients are asterisked once or twice if they are individually statistically significant at the 0.05 or 0.01 levels, respectively. This indicates a strong relationship between the predictor variable (or interaction) and the response variable. The overall model p-values of 0.05 and smaller are highlighted in yellow. This indicates that the subject model appears to explain the observed variability well.

For parameters of greatest interest, the result of the best two-factor model of performance parameter as a function of fuel properties is also illustrated graphically through the use of a contour plot. Each contour plot provides a means for assessing the region(s) of the fuel property values that optimize performance. The basic format of the contour plot is a set of lines, each representing a fixed response value of the performance parameter over the range of the two predictor variables used to create the regression relationship.

The contour plots here have been augmented by superimposing the average response levels for each of the tested fuels (with their corresponding values). This provides two valuable pieces of information. If the plotted points are close to the contour lines, it indicates that the observed data results match closely to the contour regression line results and hence that the proposed model appears to fit the observed data well. Second, it shows the span of the two predictor variables achieved in the test. This latter point is important since it is best to limit inferences in a two-factor regression model to the simultaneous range observed for both factors. One additional enhancement to the contour plots was the addition of the average indolene result in each case. This is provided strictly for reference and it should be noted that the indolene results were not modeled in the regression analysis.

A comprehensive list of all two-factor regression fits (after whatever ethanol adjustment was most applicable) is provided for each performance parameter and for each speed

---

**CUSTOMER CONFIDENTIAL**



and mode in Appendix F. The resulting models are sorted in descending order of their  $r^2$  values.

### 5.5.1. Indicated Specific Fuel Consumption (BI)

Condition-adjusted indicated specific fuel consumption appears statistically significantly related to ethanol content. For five of the six speed and mode conditions, BI increased linearly with increasing ethanol content. For 2000 rpm/RCEI, the relationship was also increasing, but was better characterized by a quadratic relationship. The data and corresponding estimated linear relationships are shown in Figure 5.7. The model coefficients are summarized in Table 5.3.

**Table 5.3 - Best Ethanol Content Statistical Model for ISFC**

Speed	Mode	Model Coefficients		
		Intercept	Ethanol	(Ethanol) <sup>2</sup>
1000	1	255.4 **	0.945 **	
1000	2	259.2 **	0.604 **	
2000	1	202.9 **	0.708 **	
2000	2	205.0 **	0.042	0.021 *
3000	1	214.7 **	0.596 **	
3000	2	212.2 **	0.658 **	

Note: Response values have been adjusted by test phase, TL22, MFB 50, and pressure (PI at 1000, 2000 rpm and PR\_CYP at 3000 rpm)

\* Statistically significant with 95 percent confidence

\*\* Statistically significant with 99 percent confidence

Example:  $ISFC [2000rpm/RBEI] = 202.9 + 0.708(\%Ethanol)$

The best two-factor with interaction model fit to the measured and condition-adjusted specific fuel consumption data for non-ethanol fuels was for the fuel properties butane and T10. This model is significant for all conditions except 1000 rpm and is shown in Table 5.4.

**Table 5.4 - Best Ranked R-Square Model for ISFC**

Speed	Mode	Predictor Variables		Model Coefficients				Standard Deviation	RSquare	Overall Model p-Value
		P1	P2	Intercept	P1	P2	P1 * P2			
1000	1	Butane	Distillation 10	169.65 *	8.52	0.61	-0.06	13.444	18%	0.524
1000	2	Butane	Distillation 10	210.62 **	9.14	0.34	-0.06	7.284	21%	0.410
2000	1	Butane	Distillation 10	126.21 **	8.25	0.52 **	-0.06 *	4.143	68%	0.003
2000	2	Butane	Distillation 10	136.59 **	12.76 *	0.46 **	-0.08 **	4.289	54%	0.021
3000	1	Butane	Distillation 10	100.47 *	25.46 **	0.77 **	-0.17 **	7.933	52%	0.026
3000	2	Butane	Distillation 10	156.70 **	11.28 *	0.37 **	-0.07 *	3.867	51%	0.032

Note: Response values have been adjusted by test phase, TL22, MFB 50, and pressure (PI at 1000, 2000 rpm and PR\_CYP at 3000 rpm)

\* Statistically significant with 95 percent confidence

\*\* Statistically significant with 99 percent confidence

Example:  $ISFC [2000rpm/RBEI] = 126.21 + 8.25(\%nbutane) + 0.52(T10) - 0.06(\%nbutane)(T10)$

To illustrate the butane and T10 relationship visually, a set of contour plots is shown below in Figure 5.8. At most speed and mode conditions, the contour plots show that best specific fuel consumption is seen for fuels with low T10. There does appear to be an exception where similarly better fuel consumption is observed for fuels with high T10 and high butane proportions.

## CUSTOMER CONFIDENTIAL

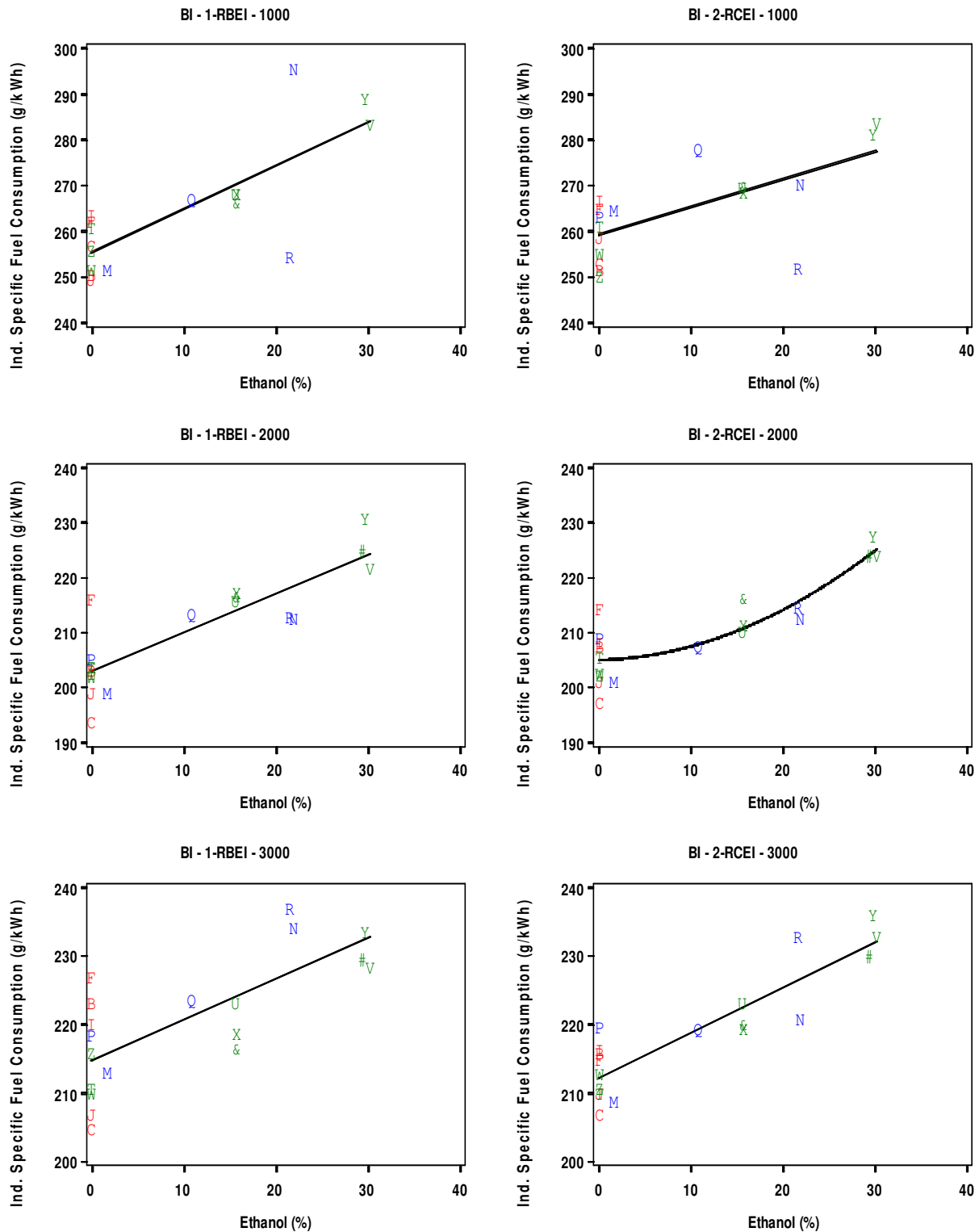


Figure 5.7 - Relationship between Ethanol Content and ISFC

**CUSTOMER CONFIDENTIAL**

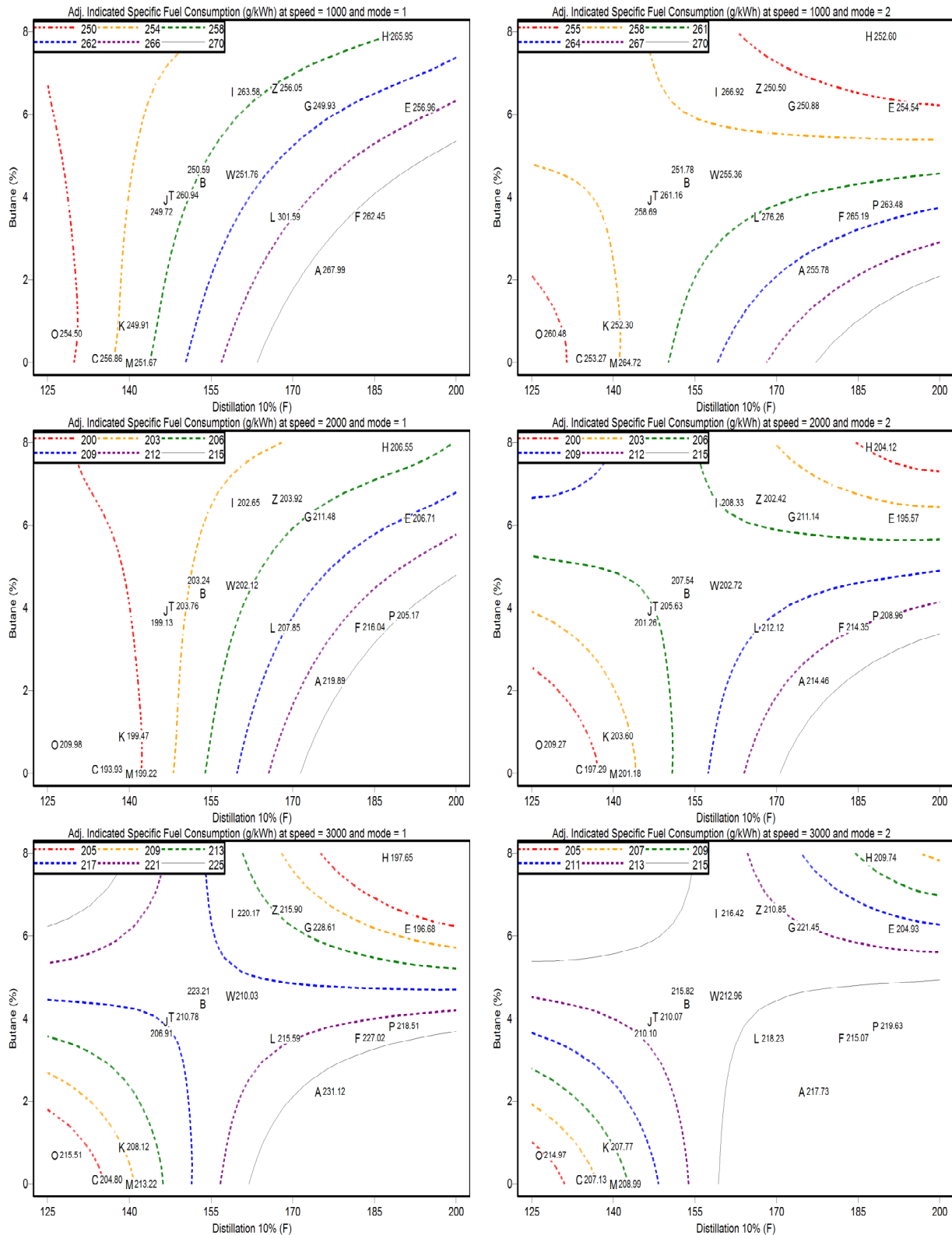


Figure 5.8 - Contour Plots of Modeled ISFC

**CUSTOMER CONFIDENTIAL**

The electronic version is the only controlled copy.  
All other copies are for reference only. Printed: 9/1/2009 4:09:13 PM  
Page 73

CA4-prg-007 Technical Report  
Originated: 01/01/04 Revised: 01/11/09



### 5.5.2. Indicated Thermal Efficiency (ITE)

Condition-adjusted indicated thermal efficiency (ITE) appears statistically significantly related to ethanol content at all conditions except for 1000 rpm/RBEI, with ITE increasing linearly with increasing ethanol content. The data and corresponding estimated linear relationships are shown in Figure 5.9. The associated tabular results are contained in Table 5.5

**Table 5.5 - Best Ethanol Content Model for ITE**

Speed	Mode	Model Coefficients		
		Intercept	Ethanol	(Ethanol) <sup>2</sup>
1000	1	32.5 **		
1000	2	31.6 **	0.079 **	
2000	1	40.6 **	0.045 *	
2000	2	40.3 **	0.071 **	
3000	1	38.7 **	0.058 *	
3000	2	39.3 **	0.050 **	

Note: Response values have been adjusted by test phase, TL22, MFB 50, and pressure (PI at 1000, 2000 rpm and PR\_CYP at 3000 rpm)

\* Statistically significant with 95 percent confidence

\*\* Statistically significant with 99 percent confidence

The best two-factor with interaction model fit to the measured and condition-adjusted indicated thermal efficiency data was for the fuel properties N-paraffins without butane and T10, although this model was only significant overall for the 2000 rpm conditions and 3000 rpm/RBEI. The tabular results for the model are shown in Table 5.6.

**Table 5.6 - Best Ranked R-Square Model for ITE**

Speed	Mode	Predictor Variables		Model Coefficients			Standard Deviation	RSquare	Overall Model p-Value	
		P1	P2	Intercept	P1	P2				P1 * P2
1000	1	n Paraffns wo C4	Distillation 10	35.09 **	-0.33	-0.02	0.002	1.332	2%	0.965
1000	2	n Paraffns wo C4	Distillation 10	35.64 **	-0.65	-0.02	0.004	0.975	20%	0.422
2000	1	n Paraffns wo C4	Distillation 10	60.30 **	-1.16 *	-0.13 **	0.01 *	0.800	60%	0.009
2000	2	n Paraffns wo C4	Distillation 10	60.93 **	-1.54 *	-0.13 **	0.01 *	1.068	51%	0.030
3000	1	n Paraffns wo C4	Distillation 10	69.25 **	-2.18 *	-0.20 **	0.01 *	1.625	55%	0.019
3000	2	n Paraffns wo C4	Distillation 10	54.39 **	-1.01	-0.1	0.01	1.182	31%	0.199

Note: Response values have been adjusted by test phase, TL22, MFB 50, and pressure (PI at 1000, 2000 rpm and PR\_CYP at 3000 rpm)

\* Statistically significant with 95 percent confidence

\*\* Statistically significant with 99 percent confidence

To illustrate the N-paraffins without butane and T10 relationship visually, a set of contour plots is shown in Figure 5.10. The plots show similar results to what was seen with specific fuel consumption. Better thermal efficiency is generally seen with low T10 fuels, but there is an exception where a few very high T10 fuels with high n-paraffin content also reach better thermal efficiency levels.

### CUSTOMER CONFIDENTIAL

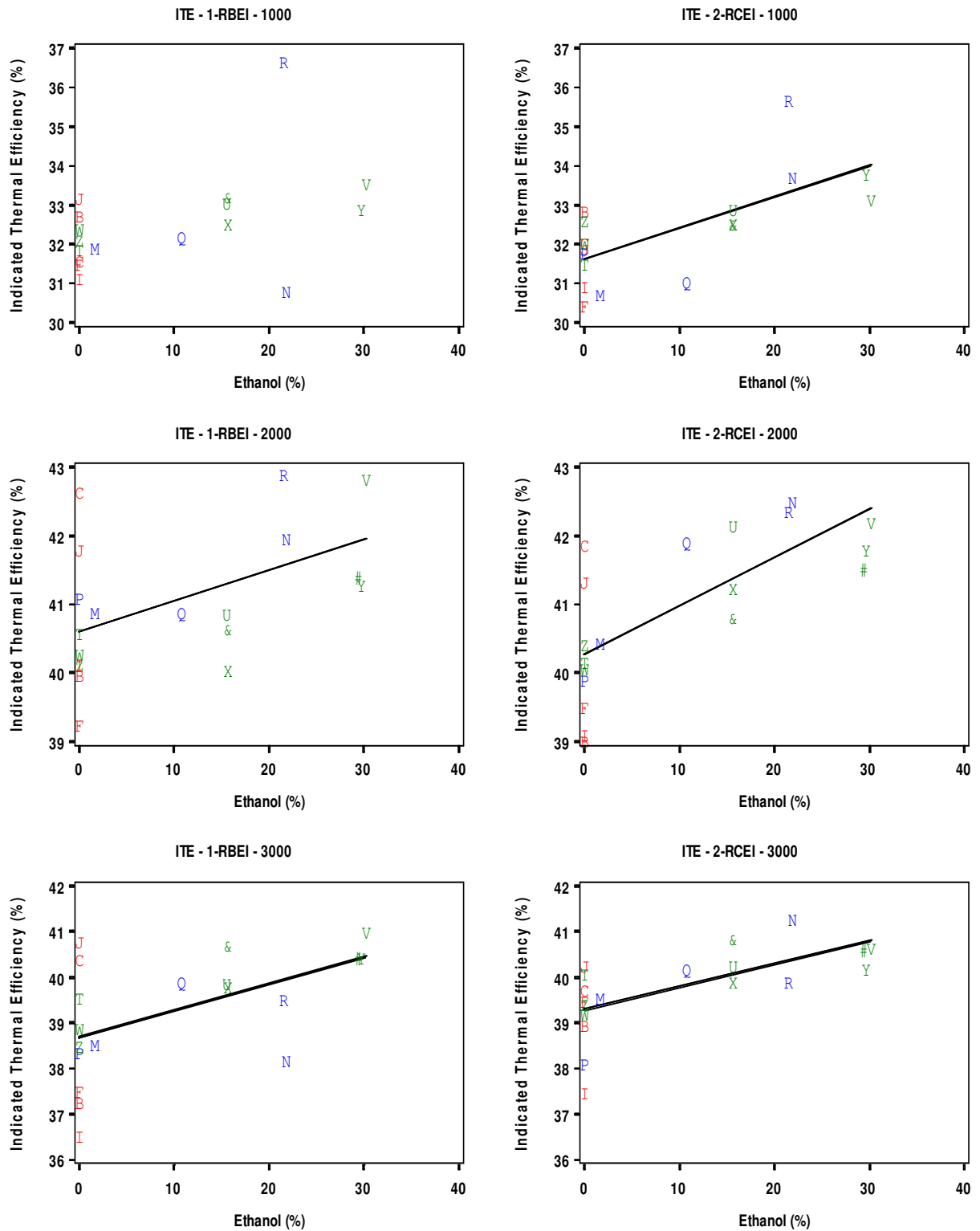


Figure 5.9 - Relationship between Ethanol Content and ITE

**CUSTOMER CONFIDENTIAL**

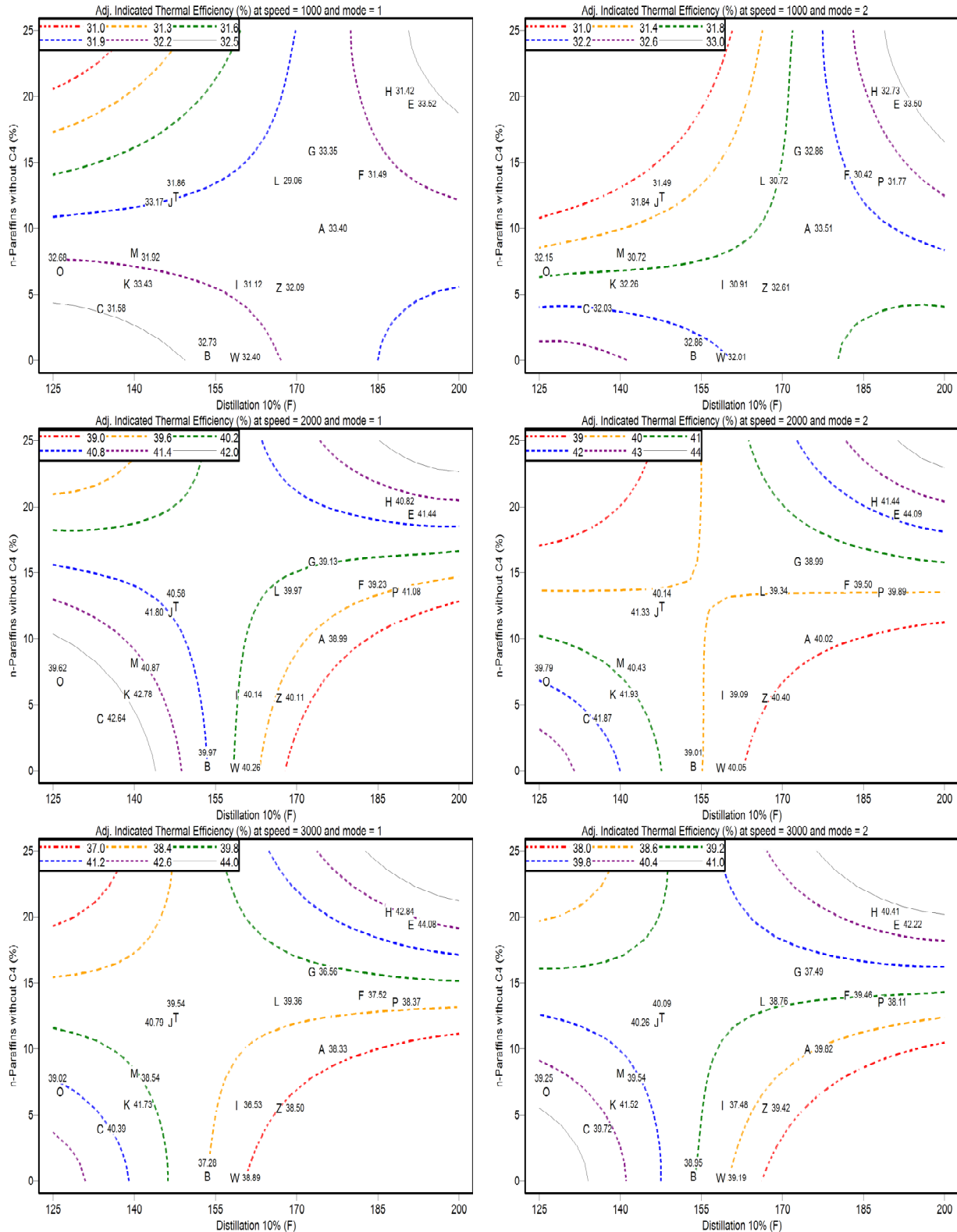


Figure 5.10 - Contour Plots of Modeled ITE

**CUSTOMER CONFIDENTIAL**

The electronic version is the only controlled copy.  
 All other copies are for reference only. Printed: 9/1/2009 4:09:13 PM  
 Page 76

CA4-prg-007 Technical Report  
 Originated: 01/01/04 Revised: 01/11/09



### 5.5.3. Indicated Specific NO<sub>x</sub> Emission (ISNO<sub>x</sub>)

Condition-adjusted indicated specific NO<sub>x</sub> emission (ISNO<sub>x</sub>) appeared statistically significantly negatively related to ethanol content of fuel for all conditions except for 1000 rpm/RBEI. Figure 5.11 shows the relationship between ISNO<sub>x</sub> and ethanol for all speed and mode conditions with the significant decreasing linear relationship overlaid on the data points. The tabular results of the model are contained in Table 5.7.

**Table 5.7 - Best Ethanol Content Model for ISNO<sub>x</sub>**

Speed	Mode	Model Coefficients		
		Intercept	Ethanol	(Ethanol) <sup>2</sup>
1000	1	0.009 *		
1000	2	0.010 **	-0.0003 *	
2000	1	0.060 **	-0.0006 *	
2000	2	0.056 **	-0.0008 *	
3000	1	0.098 **	-0.0006 *	
3000	2	0.166 **	-0.0022 *	

Note: Response values have been adjusted by test phase, TL22, MFB 50, and pressure (PI at 1000, 2000 rpm and PR\_CYP at 3000 rpm)

\* Statistically significant with 95 percent confidence

\*\* Statistically significant with 99 percent confidence

The best two-factor with interaction model fit to the measured and condition-adjusted indicated specific NO<sub>x</sub> emission data was for the fuel properties olefins and butane. Table 5.8 shows the overall model results of NO<sub>x</sub> performance.

**Table 5.8 - Best Ranked R-Square Model for ISNO<sub>x</sub>**

Speed	Mode	Predictor Variables		Model Coefficients			Standard Deviation	RSquare	Overall Model p-Value	
		P1	P2	Intercept	P1	P2				P1 * P2
1000	1	Olefins	Butane	0.01	-0.00002	-0.001	0.0003 **	0.006	66%	0.006
1000	2	Olefins	Butane	0.01 *	-0.00009	-0.002	0.0001	0.006	38%	0.115
2000	1	Olefins	Butane	0.12 **	-0.002 **	-0.01 *	-0.0001	0.018	57%	0.015
2000	2	Olefins	Butane	0.12 **	-0.002 **	-0.01 **	-0.00002	0.015	66%	0.004
3000	1	Olefins	Butane	0.18 **	-0.002 **	-0.01 *	-0.0001	0.023	54%	0.020
3000	2	Olefins	Butane	0.29 **	-0.004 **	-0.02 **	-0.0005	0.030	69%	0.002

Note: Response values have been adjusted by test phase, TL22, MFB 50, and pressure (PI at 1000, 2000 rpm and PR\_CYP at 3000 rpm)

\* Statistically significant with 95 percent confidence

\*\* Statistically significant with 99 percent confidence

To illustrate the fits visually, a set of contour plots is shown below for the olefins and butane parameters. In the contour plots shown in Figure 5.12, the adjusted indicated specific NO<sub>x</sub> values have been scaled by 100 to more easily see the values.

In the contour plots, the extremely low NO<sub>x</sub> levels for 1000 rpm make the results difficult to interpret. At 2000 and 3000 rpm, though, a consistent pattern emerges. Highest NO<sub>x</sub> levels are observed for fuels with both low olefins and low butane. The interaction terms are not significant so that both increasing olefins and increasing butane correspond to lower NO<sub>x</sub>.

#### CUSTOMER CONFIDENTIAL

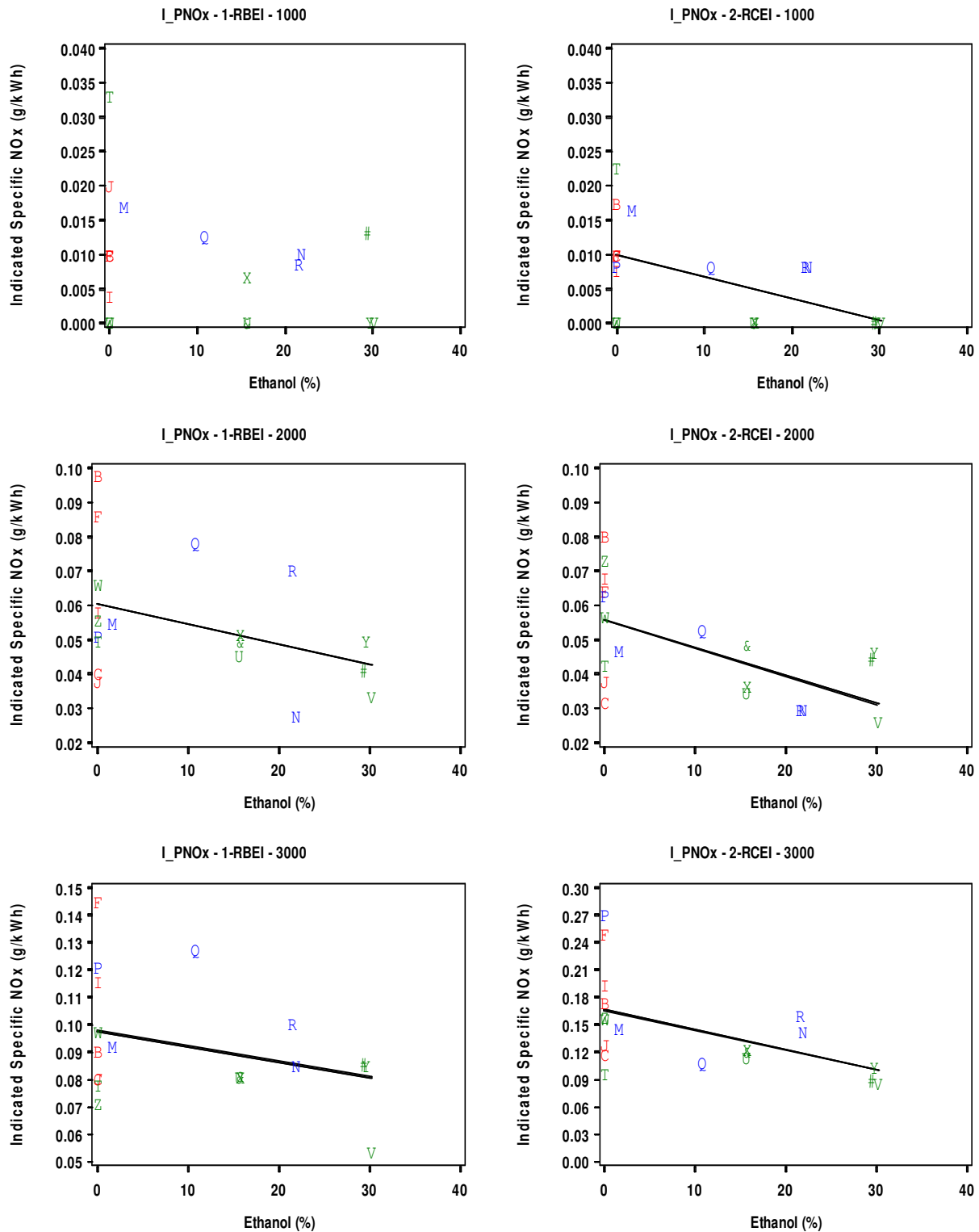


Figure 5.11 - Relationship between Ethanol Content and ISNO<sub>x</sub>

**CUSTOMER CONFIDENTIAL**

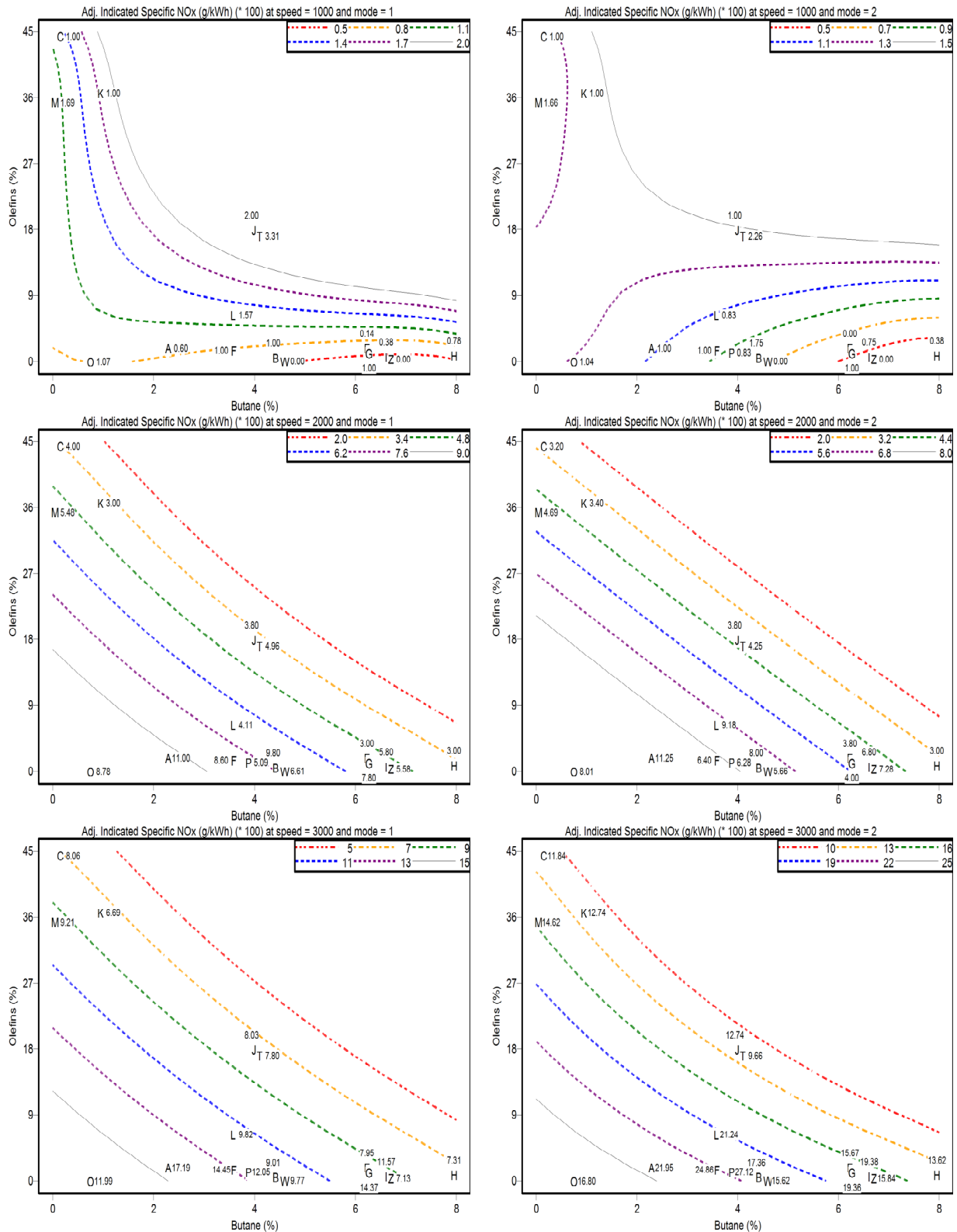


Figure 5.12 - Contour Plots of Modeled ISNO<sub>x</sub>

**CUSTOMER CONFIDENTIAL**

The electronic version is the only controlled copy.  
 All other copies are for reference only. Printed: 9/1/2009 4:09:13 PM  
 Page 79

CA4-prg-007 Technical Report  
 Originated: 01/01/04 Revised: 01/11/09



#### 5.5.4. Indicated Specific HC Emission (ISHC)

Condition-adjusted indicated specific hydrocarbon emission (ISHC) levels appear to have little relationship to ethanol content as shown in Table 5.9 and Figure 5.13. At 3000 rpm/RBEI there is indication of a statistically significant quadratic relationship with hydrocarbon levels lowest in the 10 to 20 percent range and higher for either lower or higher ethanol content.

**Table 5.9 - Best Ethanol Content Model for ISHC**

Speed	Mode	Model Coefficients		
		Intercept	Ethanol	(Ethanol) <sup>2</sup>
1000	1	17.0 **		
1000	2	17.3 **		
2000	1	8.0 **		
2000	2	5.6 **		
3000	1	7.5 **	-0.175 *	0.006
3000	2	3.9 **		

Note: Response values have been adjusted by test phase, TL22, MFB 50, and pressure (PI at 1000, 2000 rpm and PR\_CYP at 3000 rpm)

\* Statistically significant with 95 percent confidence

\*\* Statistically significant with 99 percent confidence

The best two-factor with interaction model fit to the measured and condition-adjusted indicated specific hydrocarbon emission data was for the fuel properties aromatics and iso-paraffins. This model is shown in Table 5.10.

**Table 5.10 - Best Ranked R-Square Model for ISHC**

Speed	Mode	Predictor Variables		Model Coefficients				Standard Deviation	RSquare	Overall Model p-Value
		P1	P2	Intercept	P1	P2	P1 * P2			
1000	1	Aromatics	i Paraffins	16.09 **	0.47 **	0.06 *	-0.02 **	1.257	52%	0.037
1000	2	Aromatics	i Paraffins	16.29 **	0.06	0.01	-0.002	1.137	4%	0.923
2000	1	Aromatics	i Paraffins	7.22 **	0.03	0.01	-0.0003	0.857	13%	0.613
2000	2	Aromatics	i Paraffins	5.64 **	0.17	0.01	-0.01	1.083	28%	0.245
3000	1	Aromatics	i Paraffins	6.40 **	0.08	0.01	-0.001	1.060	33%	0.171
3000	2	Aromatics	i Paraffins	2.86 **	0.04	0.01	-0.00001	0.805	36%	0.137

Note: Response values have been adjusted by test phase, TL22, MFB 50, and pressure (PI at 1000, 2000 rpm and PR\_CYP at 3000 rpm)

\* Statistically significant with 95 percent confidence

\*\* Statistically significant with 99 percent confidence

Only the 1000 rpm/RBEI condition resulted in a statistically significant overall model. It appears that hydrocarbon variability is not strongly related to the fuel properties evaluated here. With the lack of statistically significant models, contour plots were not generated for hydrocarbon emission performance.

#### CUSTOMER CONFIDENTIAL

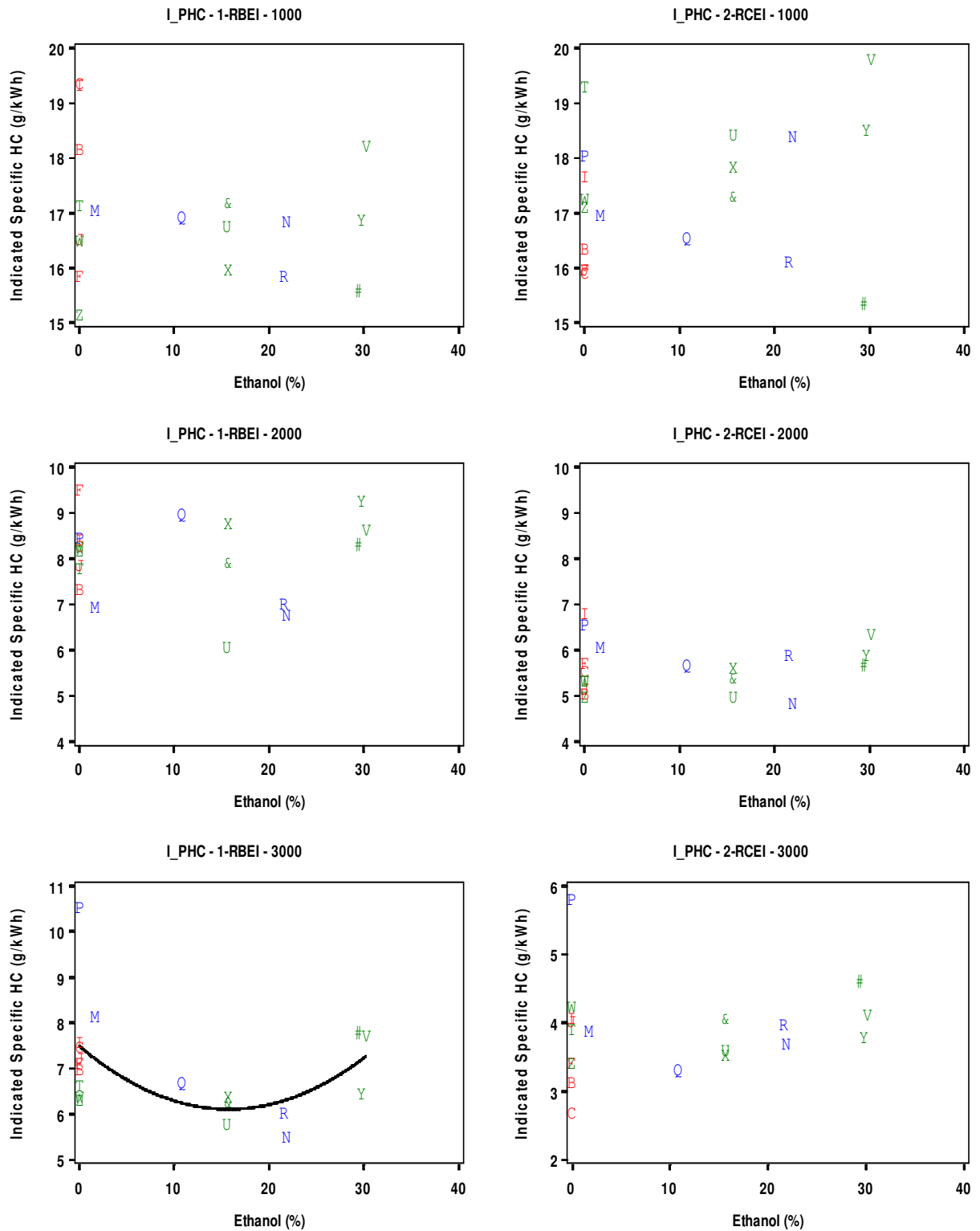


Figure 5.13 - Relationship between Ethanol Content and ISHC

**CUSTOMER CONFIDENTIAL**



### 5.5.5. Indicated Specific CO Emission (ISCO)

Condition-adjusted indicated specific CO (ISCO) emission levels increased with increasing ethanol for both modes at 1000 rpm and for RCEI at 2000 rpm. The tabular results are shown in Table 5.11.

**Table 5.11 - Best Ethanol Content Model for ISCO**

Speed	Mode	Model Coefficients		
		Intercept	Ethanol	(Ethanol) <sup>2</sup>
1000	1	37.5 **	0.559 **	
1000	2	41.9 **	0.603 **	
2000	1	4.4 **		
2000	2	4.2 **	0.034 **	
3000	1	5.8 *		
3000	2	2.6 **		

Note: Response values have been adjusted by test phase, TL22, MFB 50, and pressure (PI at 1000, 2000 rpm and PR\_CYP at 3000 rpm)

\* Statistically significant with 95 percent confidence

\*\* Statistically significant with 99 percent confidence

The best two-factor with interaction model fit to the measured and condition-adjusted indicated specific CO emission data was for the fuel properties aromatics and iso-paraffins. Table 5.12 shows the overall model results of CO performance.

**Table 5.12 - Best Ranked R-Square Model for ISCO**

Speed	Mode	Predictor Variables		Model Coefficients				Standard Deviation	RSquare	Overall Model p-Value
		P1	P2	Intercept	P1	P2	P1 * P2			
1000	1	Aromatics	i Paraffins	65.10 **	0.17	-0.30 *	-0.02	6.080	66%	0.007
1000	2	Aromatics	i Paraffins	78.59 **	-0.28	-0.46 **	-0.01	6.707	72%	0.001
2000	1	Aromatics	i Paraffins	5.27 **	-0.10	-0.02 *	0.003	0.475	36%	0.130
2000	2	Aromatics	i Paraffins	6.06 **	0.02	-0.02	-0.001	0.687	45%	0.060
3000	1	Aromatics	i Paraffins	-3.93	-0.06	0.19 *	0.004	4.230	56%	0.017
3000	2	Aromatics	i Paraffins	3.08 **	-0.09	-0.01	0.003	0.645	16%	0.549

Note: Response values have been adjusted by test phase, TL22, MFB 50, and pressure (PI at 1000, 2000 rpm and PR\_CYP at 3000 rpm)

\* Statistically significant with 95 percent confidence

\*\* Statistically significant with 99 percent confidence

With r-square values near 70 percent, these properties account for most of the observed CO variability at 1000 rpm. The results are weaker for the higher speed conditions. To illustrate the fits visually, a set of contour plots is shown in Figure 5.15 for the aromatics and iso-paraffins parameters.

The contour plots for both modes at 1000 rpm have a similar characteristic; CO levels are highest for fuels with simultaneously low aromatic and iso-paraffin content. Increases in either factor while the other is held constant resulted in lower CO. For 2000 rpm, the model is not statistically significant with very little variation in CO levels across all the fuels tested. For 3000 rpm/RBEI, the model is significant but is highly influenced by two fuels with very high CO levels.

## CUSTOMER CONFIDENTIAL

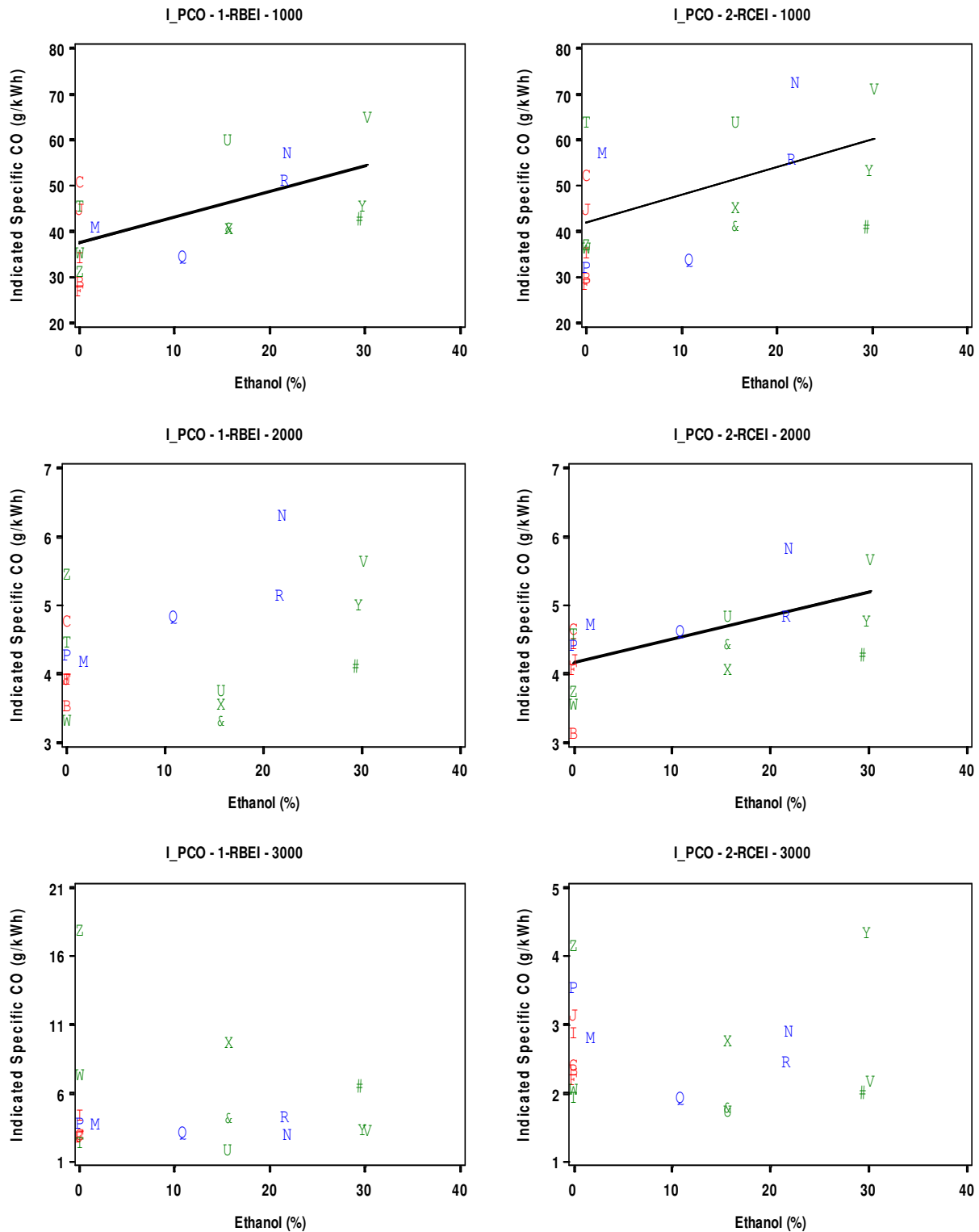


Figure 5.14 - Relationship between Ethanol Content and ISCO

**CUSTOMER CONFIDENTIAL**

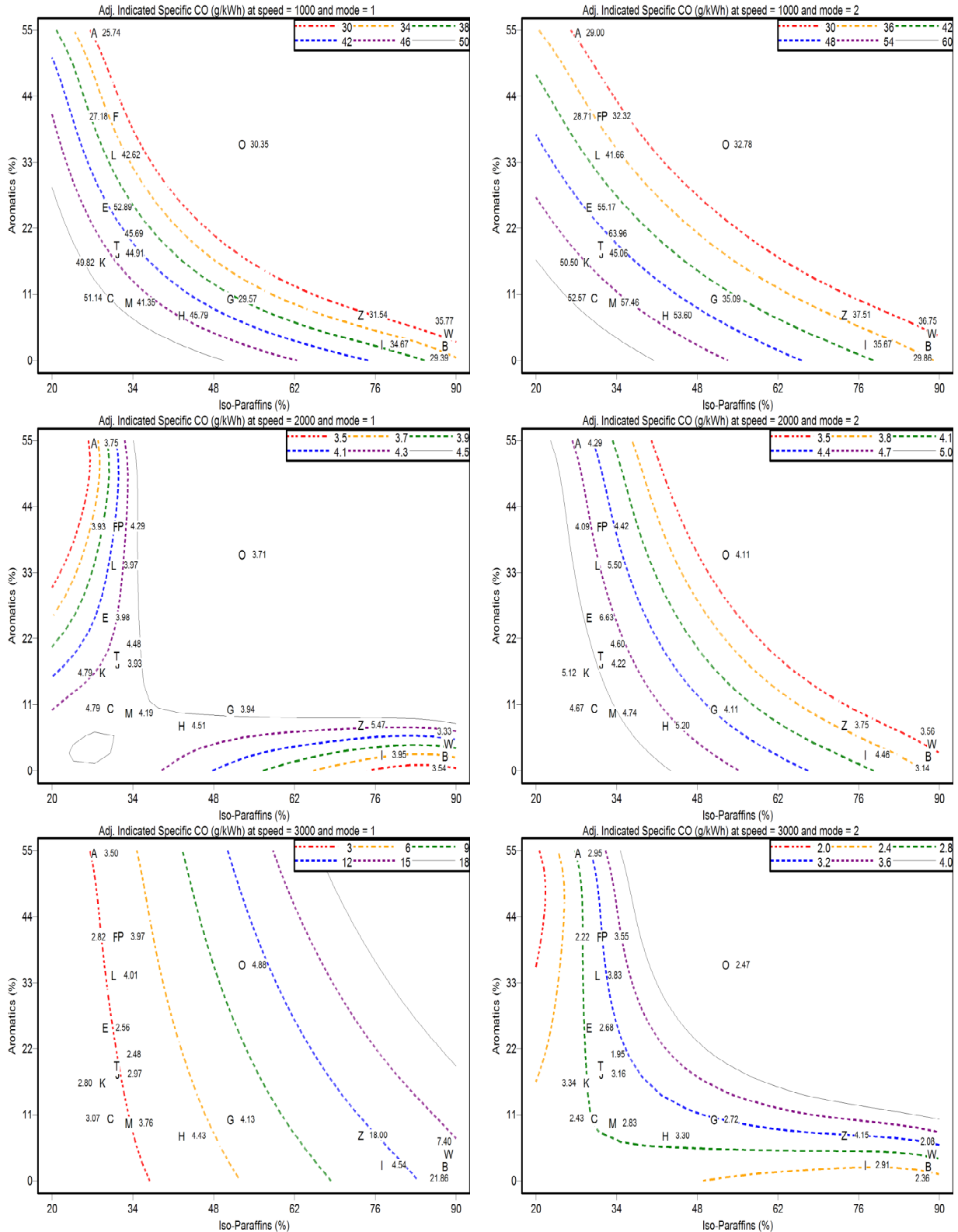


Figure 5.15 - Contour Plots of Modeled ISCO

**CUSTOMER CONFIDENTIAL**

The electronic version is the only controlled copy.  
 All other copies are for reference only. Printed: 9/1/2009 4:09:13 PM  
 Page 84

CA4-prg-007 Technical Report  
 Originated: 01/01/04 Revised: 01/11/09



### 5.5.6. Indicated Specific Smoke (IS\_SMK)

Condition-adjusted indicated specific smoke (IS\_SMK) levels were not statistically significantly related to ethanol levels (either linearly or quadratically) for any speed or mode.

The best two-factor with interaction model fit to the measured and condition-adjusted indicated specific smoke was for the properties aromatics and T10. The following table shows the model results.

**Table 5.13 - Best Ranked R-Square Model for IS\_SMK**

Speed	Mode	Predictor Variables		Model Coefficients			Standard Deviation	RSquare	Overall Model p-Value	
		P1	P2	Intercept	P1	P2				P1 * P2
1000	1	Aromatics	Distillation 10	0.004	-0.0003	-0.00002	0	0.000	42%	0.096
1000	2	Aromatics	Distillation 10	0.01	-0.0005 *	-0.00004	0.00 *	0.001	72%	0.001
2000	1	Aromatics	Distillation 10	-0.03	0.001	0.0002	0	0.005	51%	0.031
2000	2	Aromatics	Distillation 10	-0.03	0.002	0.0002	-0.00001	0.004	57%	0.016
3000	1	Aromatics	Distillation 10	-0.35	0.002	0.002	0	0.042	77%	<.001
3000	2	Aromatics	Distillation 10	0.02	-0.01	-0.00005	0.00003	0.015	51%	0.032

Note: Response values have been adjusted by test phase, TL22, MFB 50, and pressure (PI at 1000, 2000 rpm and PR\_CYP at 3000 rpm)

\* Statistically significant with 95 percent confidence

\*\* Statistically significant with 99 percent confidence

To illustrate the fits visually, a set of contour plots for the aromatics and T10 parameters is shown in Figure 5.16. The condition-adjusted indicated specific smoke results appearing on the contour plots were scaled up by a factor of 100 to make them easier to read.

While all but the 1000 rpm/RBEI condition yielded statistically significant fits, the exact region of aromatics and T10 that yielded certain levels of smoke seemed to differ between the speed and mode conditions. In general, though, higher indicated specific smoke was found for fuels with higher aromatic content.

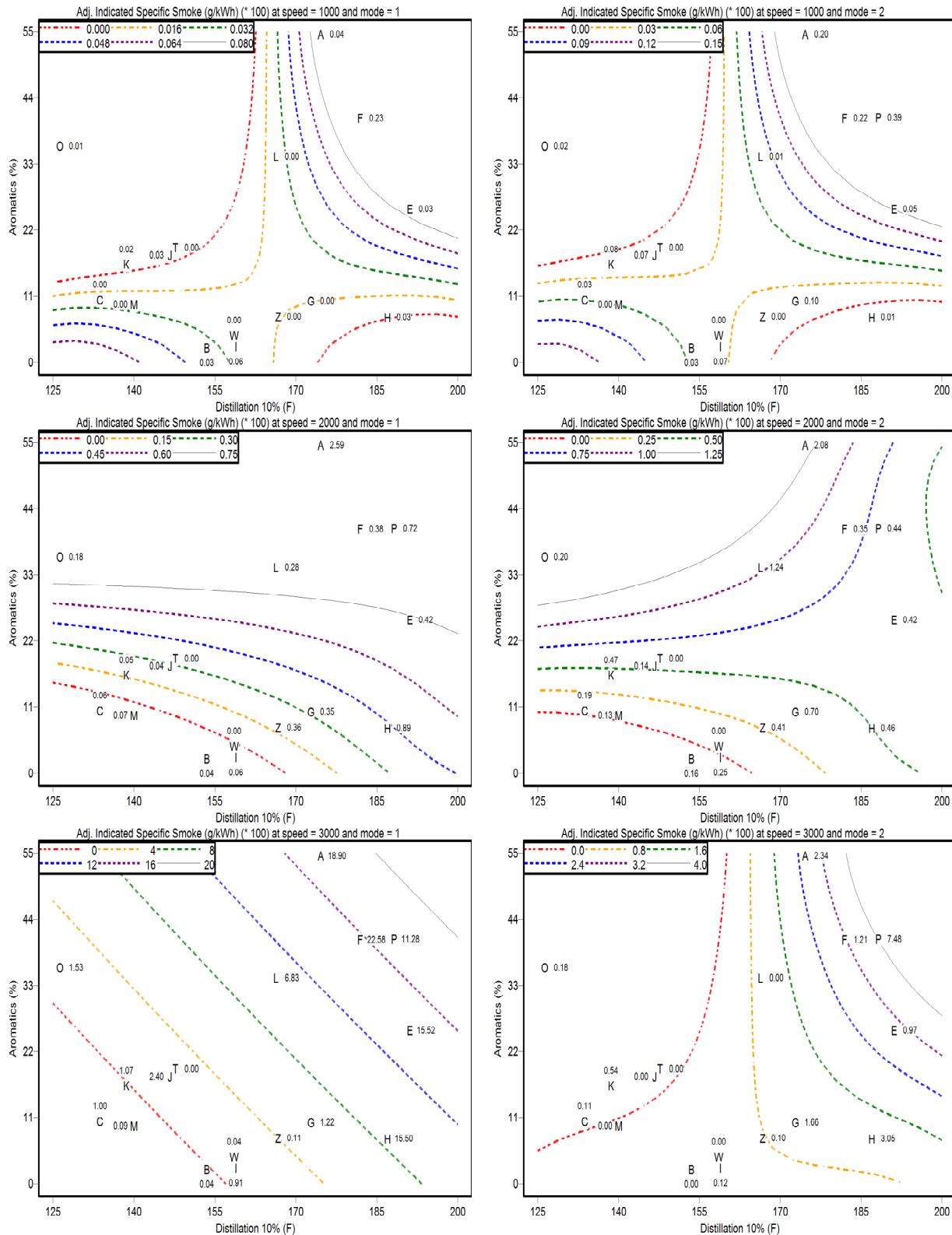


Figure 5.16 - Contour Plots of Modeled IS\_SMK

**CUSTOMER CONFIDENTIAL**

The electronic version is the only controlled copy.  
 All other copies are for reference only. Printed: 9/1/2009 4:09:13 PM  
 Page 86

CA4-prg-007 Technical Report  
 Originated: 01/01/04 Revised: 01/11/09



### 5.5.7. Combustion Duration (MFB\_Duration)

There was a statistically significant, linear, increasing trend of ethanol to condition-adjusted combustion duration for both modes at 1000 and 2000 rpm. At the 3000 rpm speed, the statistically significant relationship was better modeled as a quadratic with duration highest in the 10 to 20 percent ethanol range and lower at either higher or lower ethanol content. These results are shown in Table 5.14 and Figure 5.17.

**Table 5.14 - Best Ethanol Content Model for Combustion Duration**

Speed	Mode	Model Coefficients		
		Intercept	Ethanol	(Ethanol) <sup>2</sup>
1000	1	13.5 **	0.069 **	
1000	2	13.4 **	0.097 **	
2000	1	8.2 **	0.025 *	
2000	2	7.3 **	0.040 **	
3000	1	7.8 **	0.852 **	-0.027 **
3000	2	8.9 *	0.915 *	-0.030

Note: Response values have been adjusted by test phase, TL22, MFB 50, and pressure (PI at 1000, 2000 rpm and PR\_CYP at 3000 rpm)

\* Statistically significant with 95 percent confidence

\*\* Statistically significant with 99 percent confidence

The best two factor with interaction model fit to the measured and condition-adjusted combustion duration was olefins and T10. Table 5.15 shows the model results. However, since this relationship is not a strong one, no contour plots were created.

**Table 5.15 - Best Ranked R-Square Model for Combustion Duration**

Speed	Mode	Predictor Variables		Model Coefficients				Standard Deviation	RSquare	Overall Model p-Value
		P1	P2	Intercept	P1	P2	P1 * P2			
1000	1	Olefins	Distillation 10	6.68 *	0.44	0.04 *	-0.003	0.632	63%	0.009
1000	2	Olefins	Distillation 10	9.32 *	0.29	0.02	-0.002	0.991	23%	0.344
2000	1	Olefins	Distillation 10	7.95 **	0.63 *	0.004	-0.005 *	0.561	37%	0.127
2000	2	Olefins	Distillation 10	2.77	0.001	0.03 *	0.0002	0.431	41%	0.088
3000	1	Olefins	Distillation 10	-11.83	-1.08	0.12	0.01	2.998	26%	0.286
3000	2	Olefins	Distillation 10	-5.64	-0.45	0.08 **	0.004	1.159	53%	0.025

Note: Response values have been adjusted by test phase, TL22, MFB 50, and pressure (PI at 1000, 2000 rpm and PR\_CYP at 3000 rpm)

\* Statistically significant with 95 percent confidence

\*\* Statistically significant with 99 percent confidence

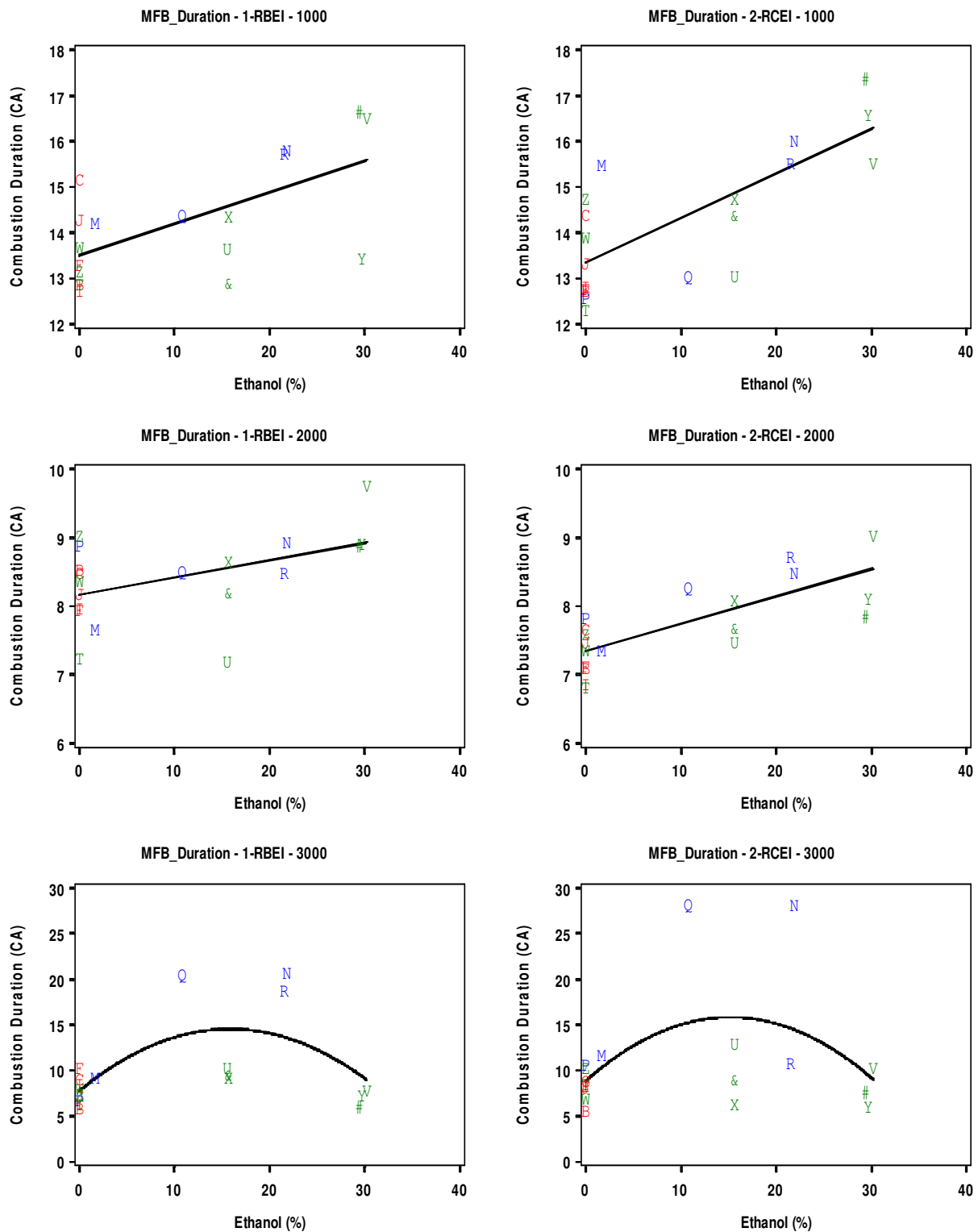


Figure 5.17 - Relationship between Ethanol Content and Combustion Duration

**CUSTOMER CONFIDENTIAL**



### 5.5.8. Coefficient of Variance (COV) of IMEP

Condition-adjusted COV of IMEP performance shows a statistically significant, linear, increasing trend with ethanol content for both modes at 1000 rpm. The 2000 rpm/RCEI mode has a significant quadratic relationship. No significant relationships were seen at the 3000 rpm speeds.

**Table 5.16 - Best Ethanol Content Model for COV of IMEP**

Speed	Mode	Model Coefficients		
		Intercept	Ethanol	(Ethanol) <sup>2</sup>
1000	1	12.2 **	0.139	
1000	2	13.6 **	0.277 **	
2000	1	2.6 **		
2000	2	2.3 **	0.034 *	-0.001 *
3000	1	4.0 **		
3000	2	3.0 **		

Note: Response values have been adjusted by test phase, TL22, MFB 50, and pressure (PI at 1000, 2000 rpm and PR\_CYP at 3000 rpm)

\* Statistically significant with 95 percent confidence

\*\* Statistically significant with 99 percent confidence

Because of its primary importance to assessing idle combustion stability, COV of IMEP two-factor with interaction model analysis is evaluated for just the 1000 rpm test conditions. The best two-factor with interaction model for the 1000 rpm condition only was for RON and T10.

**Table 5.17 - Best Ranked R-Square Model for COV of IMEP**

Speed	Mode	Predictor Variables		Model Coefficients				Standard Deviation	RSquare	Overall Model p-Value
		P1	P2	Intercept	P1	P2	P1 * P2			
1000	1	RON	Distillation 10	-281.16 **	3.61 **	1.74 **	-0.02 **	2.720	70%	0.003
1000	2	RON	Distillation 10	-210.2	2.7	1.24	-0.02	4.054	29%	0.234

Note: Response values have been adjusted by test phase, TL22, MFB 50, and pressure (PI at 1000, 2000 rpm and PR\_CYP at 3000 rpm)

\* Statistically significant with 95 percent confidence

\*\* Statistically significant with 99 percent confidence

A set of contour plots is provided for the statistical model. The contours show that COV of IMEP is influenced by RON and distillation temperature T10. The contour plots can be conceptually divided into four quadrants, which are defined as follows.

- (I) T10 < ~165 F (RBEI, 180F for RCEI) & RON > 80 (RBEI, 82 for RCEI);
- (II) T10 > ~165 F (RBEI, 180F for RCEI) & RON > 80 (RBEI, 82 for RCEI);
- (III) T10 < ~165 F (RBEI, 180F for RCEI) & RON < 80 (RBEI, 82 for RCEI);
- (IV) T10 > ~165 F (RBEI, 180F for RCEI) & RON < 80 (RBEI, 82 for RCEI).

In quadrant (I), higher RON and lower T10 lead to greater COV of IMEP. In quadrant (IV), lower RON and higher T10 similarly lead to greater COV of IMEP. There are not enough fuels tested in quadrants (II) and (III) to validate the appropriateness of the statistical model.

#### CUSTOMER CONFIDENTIAL

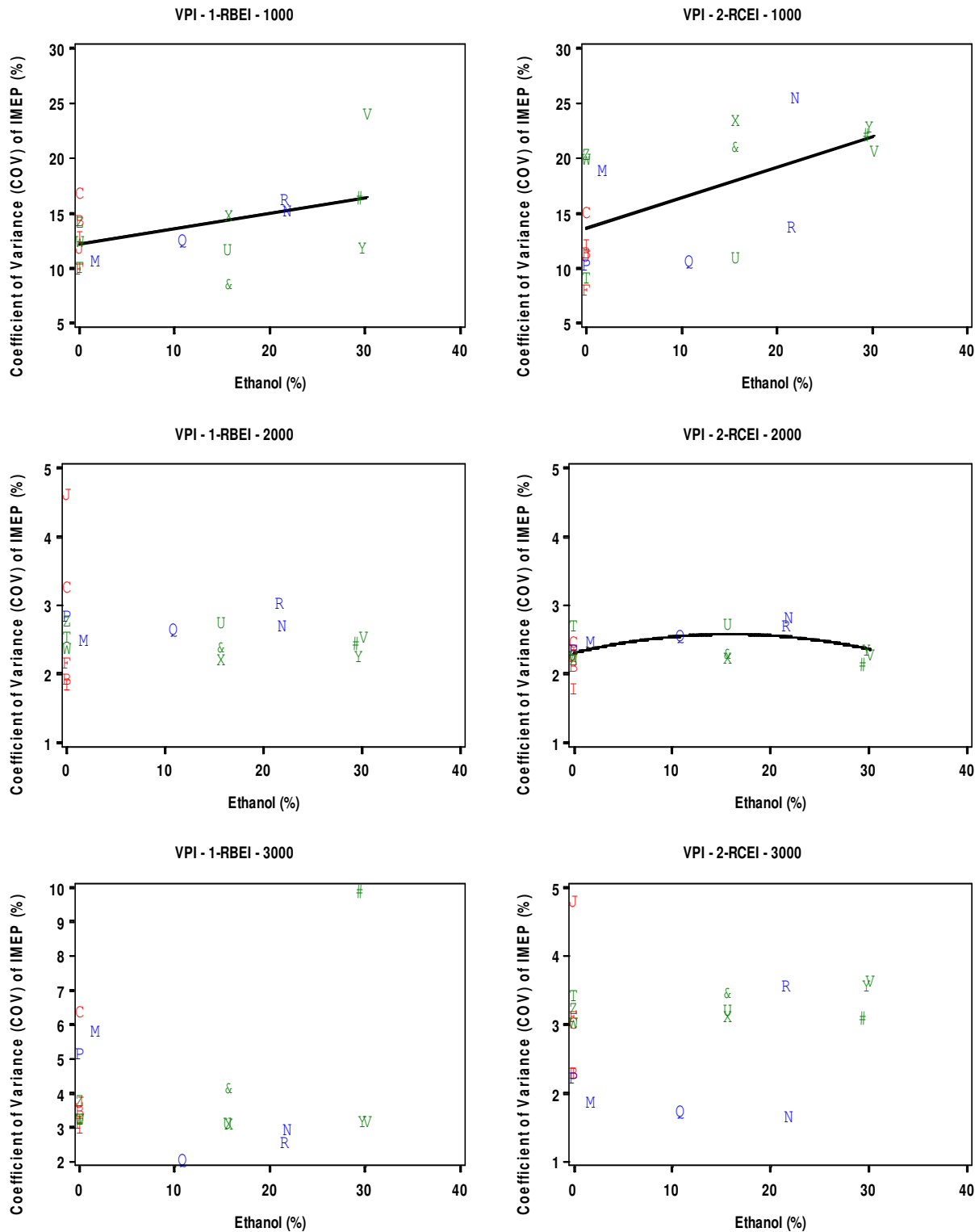
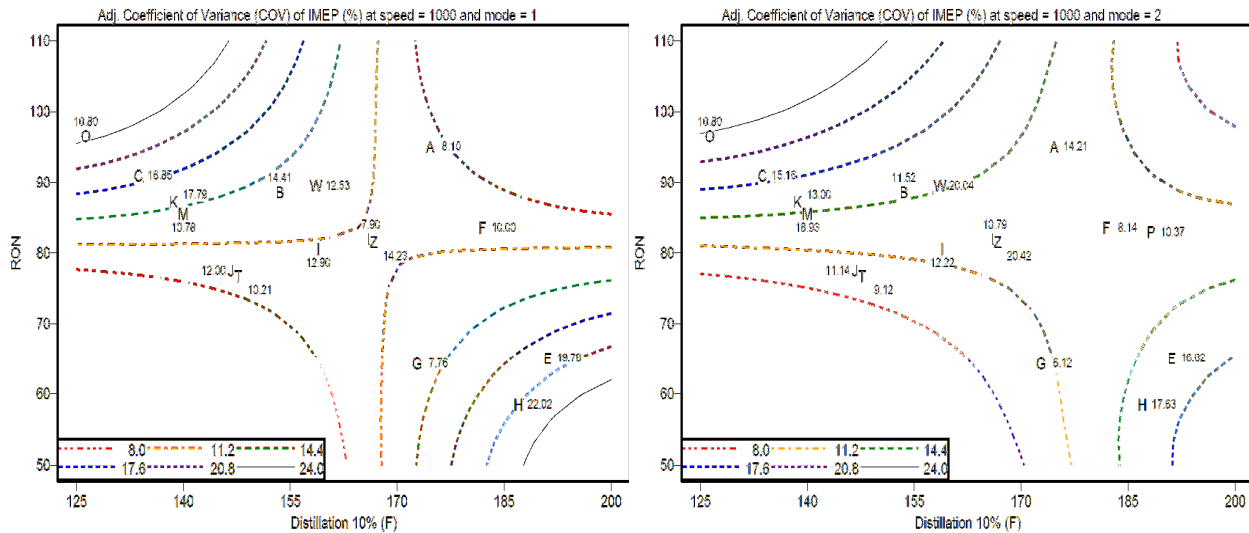


Figure 5.18 - Relationship between Ethanol Content and COV of IMEP

**CUSTOMER CONFIDENTIAL**



**Figure 5.19 - Contour Plots of Modeled COV of IMEP**

### 5.5.9. Combustion Noise

As shown in Table 5.18 and Figure 5.20, condition-adjusted combustion noise levels showed a statistically significant linear decrease with increasing ethanol content only for the 2000 rpm/RCEI mode.

**Table 5.18 - Best Ethanol Content Model for Noise**

Speed	Mode	Model Coefficients		
		Intercept	Ethanol	(Ethanol) <sup>2</sup>
1000	1	74.1 **		
1000	2	73.9 **		
2000	1	86.0 **		
2000	2	87.1 **	-0.068 **	
3000	1	93.7 **		
3000	2	93.1 **		

Note: Response values have been adjusted by test phase, TL22, MFB 50, and pressure (PI at 1000, 2000 rpm and PR\_CYP at 3000 rpm)

\* Statistically significant with 95 percent confidence

\*\* Statistically significant with 99 percent confidence

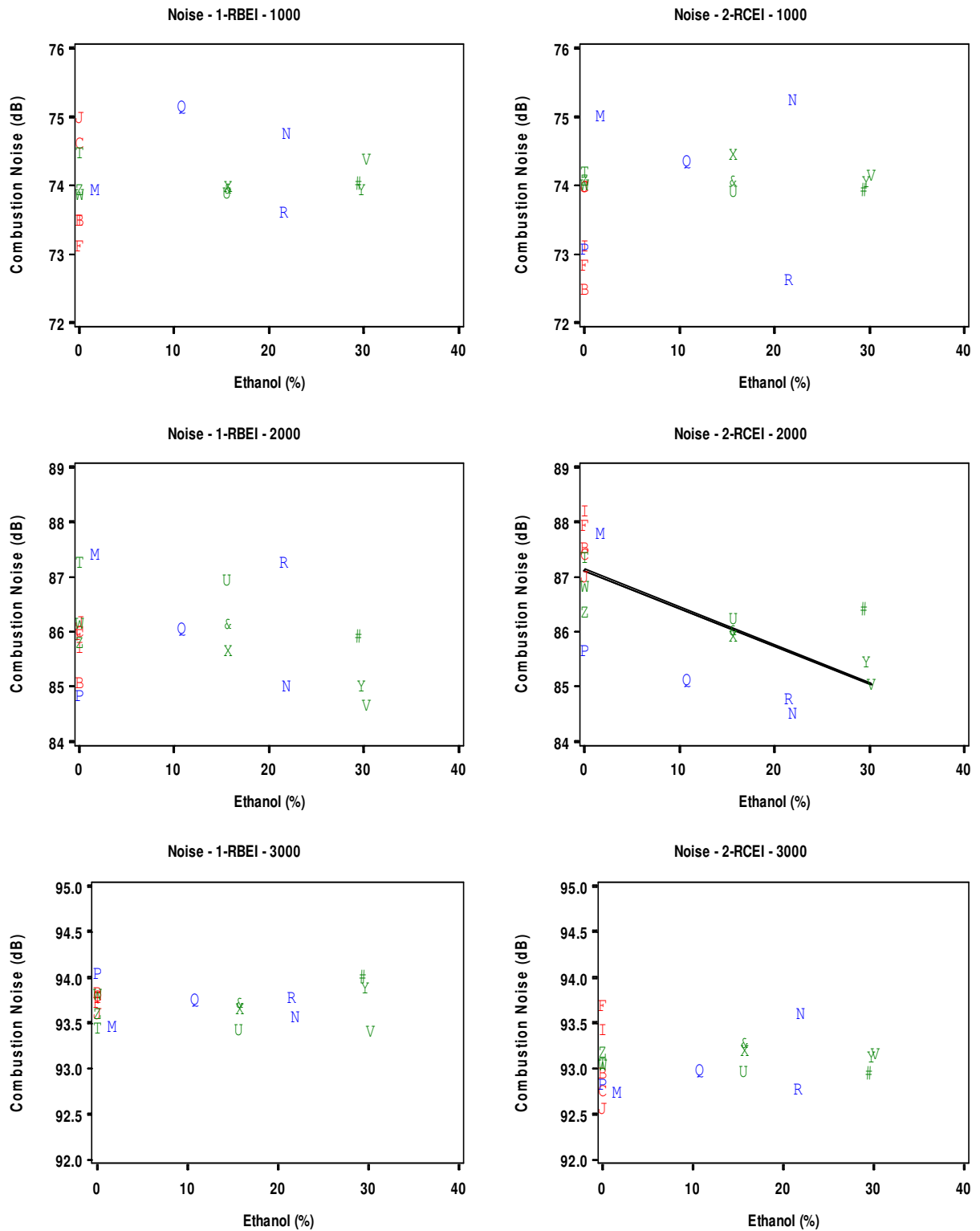


Figure 5.20 - Relationship between Ethanol Content and Noise

**CUSTOMER CONFIDENTIAL**



The best two-factor with interaction model, shown in Table 5.19, was for the parameters aromatics and n-paraffins without butane; however, it is only significant at 1000 rpm. The noise levels are relatively low at 2000 rpm and 1000 rpm, so these results are not of particular interest.

**Table 5.19 - Best Ranked R-Square Model for Noise**

Speed	Mode	Predictor Variables		Model Coefficients			Standard Deviation	RSquare	Overall Model p-Value	
		P1	P2	Intercept	P1	P2				P1 * P2
1000	1	Aromatics	n Paraffns wo C4	72.77 **	0.11 *	0.18 **	-0.01 *	0.692	58%	0.020
1000	2	Aromatics	n Paraffns wo C4	72.50 **	0.11	0.21 **	-0.01 *	0.859	48%	0.044
2000	1	Aromatics	n Paraffns wo C4	85.85 **	0.01	-0.01	0.001	1.052	11%	0.705
2000	2	Aromatics	n Paraffns wo C4	87.34 **	0.03	-0.03	-0.003	0.803	21%	0.396
3000	1	Aromatics	n Paraffns wo C4	94.08 **	-0.04 *	-0.04 *	0.003 *	0.224	43%	0.070
3000	2	Aromatics	n Paraffns wo C4	93.06 **	0.001	-0.02	0.0006	0.385	10%	0.717

Note: Response values have been adjusted by test phase, TL22, MFB 50, and pressure (PI at 1000, 2000 rpm and PR\_CYP at 3000 rpm)

\* Statistically significant with 95 percent confidence

\*\* Statistically significant with 99 percent confidence

### 5.5.10. Peak Cylinder Pressure

The ethanol relationship to condition-adjusted peak cylinder pressure performance shown in Table 5.20 is significant as a linearly decreasing relationship for 2000 rpm/RCEI only. The best two factor with interaction model fit to the condition-adjusted peak cylinder pressure was for the parameters RON and T10. Table 5.21 shows the model results. This best model is only statistically significant for 2000 rpm/RCEI and 3000 rpm/RBEI. As such neither model is a good generally predictive model of peak cylinder pressure.

**Table 5.20 - Best Ethanol Content Model for Peak Cylinder Pressure**

Speed	Mode	Model Coefficients		
		Intercept	Ethanol	(Ethanol) <sup>2</sup>
1000	1	28.5 **		
1000	2	28.6 **		
2000	1	37.9 **		
2000	2	39.6 **	-0.033 **	
3000	1	40.4 **		
3000	2	37.7 **		

Note: Response values have been adjusted by test phase, TL22,

MFB 50, and pressure (PI at 1000, 2000 rpm and PR\_CYP at 3000 rpm)

\* Statistically significant with 95 percent confidence

\*\* Statistically significant with 99 percent confidence

**Table 5.21 - Best Ranked R-Square Model for Peak Cylinder Pressure**

Speed	Mode	Predictor Variables		Model Coefficients			Standard Deviation	RSquare	Overall Model p-Value	
		P1	P2	Intercept	P1	P2				P1 * P2
1000	1	RON	Distillation 10	17.97	0.12	0.05	-0.0006	0.413	13%	0.652
1000	2	RON	Distillation 10	21.72 *	0.11	0.04	-0.0006	0.339	37%	0.125
2000	1	RON	Distillation 10	35.86	0.07	0.02	-0.0005	0.791	19%	0.444
2000	2	RON	Distillation 10	39.99 **	0.05	-0.001	-0.0003	0.302	76%	<.001
3000	1	RON	Distillation 10	2.7	0.45 **	0.22 **	-0.003 **	0.421	60%	0.010
3000	2	RON	Distillation 10	19.2	0.24	0.12	-0.002	0.553	40%	0.099

Note: Response values have been adjusted by test phase, TL22, MFB 50, and pressure (PI at 1000, 2000 rpm and PR\_CYP at 3000 rpm)

\* Statistically significant with 95 percent confidence

\*\* Statistically significant with 99 percent confidence

## CUSTOMER CONFIDENTIAL

The electronic version is the only controlled copy.

All other copies are for reference only. Printed: 9/1/2009 4:09:13 PM

Page 93

CA4-prg-007 Technical Report  
Originated: 01/01/04 Revised: 01/11/09

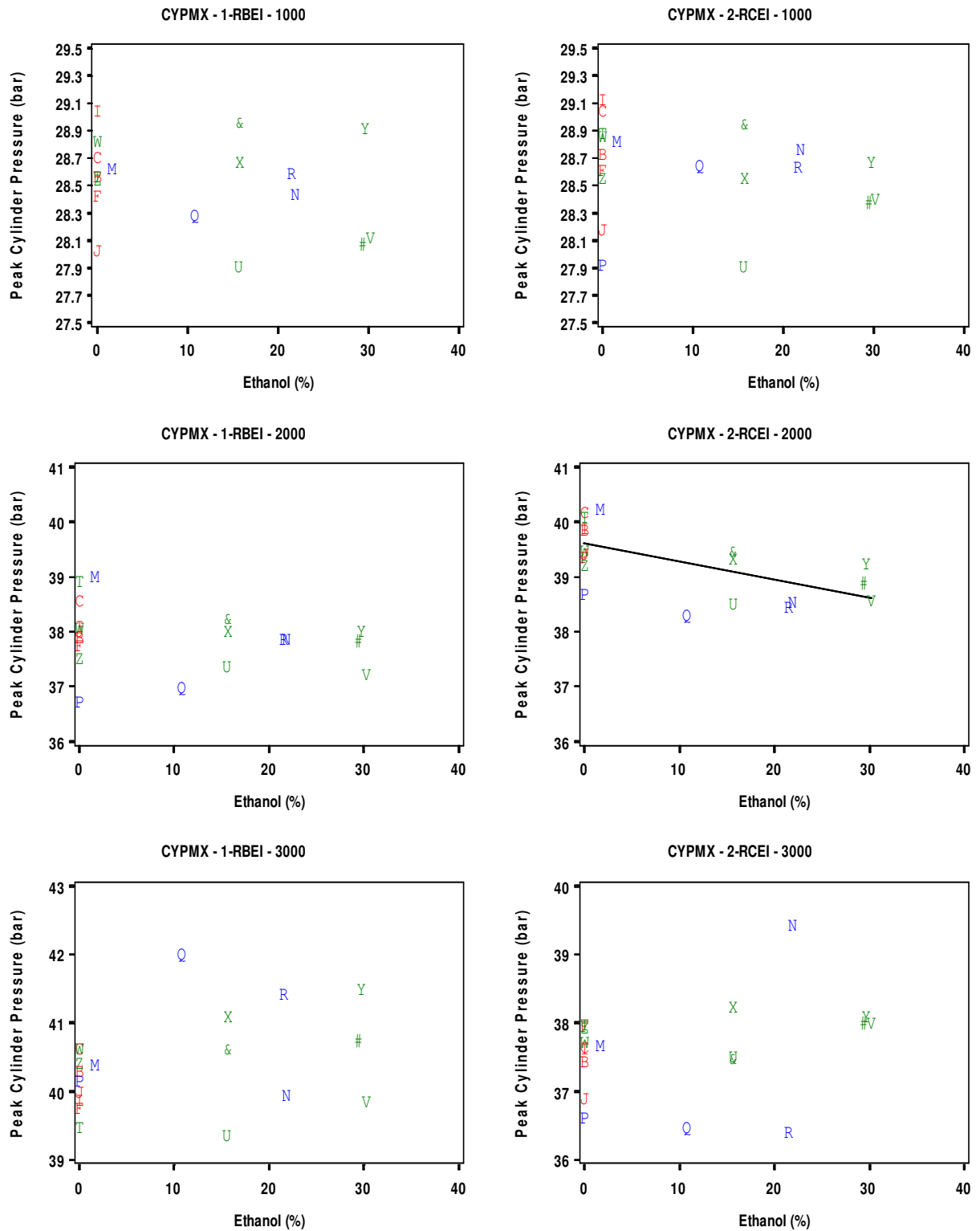


Figure 5.21 - Relationship between Ethanol Content and Peak Cylinder Pressure



### 5.5.11. Exhaust Valve Close Angle (EVC)

The ethanol relationship to condition-adjusted exhaust valve close angle is only significant for 2000 rpm/RBEI. This is illustrated in Table 5.22 and Figure 5.22.

**Table 5.22 - Best Ethanol Content Model for EVC**

Speed	Mode	Model Coefficients		
		Intercept	Ethanol	(Ethanol) <sup>2</sup>
1000	1	236.4 **		
1000	2	236.1 **		
2000	1	250.3 **	0.950 *	-0.031 *
2000	2	245.3 **		
3000	1	288.0 **		
3000	2	268.1 **		

Note: Response values have been adjusted by test phase, TL22, MFB 50, and pressure (PI at 1000, 2000 rpm and PR\_CYP at 3000 rpm)

\* Statistically significant with 95 percent confidence

\*\* Statistically significant with 99 percent confidence

The best two factor with interaction model fit to the measured and condition-adjusted exhaust valve close angle was for the properties sensitivity and T90. However, the model was only statistically significant for 1000 rpm/RBEI and 3000 rpm/RCEI. Table 5.23 shows the model results.

**Table 5.23 - Best Ranked R-Square Model for EVC**

Speed	Mode	Predictor Variables		Model Coefficients				Standard Deviation	RSquare	Overall Model p-Value
		P1	P2	Intercept	P1	P2	P1 * P2			
1000	1	Sensitivity	Distillation_90	181.42 **	7.30 **	0.15 **	-0.02 **	3.843	64%	0.009
1000	2	Sensitivity	Distillation_90	248.18 **	1.99	-0.04	-0.01	4.160	35%	0.152
2000	1	Sensitivity	Distillation_90	222.73 **	3.56	0.08	-0.01	4.877	25%	0.319
2000	2	Sensitivity	Distillation_90	209.86 **	3.45	0.1	-0.01	4.056	29%	0.242
3000	1	Sensitivity	Distillation_90	252.42 **	4.32	0.09	-0.01	5.557	26%	0.289
3000	2	Sensitivity	Distillation_90	220.27 **	4.90 **	0.14 **	-0.01 *	3.481	50%	0.034

Note: Response values have been adjusted by test phase, TL22, MFB 50, and pressure (PI at 1000, 2000 rpm and PR\_CYP at 3000 rpm)

\* Statistically significant with 95 percent confidence

\*\* Statistically significant with 99 percent confidence

Because the exhaust valve closing angle is subject to the variability of the hydraulically controlled valve actuation system, no consistent relationship to fuel composition would be expected.

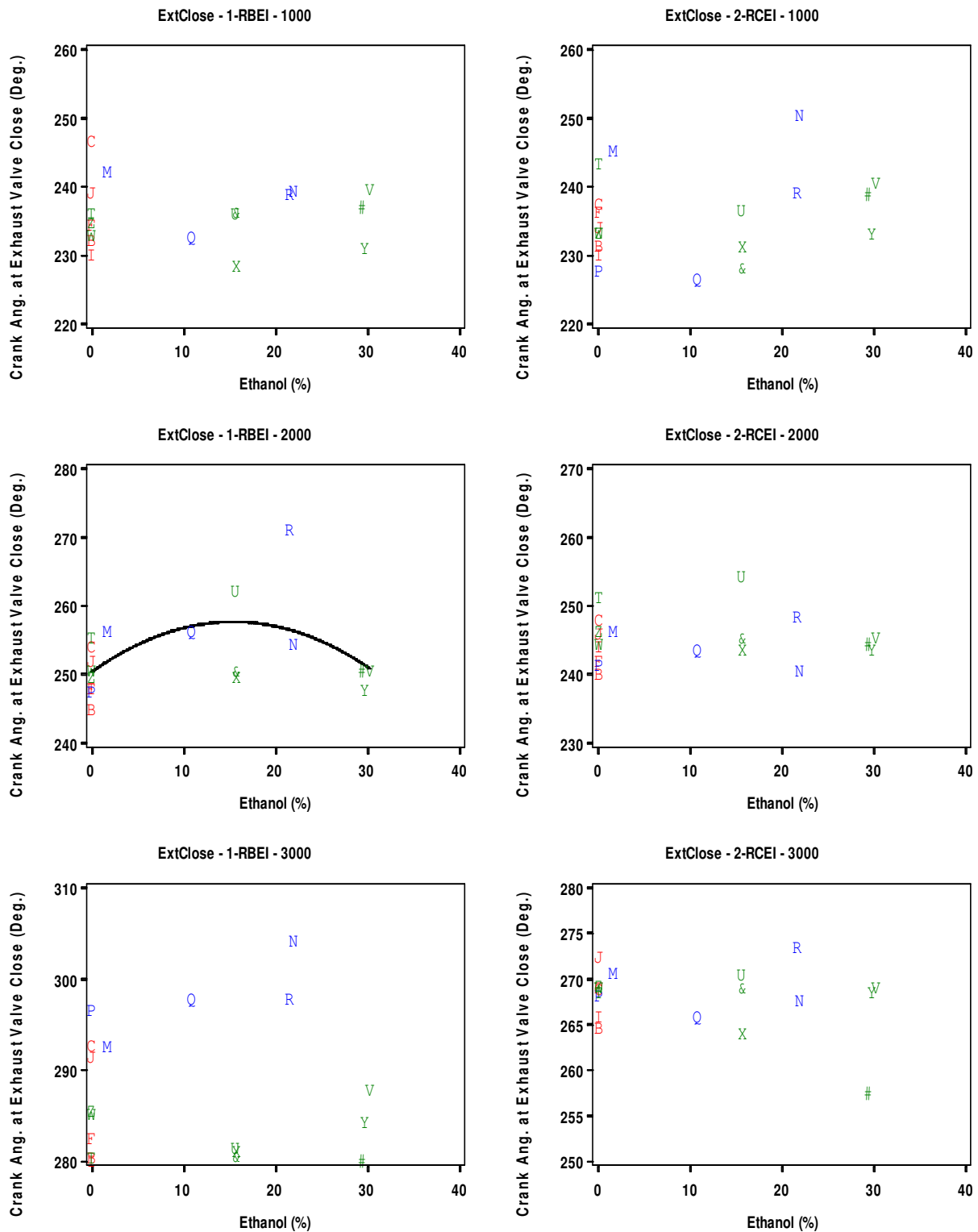


Figure 5.22 - Relationship between Ethanol Content and EVC

**CUSTOMER CONFIDENTIAL**



### 5.5.12. Indicated Mean Effective Pressure (IMEP)

The ethanol relationship to condition-adjusted IMEP is linearly increasing and statistically significant for both modes at 3000 rpm. The tabular results are listed in Table 5.24 and are illustrated in Figure 5.23.

**Table 5.24 - Best Ethanol Content Model for IMEP @ 3000 rpm**

Speed	Mode	Model Coefficients		
		Intercept	Ethanol	(Ethanol) <sup>2</sup>
3000	1	2.9 **	0.006 *	
3000	2	2.8 **	0.004 *	

Note: Response values have been adjusted by test phase, TL22, MFB 50, and pressure (PI at 1000, 2000 rpm and PR\_CYP at 3000 rpm)

\* Statistically significant with 95 percent confidence

\*\* Statistically significant with 99 percent confidence

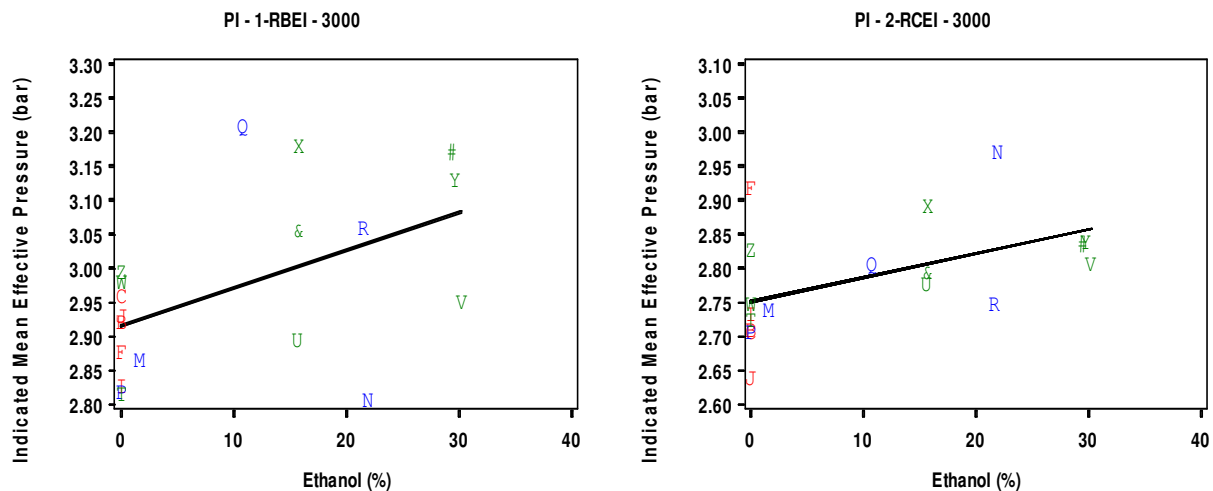


**Figure 5.23 - Relationship between Ethanol Content and IMEP**

The best two factor with interaction model was for butane and T10 and is shown in Table 5.25. It is statistically significant for both modes at 3000 rpm. This means that while the 3000 rpm testing was conducted and later normalized to a specific maximum rate of cylinder pressure rise, indicated mean effective pressure will vary in a predictable way with the fuel properties Butane and T10.

**Table 5.25 - Best Ranked R-Square Model for IMEP @ 3000 rpm**

Speed	Mode	Predictor Variables		Model Coefficients				Standard Deviation	RSquare	Overall Model p-Value
		P1	P2	Intercept	P1	P2	P1 * P2			
3000	1	Butane	Distillation_10	3.99 **	-0.35 **	-0.01 **	0.002 **	0.079	74%	<.001
3000	2	Butane	Distillation_10	2.97 **	-0.17 *	-0.002	0.001 *	0.072	54%	0.022

Note: Response values have been adjusted by test phase, TL22, MFB 50, and pressure (PI at 1000, 2000 rpm and PR\_CYP at 3000 rpm)

\* Statistically significant with 95 percent confidence

\*\* Statistically significant with 99 percent confidence

### CUSTOMER CONFIDENTIAL

### 5.5.13. Maximum Rate of Cylinder Pressure Rise (MRPR)

The condition-adjusted maximum rate of cylinder pressure rise showed a statistically significant, linearly decreasing, trend with increased ethanol for both 1000 rpm modes and for 2000 rpm/RCEI. This is shown in Table 5.26 and Figure 5.24.

**Table 5.26 - Best Ethanol Content Model for MRPR**

Speed	Mode	Model Coefficients		
		Intercept	Ethanol	(Ethanol) <sup>2</sup>
1000	1	0.78 **	-0.003 **	
1000	2	0.80 **	-0.003 **	
2000	1	3.34 **		
2000	2	3.58 **	-0.022 **	

Note: Response values have been adjusted by test phase, TL22, MFB 50, and pressure (PI at 1000, 2000 rpm and PR\_CYP at 3000 rpm)

\* Statistically significant with 95 percent confidence

\*\* Statistically significant with 99 percent confidence

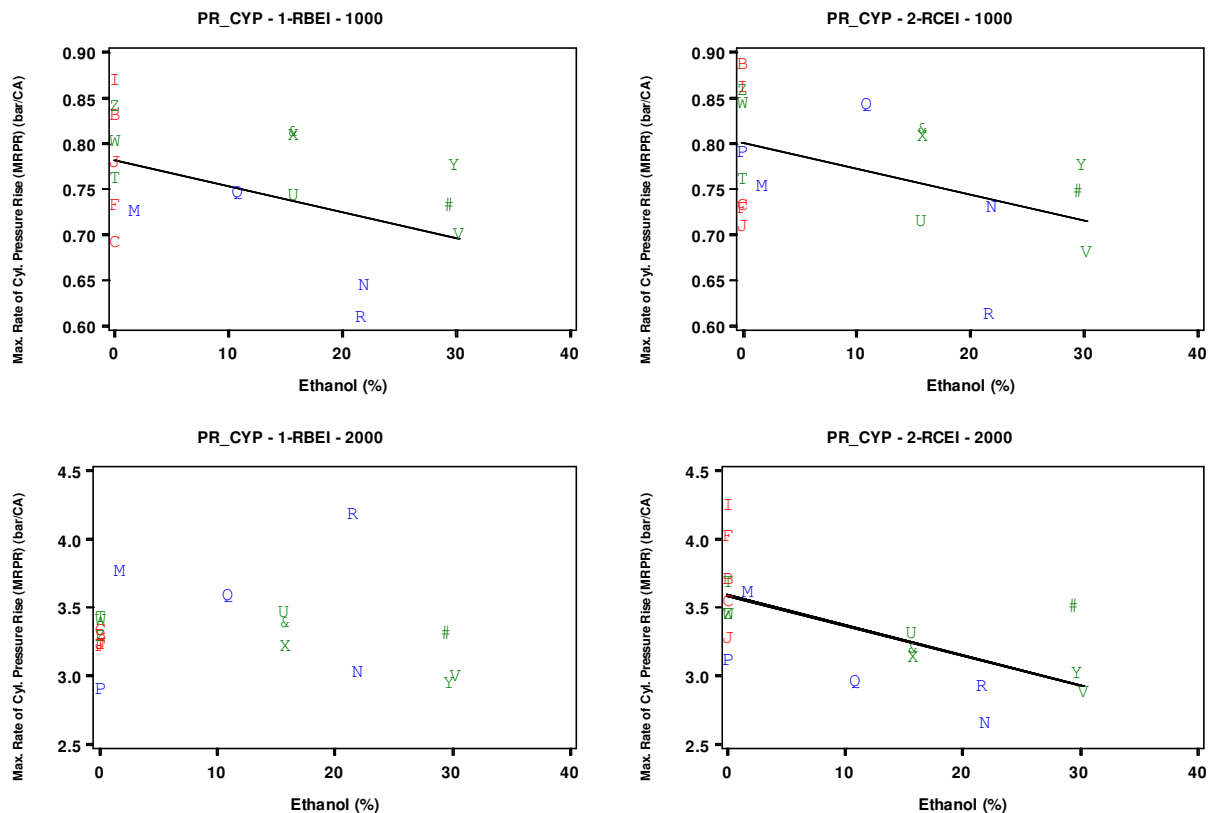


**Figure 5.24 - Relationship between Ethanol Content and MRPR**



The best two factor with interaction model for condition-adjusted maximum rate of cylinder pressure rise across both modes was for aromatics and iso-paraffins. These models were statistically significant only for the two 1000 rpm conditions and are listed in Table 5.27. This means that while the 1000 rpm testing was conducted and later normalized to a specific indicated mean effective pressure, maximum rate of cylinder pressure rise will vary in a predictable way with the fuel properties aromatics and iso-paraffins.

**Table 5.27 - Best Ranked R-Square Model for MRPR**

Speed	Mode	Predictor Variables		Model Coefficients			Standard Deviation	RSquare	Overall Model p-Value	
		P1	P2	Intercept	P1	P2				P1 * P2
1000	1	Aromatics	i Paraffins	0.54 **	0.01	0.004 *	-0.0002	0.072	56%	0.024
1000	2	Aromatics	i Paraffins	0.60 **	0.0008	0.003 **	0.00005	0.046	66%	0.004
2000	1	Aromatics	i Paraffins	3.12 **	0.02	0.004	-0.0006	0.323	6%	0.846
2000	2	Aromatics	i Paraffins	3.22 **	0.07 *	0.01 *	-0.002 *	0.270	35%	0.143

Note: Response values have been adjusted by test phase, TL22, MFB 50, and pressure (PI at 1000, 2000 rpm and PR\_CYP at 3000 rpm)

\* Statistically significant with 95 percent confidence

\*\* Statistically significant with 99 percent confidence



## 6. Conclusions

### 6.1. Volumetric Ethanol Content

As the volumetric ethanol content of each fuel is increased, the smaller LHV causes a predictable increase in ISFC. However, ethanol also has a cooling effect on the combustion temperatures which decreases ISNO<sub>x</sub> emissions and increases thermal efficiency by reducing heat transfer losses at 2000 rpm and 3000 rpm. At these higher speeds, the ethanol has no apparent effect on the ISHC or ISCO emissions.

The cooler combustion temperatures cause a reduced rate of pressure rise and longer combustion durations at 1000 rpm and 2000 rpm. Under engine idle conditions, these longer durations result in a detrimental effect on HCCI combustion stability and causes an associated increase in ISCO emissions. At 2000rpm, the combustion stability is not affected by the longer combustion durations. However, if the ethanol content of the fuel were increased further, the combustion stability would eventually degrade.

Ethanol has been shown to have the effect of mitigating knock under full-load conditions in spark-ignited engines due to the higher octane number. The observed cooling effect and the higher octane number also seem to aid in reducing knock during part load HCCI operation. This is indicated as an increase in IMEP for a given MRPR at 3000 rpm. This observed effect implies that for a given IMEP at higher engine speeds, the HCCI noise levels would decrease with increased ethanol content due to the reduced engine knock and the associated lower MRPR.

In conclusion, increased ethanol content would be beneficial to a strategy that combines part-load HCCI operation with traditional spark-ignited operation. However, the thermal efficiency, NO<sub>x</sub> emission and knock-mitigation benefits must be carefully balanced with the loss in idle stability.

### 6.2. Base Fuel Composition

At the conclusion of Phase I, after testing ten base fuel blends, the best 2-factor models were chosen for each of ten engine performance parameters. Nine fuel properties were used at the predictor variables for this analysis. During Phase II, one additional fuel was tested and five fuels were repeated. This additional data resulted in different 2-factor models for each of the engine performance parameters. However, this does not mean that the original conclusions stated at the beginning of the report were wrong. This change only indicates that, with the addition of data, other 2-factor models became more significant than the best models chosen in Phase I.

Fuel consumption showed a significant relationship to T10 and butane at 2000 rpm and 3000 rpm. In general, low T10 numbers were associated with better fuel consumption. However, fuels with high T10 numbers and high butane content also had better fuel

---

#### CUSTOMER CONFIDENTIAL



consumption. Similarly, fuels with low T10 numbers exhibited better thermal efficiency at 2000 rpm and 3000 rpm. Fuels with high T10 numbers and high normal paraffins (excluding butane) also showed improved thermal efficiency. At 3000rpm, the IMEP was also related to T10 and butane. Overall engine performance using HCCI combustion seems to be strongly related to T10 and normal paraffin content.

At the higher engine speeds, lower ISNO<sub>x</sub> emissions were observed with higher olefin content and/or butane content. These fuel components may therefore have a cooling effect on the combustion temperatures similar to ethanol. Further investigation would be required to verify this conclusion.

Testing fuels with low aromatic content and low iso-paraffin content resulted in higher ISCO emissions under idle conditions. These two predictor variables also showed a significant effect on MRPR at 1000rpm. However, they did not have any apparent effect on combustion stability, indicated by COV of IMEP, or combustion duration. In fact, no 2-factor model was found to act as a good predictive model for either of these engine performance parameters or the peak cylinder pressure.

In general, fuels with high aromatic content led to higher smoke emissions at all engine conditions.



## 7. Recommendations

Due to increased demand and rising oil prices, there is an increased interest in renewable fuels. As a result, E85 fuel, a blend of 85% ethanol and 15% gasoline, is becoming more readily available to the consumer. If HCCI combustion were to be used in conjunction with spark-ignited operation to increase thermal efficiency and reduce NO<sub>x</sub> emissions under part load conditions, an investigation into flexible fuel compatibility should be conducted. In this study, fuels with high ethanol content showed improved thermal efficiency and low NO<sub>x</sub> emissions. However, increased ethanol content also degraded HCCI idle stability. The highest level of volumetric ethanol tested was only 30%. Despite lower combustion temperatures and longer combustion durations at 2000 rpm with this level of ethanol content, the combustion stability seems unaffected. However, if the ethanol content were increased to 85%, HCCI combustion may be disabled by the decreased combustion temperatures. On the other hand, at 3000 rpm, the higher octane mitigates the knocking that is inherent to HCCI operation and limits its overall range of use. Thus, using higher levels of ethanol may help to increase the effective operating range of HCCI combustion. Investigating fuel blends with volumetric ethanol content in the range of 50% to 85% may be useful in answering these questions.



## 8. References

1. Shen, Y., "Fuel Chemistry Impacts in Gasoline HCCI," Coordinating Research Council Project No. AVFL-13 Final Report, November, 2006.
2. Morrison, D.F. (1976) Multivariate Statistical Methods. McGraw Hill Series in Probability and Statistics.
3. Orban, J.E.; Tsai, H; and Whitacre, S.D., "Statistical Design and Analysis Methods for Evaluating the Effects of Lubricant Formulations on Diesel Engine Emissions." JSAE 20030201 and SAE 2003-01-2222, 2003.
4. Zheng, J., Yang, W., et al, ( "A Skeletal Chemical Kinetic Model for the HCCI Combustion Process," SAE Technical Paper 2002-01-0423, 2002.
5. Law, D., Allen, J., et al, "Controlled combustion in an IC-Engine with a fully variable valve train," SAE Technical Paper 2001-01-0251, 2001.
6. Sun, R., Thomas, and R., Gray, C., "An HCCI Engine: Power Plant for a Hybrid Vehicle," SAE Technical Paper 2004-01-0933, 2004.
7. Marriott, C. and Reitz, R., ( "Experimental Investigation of Direct Injection Gasoline for Premixed Compression-Ignited Combustion-Phasing Control," 2002-01-0418, 2002.
8. Peng, Z., Zhao, H., and Ladommatos, N., "Effects of Air/Fuel Ratios and EGR Rates on HCCI Combustion of n-heptane, a Diesel Type Fuel," SAE Technical Paper 2003-01-0747, 2003.
9. Sjoberg, M., Edling, L., et al, "GDI HCCI: Effects of Injection Timing and Air Swirl on Fuel Stratification, Combustion and Emissions Formation," SAE Technical Paper 2002-01-0106, 2002.
10. Olsson, J., Tunestal, P., et al, "The Effect of Cooled EGR on Emissions and Performance of a Turbocharged HCCI Engine," SAE Technical Paper 2003-01-0743, 2003.
11. Kaneko, M., Morikawa, K., et al, "Study on Homogeneous Charge Compression Ignition Gasoline Engine," The Fifth International Symposium on Diagnostics and Modeling of Combustion in Internal Combustion Engines (COMODIA 2001), Nagoya, Japan, July, 2001.
12. Milovanovic, N., Chen, R. and Turner, J., "Influence of the Variable Valve Timing Strategy on the Control of a Homogeneous Charge Compression (HCCI) Engine," SAE Technical Paper 2004-01-1899, 2004.
13. Fuerhapter, A., Piock, W.F. and Fraidl, G.K., "CSI – Controlled Auto Ignition – The Best Solution for the Fuel Consumption – Versus Emission Trade-Off?" SAE Technical Paper 2003-01-0754, 2003.

---

### CUSTOMER CONFIDENTIAL



14. Kaahaaina, N.B., Simon, A.J., et al, "Use of Dynamic Valving to Achieve Residual-Affected Combustion," SAE Technical Paper 2001-01-0549, 2001.
15. Nehmer, D.A., Fluechinger, L., et al, "Development of a Fully Flexible Hydraulic Valve Actuation Engine, Part I: Hydraulic Valve Actuation System Development," Proceedings of the 2002 Global Powertrain Congress (GPC) on Advanced Engine Design and Performance, Ann Arbor, Michigan, September 24 – 26, 2002.
16. Schock, H. J., Shen, Y., et al, "The Measurement and Control of Cyclic Variations of Flow in a Piston Cylinder Assembly," SAE Technical Paper 2003-01-1357, 2003.
17. Urushihar, T., Murayama, T., et al, "Turbulence and Cycle-by-cycle Variations of Mean Velocity Generated by Swirl and Tumble Flow and Their Effects on Combustion," SAE Technical Paper 950813, 1995.
18. Marriott, C., Wiles, M., Gwidt, J., and Parrish, S., "Development of a Naturally Aspirated Spark Ignition Direct-Injection Flex-Fuel Engine", SAE 2008-01-0319, 2008.
19. Nakata, K., Utsumi, S., Ota, A., Kawatake, K., Kawai, T. and Tsunooka T., "The Effect of Ethanol Fuel on a Spark Ignition Engine", SAE 2006-01-3380, 2006.

## Appendix A – Definition of Acronyms

ABDC	After Bottom Dead Center
AFR	Air-to-Fuel Ratio
API	American Petroleum Institute
ATDC	After Top Dead Center
AVFL	Advanced Vehicles, Fuels and Lubricants
AVL	Anstalt für Verbrennungskraftmaschinen, List ( <i>Institute for Internal Combustion Engines, List</i> )
BTDC	Before Top Dead Center
COV	Coefficient of Variation
CRC	Coordinating Research Council
EGR	Exhaust Gas Recirculation
EGT	Exhaust Gas Temperature
ETBE	Ethyl Tert-Butyl Ether
ETOH	Ethanol
EVC	Exhaust Valve Closing
EVL	Exhaust Valve Lift
EVO	Exhaust Valve Opening
FSN	Filter Smoke Number
GDI	Gasoline Direct Injection
HCCI	Homogeneous Charge Compression Ignition
HVA	Hydraulic Valve Actuation
IAT	Intake Air Temperature
IBP	Initial Boiling Point
ICE	Internal Combustion Engine
IMEP	Indicated Mean Effective Pressure
IPW	Injection Pulse Width
ISCO	Indicated Specific Carbon Monoxide
ISFC	Indicated Specific Fuel Consumption
ISHC	Indicated Specific Hydrocarbon
ISNO <sub>x</sub>	Indicated Specific Oxides of Nitrogen
IS_SMK	Indicated Specific Smoke Emissions
ITE	Indicated Thermal Efficiency
IVC	Intake Valve Closing
IVL	Intake Valve Lift
IVO	Intake Valve Opening
LHV	Lower Heating Value
MAP	Manifold Absolute Pressure
MFB	Mass Fraction Burned
MON	Motor Octane Number
MRPR	Maximum Rate of Pressure Rise
MTBE	Methyl Tert-Butyl Ether
NDR	Normalized Dilution Ratio
ORNL	Oakridge National Laboratory
PFI	Port Fuel Injection
PP	Peak Cylinder Pressure
RBEI	Re-Breathing Early Injection
RCEI	Re-Compression Early Injection
RCSI	Re-Compression Split Injection
ROAD	Road Octane Number (R+M)/2
RON	Research Octane Number
RVP	Reed Vapor Pressure
SCRE	Single Cylinder Research Engine
SI	Spark Ignition
SOC	Start of Combustion
V/L	Vapor/Liquid Ratio
VVT	Variable Valvetrain
WOT	Wide Open Throttle

## Appendix B – Measured and Calculated Parameters

**Table B.1 – Measured & Calculated Parameters**

NORMNAME	DESCRIPTION	UNIT
N	Actual Dynamometer Speed	rpm
PI	Net Indicated Mean Effective Pressure (IMEP)	bar
ITE	Net Indicated Thermal Efficiency (ITE)	%
TL22	Intake Manifold Temperature (IAT)	°C
MFB 50%	50% Mass Fraction Burn Location (MFB50)	°ATDC
MFB Duration	Mass Fraction Burn Duration from 10% to 90%	°CA
VPI	Co-efficient of variance of IMEP (COV of IMEP)	%
CYPMX	Peak Cylinder Pressure (PP)	bar
PR_CYP	Maximum Rate of Pressure Rise (MRPR)	bar/°CA
IntAOpen	Intake A Open Demand (IVO)	°ATDC
IntAClos	Intake A Close Demand (IVC)	°ATDC
IntALift	Intake A Lift Demand (IVL)	mm
ExtOpen	Exhaust Valve Open Demand (EVO)	°BTDC
ExtClose	Exhaust Valve Close Demand (EVC)	°BTDC
ExtLift	Exhaust Valve Lift Demand (EVL)	mm
ExtBOpen	2nd Exhaust Valve Open Demand (EVOB)	°BTDC
ExtBClos	2nd Exhaust Valve Close Demand (EVCB)	°BTDC
ExtBlift	2nd Exhaust Valve Lift Demand (EVLB)	mm
P_RAIL	Fuel Rail Pressure	bar
InjAngle	Injector Pulse Demand Angle	°BTDC
InjPulse	Injector Pulse Width Demand (IPW)	µs
InjAngB	Injector Pulse Demand Angle B	°BTDC
InjPulB	Injector Pulse Width Demand B (IPWB)	µs
GL	Mass Air Flow (MAF)	kg/h
BH	Fuel Flow	kg/h
BI	Indicated Specific Fuel Consumption (ISFC)	g/kWh
LAV	Lambda (Normalized A/F Ratio)	-
HC	HC - Emission	ppm
CO	CO - Emission	ppm
NOX	NO <sub>x</sub> - Emission	ppm
CO2	CO2 - Emission	%
O2	O2 - Emission	%
SMKS FSN	AVL 415 Filter Smoke Number (FSN)	-
I_PHC	Net Indicated Specific HC Emissions (ISHC)	g/kWh
I_PCO	Net Indicated Specific CO Emissions (ISCO)	g/kWh
I_PNOX	Net Indicated Specific NO <sub>x</sub> Emissions (ISNO <sub>x</sub> )	g/kWh
I_PSMK	Net Indicated Specific Smoke Emissions	g/kWh
NOISE	Combustion Noise Calculation from Indicom	dB
POEL	Oil Pressure	bar
P0	Ambient Air Pressure	mbar
P22	Intake Manifold Pressure	bar
P41	Exhaust Pressure	mbar
PKR	Fuel Pressure	bar
T_Rail	Fuel Rail Temperature	Celsius
TAZ1	Exhaust Gas Temperature (EGT)	Celsius
TOEL	Oil Temperature	Celsius
TWA	Temperature Water Outlet	Celsius
TWE	Temperature Water Inlet	Celsius
Comb Eff	Combustion Efficiency	%
EGR_EST	Estimated EGR	%
X	Humidity	g/kg
RTCBAL	Carbon Balance	%
Q_MEAN	Average Heat Release	kg/h

## Appendix C – Fuel Analysis

**Table C.1 – Phase I (AVFL-13) Fuel Analysis**

	Phase I (AVFL-13)									
	A100	B100	C100	B50D50	C85D15	B77D23	B30D70	A79D21	C50D50	A33D67
RON	95.5	89.1	91.5	58.9	87.7	81.0	64.7	84.0	78.0	65.5
MON	84.8	89.3	80.3	61.1	77.3	81.9	63.7	76.2	71.5	62.8
ROAD	90.2	89.2	85.9	60.0	82.5	81.5	64.2	80.1	74.7	64.2
Sensitivity	10.7	-0.2	11.1	-2.1	10.4	-0.8	1.1	7.9	6.4	2.7
API Gravity	46.2	71.1	65.8	56.8	61.2	67.0	60.3	49.6	59.4	53.2
Density (60F/60F)	0.7963	0.6984	0.7173	0.7516	0.7343	0.7128	0.7376	0.7813	0.7412	0.7662
RVP (psi)	7.34	6.99	7.53	7.48	7.15	7.09	7.34	6.93	7.31	6.99
Total Sulfur (ppm)	2	2	72	808	306	400	1086	347	788	1007
Distillation (F)										
IBP	103.6	99.5	103.1	109.2	102.0	101.1	101.1	105.6	99.1	113.4
5%										
10%	174.6	153.5	133.7	187.0	138.6	158.9	172.8	181.9	146.7	191.1
20%										
30%	241.2	198.0	152.4	280.9	172.2	210.4	234.0	243.7	201.2	251.6
40%										
50%	266.2	212.2	178.7	321.4	212.9	224.1	253.8	266.0	242.2	271.8
60%										
70%	290.5	225.5	212.2	363.7	251.8	246.7	286.7	290.5	274.8	298.0
80%										
90%	327.2	338.4	255.7	420.8	297.1	337.1	344.1	329.5	319.8	338.5
95%	346.6	396.7	276.6	462.0	317.7	380.8	367.9	349.0	341.4	356.7
EP	403.5	435.2	309.2	502.2	356.4	449.2	401.2	398.8	381.0	393.6
Composition (vol%)										
Total Paraffins	43.0%	96.5%	44.5%	91.1%	46.5%	96.2%	88.4%	57.3%	63.6%	72.0%
% n-Paraffins	12.5%	5.0%	4.3%	28.5%	6.9%	12.5%	22.3%	17.9%	16.2%	25.8%
% n-Paraffins w/o C4	10.2%	0.6%	4.1%	20.6%	6.0%	5.9%	16.0%	14.3%	12.2%	19.6%
% Butane	2.3%	4.4%	0.2%	8.0%	0.9%	6.6%	6.3%	3.6%	4.0%	6.2%
% i-Paraffins	27.3%	88.1%	30.1%	42.4%	28.7%	77.1%	50.9%	31.0%	31.3%	29.2%
% Cyclo-Par	3.3%	3.5%	10.1%	20.1%	10.9%	6.5%	15.2%	8.4%	16.1%	16.9%
Olefins	2.1%	0.8%	44.7%	1.1%	36.9%	0.9%	1.4%	1.8%	18.2%	2.1%
Aromatics	55.0%	2.8%	10.8%	7.9%	16.7%	3.0%	10.6%	41.0%	18.2%	25.9%
Oxygenates: (vol%)										
ETBE	0	0	0	0	0	0	0	0	0	0
ETOH	0	0	0	0	0	0	0	0	0	0
MTBE	0	0	0	0	0	0	0	0	0	0
C, wt %										
C, wt %	88.3%	83.8%	85.2%	82.6%	85.9%	82.9%	85.0%	87.5%	85.9%	86.4%
H, wt %										
H, wt %	11.7%	16.2%	14.8%	15.6%	14.0%	15.3%	15.0%	12.5%	14.1%	13.6%
O, wt %										
O, wt %	0.0%	0.0%	0.0%	0.0%	0.0%	0.0%	0.0%	0.0%	0.0%	0.0%
LHV, kJ/kg										
LHV, kJ/kg	42005	44478	43629	42671	42147	44231	43685	42489	43217	41984

**Table C.2 – Phase II-a (AVFL-13b) Fuel Analysis**

	Phase II-a (AVFL-13b)						
	C100	C100E20	A79D21	A79D21E10	A79D21E20	A79D21E30	A50C20D30
RON	86.0	95.1	83.4	88.5	94.7	99.1	82.4
MON	76.6	82.4	76.5	80.4	83.4	86.9	75.8
ROAD	81.3	88.8	80.0	84.5	89.1	93.0	79.1
Sensitivity	9.4	12.7	6.9	8.1	11.3	12.2	6.6
API Gravity	66.8	62.8	49.6	49.6	49.3	49.2	52.6
Density (60F/60F)	0.7127	0.7274	0.7807	0.7806	0.7820	0.7824	0.7678
RVP (psi)	6.79	7.86	6.60	7.53	7.16		6.80
Total Sulfur (ppm)	45	35	264	236	207	173	351
Distillation (F)							
IBP	110.1	110.1	106.3	114.8	119.5	119.1	102.7
5%	134.8	126.1	148.6	138.4	144.0	147.2	142.7
10%	140.0	129.2	188.2	152.8	155.8	157.6	166.3
20%	147.2	134.4	229.3	165.0	163.9	165.0	201.2
30%	155.3	139.5	244.8	207.0	167.2	167.4	223.7
40%	164.3	144.5	255.7	249.4	171.5	169.2	240.3
50%	174.6	149.4	266.9	261.3	251.6	170.8	254.7
60%	186.1	153.7	278.8	273.2	266.2	224.2	268.5
70%	199.0	157.8	292.3	287.2	279.1	271.2	283.6
80%	216.0	175.1	308.3	304.2	298.9	292.6	301.6
90%	239.7	233.4	331.9	327.2	322.7	318.9	325.0
95%	259.7	257.2	351.3	350.8	345.4	340.9	344.8
EP	287.6	292.6	399.0	396.0	392.0	384.3	391.1
Composition (vol%)							
Total Paraffins	52.8%	41.5%	57.4%	51.0%	44.3%	36.7%	58.3%
% n-Paraffins	8.4%	6.7%	17.6%	15.5%	13.6%	11.0%	17.4%
% n-Paraffins w/o C4	8.4%	6.7%	13.7%	12.2%	10.7%	8.9%	13.8%
% Butane	0.0%	0.0%	3.9%	3.3%	2.9%	2.1%	3.6%
% i-Paraffins	33.3%	26.3%	31.9%	28.5%	24.6%	20.5%	30.7%
% Cyclo-Par	11.1%	8.6%	7.9%	7.1%	6.1%	5.1%	10.2%
Olefins	35.6%	27.5%	1.5%	1.3%	1.2%	1.1%	6.6%
Aromatics	10.0%	9.1%	41.1%	36.9%	32.9%	27.5%	34.6%
Oxygenates: (vol%)							
ETBE	1.2%	1.0%	0.0%	0.0%	0.0%	0.0%	0.4%
ETOH	0.0%	20.6%	0.0%	10.8%	21.6%	34.8%	0.0%
MTBE	0.5%	0.4%	0.0%	0.0%	0.0%	0.0%	0.1%
C, wt %							
C, wt %	86.0%	77.8%	87.7%	84.1%	80.3%	75.8%	87.1%
H, wt %							
H, wt %	13.8%	13.1%	11.3%	11.4%	12.0%	11.7%	11.7%
O, wt %							
O, wt %	0.3%	7.4%	0.0%	3.7%	7.5%	12.1%	0.1%
LHV, kJ/kg							
LHV, kJ/kg	44217	40356	43147	41403	39635	37844	43357

**Table C.3 – Phase II-b (AVFL-13b) Fuel Analysis**

	Phase II-b (AVFL-13b)								
	C50D50	C50D50E15	C50D50E30	B100	B100E15	B100E30	B77D23	B77D23E15	B77D23E30
RON	77.2	87.3	94.6	90.0	100.4	105.9	82.0	94.2	101.2
MON	72.6	78.8	82.5	89.9	92.7	94.0	81.7	88.5	90.8
ROAD	74.9	83.1	88.6	90.0	96.5	99.9	81.9	91.4	96.0
Sensitivity	4.7	8.5	12.1	0.0	7.7	11.9	0.3	5.7	10.4
API Gravity	59.3	57.5	55.5	71.1	67.3	63.4	66.9	63.9	61.2
Density (60F/60F)	0.7412	0.7486	0.7564	0.6980	0.7116	0.7257	0.7128	0.7240	0.7341
RVP (psi)	7.34	8.15	7.6	7.41	8.06	7.64	7.35	8.12	7.72
Total Sulfur (ppm)	592	492	388	<1	2	2	340	262	211
Distillation (F)									
IBP	97.3	107.1	111.9	97.8	108.8	113.0	100.2	115.6	115.2
5%	131.3	128.1	133.6	139.8	132.9	137.2	142.7	135.7	138.9
10%	147.7	137.2	142.9	158.6	141.0	145.0	166.7	144.8	148.4
20%	176.1	149.7	154.8	186.0	150.8	153.9	199.4	155.7	158.3
30%	203.0	157.7	161.4	201.5	156.4	158.1	212.4	160.5	161.7
40%	227.0	162.8	165.3	210.0	159.6	160.5	219.0	163.6	163.7
50%	244.5	191.7	167.8	215.8	165.1	162.0	224.7	214.7	165.2
60%	260.7	249.1	169.7	221.1	217.1	163.6	234.4	230.2	166.0
70%	277.5	265.7	252.1	229.5	222.7	165.1	249.1	240.5	218.6
80%	298.0	288.7	279.7	246.2	237.4	228.1	280.2	267.7	257.5
90%	323.4	317.3	310.9	354.0	316.0	279.2	343.0	335.3	324.0
95%	342.5	341.4	336.1	402.2	398.2	392.8	383.9	380.2	374.5
EP	385.3	376.3	372.1	437.9	417.8	429.7	441.8	446.4	436.7
Composition (vol%)									
Total Paraffins	63.2%	53.5%	44.0%	94.8%	79.8%	66.7%	91.4%	76.7%	64.2%
% n-Paraffins	16.7%	14.1%	11.7%	5.0%	4.0%	3.3%	12.4%	10.4%	8.3%
% n-Paraffins w/o C4	12.6%	10.8%	9.1%	0.4%	0.4%	0.5%	5.7%	4.9%	3.8%
% Butane	4.1%	3.3%	2.6%	4.6%	3.6%	2.8%	6.7%	5.5%	4.5%
% i-Paraffins	31.2%	26.9%	21.9%	88.7%	74.8%	62.5%	73.5%	61.6%	51.8%
% Cyclo-Par	15.2%	12.5%	10.4%	1.1%	1.0%	0.9%	5.5%	4.7%	4.1%
Olefins	17.4%	14.6%	12.1%	0.3%	0.3%	0.2%	0.6%	0.6%	0.5%
Aromatics	19.5%	16.3%	13.7%	4.9%	4.2%	3.4%	8.0%	7.0%	5.9%
Oxygenates: (vol%)									
ETBE	0.0%	0.0%	0.0%	0.0%	0.0%	0.0%	0.0%	0.0%	0.0%
ETOH	0.0%	15.6%	30.2%	0.0%	15.7%	29.7%	0.0%	15.7%	29.4%
MTBE	0.0%	0.0%	0.0%	0.0%	0.0%	0.0%	0.0%	0.0%	0.0%
C, wt %	86.2%	80.6%	75.4%	84.4%	78.8%	73.8%	84.6%	79.0%	74.4%
H, wt %	13.8%	13.6%	13.5%	15.6%	15.2%	14.9%	15.4%	15.0%	14.7%
O, wt %	0.0%	5.8%	11.1%	0.0%	6.0%	11.3%	0.0%	6.0%	10.9%
LHV, kJ/kg	43534	40749	38135	44310	41368	37949	44171	40849	38751

**Table C.4 – Indolene Fuel Analysis**

	Indolene		
	Phase I (AVFL-13)	Phase II-a (AVFL-13b)	Phase II-b (AVFL-13b)
RON	95.6	97.0	96.3
MON	89.0	88.8	88.1
ROAD	92.3	92.9	92.2
Sensitivity	6.6	8.2	8.2
API Gravity	58.9	58.9	58.9
Density (60F/60F)	0.7433	0.7438	0.7423
RVP (psi)	9.09	8.77	9
Total Sulfur (ppm)	36	36	36
Distillation (F)			
IBP	97.9	88.3	85.8
5%		111.5	111.3
10%	127.0	126.3	125.7
20%		146.3	149.3
30%	174.0	170.0	174.5
40%		198.8	202.4
50%	221.0	221.5	220.3
60%		233.4	230.6
70%	244.0	244.7	242.9
80%		265.1	265.3
90%	322.3	316.4	316.1
95%	339.4	329.1	335.6
EP	402.8	393.9	385.3
Composition (vol%)			
Total Paraffins	71.3%	63.4%	65.1%
% n-Paraffins	8.2%	7.7%	6.5%
% n-Paraffins w/o C4	7.4%	7.0%	5.9%
% Butane	0.8%	0.8%	0.6%
% i-Paraffins	57.3%	52.9%	54.5%
% Cyclo-Par	5.8%	2.8%	4.1%
Olefins	1.4%	0.3%	0.4%
Aromatics	27.4%	36.4%	34.4%
Oxygenates: (vol%)			
ETBE	0.0%	0.0%	0.0%
ETOH	0.0%	0.0%	0.0%
MTBE	0.0%	0.0%	0.0%
C, wt %			
	86.6%	86.6%	86.2%
H, wt %			
	13.3%	13.4%	13.8%
O, wt %			
	0.0%	0.0%	0.0%
LHV, kJ/kg			
	43500	43271	43231

## Appendix D – Motored Engine Pressure Data

**Table D.1 – Motored Pressure Data 5/25/07**

Test Cell 3 Motor Traces Performed 5/25/07														
Run #	N	PP	MRPR	IVO	IVC	IVL	EVO	EVC	EVL	EVOB	EVCB	EVLB	NOISE	P41
-	rpm	bar	bar/CA	Deg.	Deg.	mm	Deg.	Deg.	mm	Deg.	Deg.	mm	dB	mbar
1	1999	31.4	0.8	268	168	60	166	248	40	0	0	0	70.61	4
2	1999	31.5	0.9	268	168	60	166	256	40	230	180	30	71.15	4
3	3000	28.5	0.8	276	164	70	178	270	50	0	0	0	74.74	9
4	3000	29.3	0.8	276	164	70	176	287	50	270	170	25	74.89	14
5	999	30.3	0.8	240	164	30	164	226	20	0	0	0	72.18	-4
6	999	29.7	0.8	245	164	30	164	253	20	220	180	15	72.41	1

**Table D.2 – Motored Pressure Data 11/23/08**

Test Cell 3 Motor Traces Performed 11/23/08														
Run #	N	PP	MRPR	IVO	IVC	IVL	EVO	EVC	EVL	EVOB	EVCB	EVLB	NOISE	P41
-	rpm	bar	bar/CA	Deg.	Deg.	mm	Deg.	Deg.	mm	Deg.	Deg.	mm	dB	mbar
1	1997	31.3	0.9	268	168	60	166	248	40	0	0	0	76.92	0
2	1996	31.6	0.9	268	168	60	166	256	40	230	180	30	77.06	-5
3	2997	28.6	0.8	276	164	70	178	270	50	0	0	0	76.55	3
4	2997	30.4	0.9	276	164	70	176	287	50	270	170	25	77.57	16
5	999	29.5	0.8	240	164	30	164	226	20	0	0	0	78.72	-11
6	997	29.1	0.8	245	164	30	164	253	20	220	180	15	78.55	-7

## **Appendix E – Numerical Results**

The numerical results of all three phases are contained in an Excel file titled:

[PEI0341-AppendixE\\_CRC\\_Test\\_Data.XLS](#)

## **Appendix F – Regression Models**

A comprehensive list of all the 2-factor regression models for the 10 engine performance parameters based on the nine fuel property predictor variables is contained in an Excel file titled:

[PEI0341-AppendixF All 2 Factor Models Results.xls](#)